

AD-750 871

SHIPBOARD RADARS AND THEIR USE

Ya. I. Berman, et al

Naval Intelligence Support Center
Washington, D. C.

29 September 1972

DISTRIBUTED BY:

NTIS

National Technical Information Service
U. S. DEPARTMENT OF COMMERCE
5285 Port Royal Road, Springfield Va. 22151



DEPARTMENT OF THE NAVY
NAVAL INTELLIGENCE SUPPORT CENTER

TRANSLATION SERVICES DIVISION
4301 SUTTLAND ROAD
WASHINGTON, D. C. 20390

AD 750871

CLASSIFICATION:

UNCLASSIFIED

APPROVED FOR PUBLIC RELEASE, DISTRIBUTION UNLIMITED

TITLE:

Shipboard Radars and Their Use

Sudovyye Radiolokatsionnyye Stantsii i Ikh Primeneniye

AUTHOR(S):

Berman, Ya. I., Vlasov, V. I., Kogan, N. L.,
Rakov, V. I., Skvortsov, V. L. and Slutskiy, P. I.

PAGES:

128

SOURCES:

Izdatel'stvo "Sudostroyeniye", Vol. 2, 1970, Leningrad
Pages 274-342 and 437-503

Reproduced from
best available copy.

DDC
RECEIVED
NOV 10 1972
C

ORIGINAL LANGUAGE: Russian

TRANSLATOR: C

NISC TRANSLATION NO. 3348

APPROVED P.T.K.

DATE 29 September 1972

Reproduced by
NATIONAL TECHNICAL
INFORMATION SERVICE
U S Department of Commerce
Springfield VA 22151

**Best
Available
Copy**

SHIPBOARD RADARS AND THEIR USE

[German, Vlasov, Kozan, Rakov, Skvortsov, and Slutskiy, Sudovyye Radio-
lokatsionnyye Stantsii i Ikh Primeneniye (Spravochnoye Rukovodstvo), Vol. 2,
Shipbuilders Publishing House, Leningrad, 1970, Pages 274-342, Russian]

CHAPTER IV

ANTENNA SYSTEMS.- CONTROLLING ANTENNA PATTERNS

1. Purposes of Antennas and Their Principal Parameters

General Information

[274]

Shipboard radar antennas receive and transmit electromagnetic energy. Their main purpose is to convert high frequency current energy into radio-wave energy and the reverse, convert the energy of an incoming signal into high frequency current energy.

In addition, an antenna is required to concentrate source energy in space, a fact necessitated by the requirement to extend the effective range of action of the equipment, and, secondly, by the need for spatial selectivity of detected objects. Sometimes, antennas are designed to produce a rational redistribution of energy in space, as, for example, when providing uniformity of signal power in reception at different angles of site from a radar target.

The essential parameters of an antenna are governed by the purpose for which the radar unit was designed.

Basic Antenna Parameters

The antenna of a shipborne radar unit is characterized by a number of electrical and structural parameters.

The electrical parameters include the following:

- amplitude radiation pattern;
 - phase radiation pattern;
 - polarization characteristic;
 - input impedance;
 - coefficient of directivity (or the effective absorption area of a receiving antenna);
 - radiation efficiency;
 - transmission frequency characteristic;
 - effective transmitted power;
 - scanning beam frequency and scanning arc.
- The structural parameters include the following:
- type of antenna focusing element (reflector, lens, etc) and antenna exciter;
 - basic antenna dimensions (height, width, and sweep radius);
 - mutual disposition of antenna elements;

Reproduced from
best available copy.

- antenna speed of rotation and scanning arc in the horizontal and vertical planes;
- the presence of a radar dome;
- weight of the antenna;
- type of stabilization system use.

The electrical parameters of the antenna are closely related to its structural features.

2. Electrical Parameters of Antennas

Amplitude and Phase Patterns

The law governing the distribution of a field radiated into space in the different directions φ , θ (IV.1) is illustrated by the antenna's radiation pattern.

The composite amplitude of directivity of an electrical field of any radiator with finite dimensions at an arbitrary point M in a far zone is determined by the expression

$$E = \frac{A}{r} f(\varphi, \theta) e^{-jkr}, \quad (\text{IV.1})$$

in which

A is a constant usually taken as the amplitude of the current at a certain point of the antenna; r , φ , θ are the coordinates of a spherical system of coordinates which determine the position of a distant point of observation M in space; $k = 2\pi/\lambda$ is the wave number; $f(\varphi, \theta) = |f(\varphi, \theta)| e^{j\varphi(\varphi, \theta)}$ is a certain complex function depending on the design of a particular antenna, which at $r = \text{constant}$ determines the radiation pattern of the antenna.

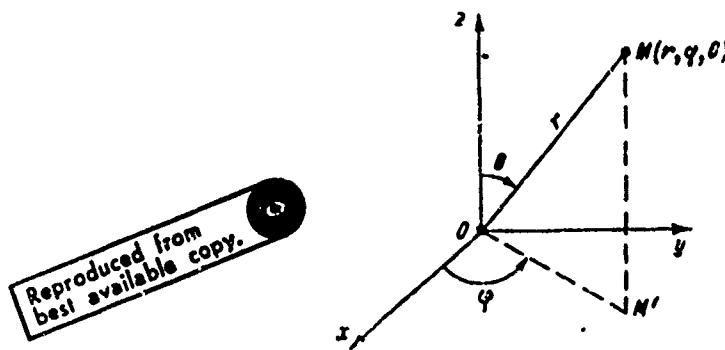


Fig. IV. 1. Spherical system of coordinates

The modulus of the function $f(\varphi, \theta)$, which determines the relationship of the amplitude of the antenna field voltage (at points in the far zone equidistant from it) to the direction of observation is called the antenna amplitude characteristic or radiation pattern. Geometrically, it is formed by the surface described by the end of the radius vector r of a ^[275] spherical system of coordinates whose magnitude is proportional to the amplitude of the field voltage produced by the antenna in a given direction.

Spatial radiation patterns are not convenient to describe a situation hence plane diagrams are most frequently used. These diagrams lie in sections of a spatial diagram which are formed by planes passing through the directions of maximum radiation. Two mutually perpendicular planes are [276] selected for this purpose. In the case of linear polarization one of these planes coincides with the plane of polarization and is referred to as the E plane, and the other is called the H plane.

Planar radiation patterns are represented in a polar or rectilinear system of coordinates. When depicted in a polar system they offer a more effective visual representation, whereas in a rectilinear system they insure greater accuracy.

Antennas with multiple lobed radiation patterns are most commonly used in shipborne radar. The principal indicators of a multiple-lobed radiation pattern are the width of the major lobe at the half power points of measurement $2\theta_{0.5P_m}$, the width of the major lobe at zero points $2\theta_0$, and the level of the side lobes close to the major lobe.

Ordinarily, a standardized amplitude pattern of directivity is used that is represented by the formula

$$F(\varphi, \theta) = \frac{f(\varphi, \theta)}{f_{\max}} \quad (\text{IV.2})$$

The maximum value of the standardized pattern $F(\varphi, \theta)$ is equal to unity.

Not infrequently, the following power radiation pattern is used

$$F_p(\varphi, \theta) = F^2(\varphi, \theta).$$

To describe a pattern of directivity with very low level side lobes use is made of the logarithmic scale in which the function $F(\varphi, \theta)$ is measured in decibels

$$F(\varphi, \theta) = 10 \lg F_p(\varphi, \theta) = 20 \lg F(\varphi, \theta).$$

Antennas in which one of the plane diagrams is close to circular in form are used in radio navigation, and antennas with needle-shaped patterns (with approximately the same directivity in both planes) are used in sets for tracking targets by two angular coordinates. When it is necessary to determine only one angular coordinate, antennas with fan-shaped radiation patterns are used.

The phase pattern of directivity $\phi(\varphi, \theta)$ characterizes the relationship of the phase of the radiated field to the direction at an equal distance from the antenna. This pattern can also be regarded as the geometric position of points in the far zone in which the field intensity is of [277] the same phase. This kind of a distribution coincides with the wave front or equi-phase surface concept.

The antenna phase pattern equation may be written as

(IV.3)

Reproduced from
best available copy.

$$D(\varphi, \theta) = D_0 e^{-jk \Delta\phi(\varphi, \theta)}$$

in which D_0 is the distance in the direction $\varphi = \theta = 0$; $k = 2\pi/\lambda$ is the wave number;

If equation (IV.3) describes the surface of a sphere, the antenna can be regarded as a point source radiator, and, therefore, the center of the sphere is the phase center of the antenna. Generally, the phase pattern will differ from the spherical pattern, and in such case the phase center is missing. In linear antennas the phase center is disposed in the center of the antenna with an even distribution of current amplitude relative to the antenna and with a zero phase distribution [20].

If there is no phase center a piecemeal approximation of the antenna phase diagram can be achieved by means of portions of several spherical surfaces with their own phase centers.

Like the amplitude radiation patterns, phase patterns are depicted in the principal planes. The planar phase pattern of a multiple lobed antenna is step-shaped in character since the field phase changes abruptly by 180° on transitting through zero radiation.

Polarization Characteristics of an Antenna

The antenna field also has the quality of polarization, i.e. time change in direction of the voltage vector of the electrical field in a plane perpendicular to the direction of wave propagation. The kind of polarization depends on the type of antenna used and its orientation in space. Generally, the antenna has elliptical polarization when the hodograph of the \vec{E} vector is in the form of an ellipse (fig. IV. 2).

The field of elliptical can be represented as the sum of two coherent orthogonal, linearly polarized fields E_θ and E_φ shifted in phase by angle δ .

The elliptical polarization equation which combines the instantaneous values of the orthogonal components e_θ and e_φ appears as

$$\left(\frac{e_\varphi}{E_\varphi}\right)^2 + \left(\frac{e_\theta}{E_\theta}\right)^2 - 2\frac{e_\theta}{E_\theta}\frac{e_\varphi}{E_\varphi}\cos\delta = \sin^2\delta. \quad (\text{IV.4})$$

From (IV.4) it follows that when $\delta = n\pi$ ($n = 0, 1, 2, \dots$) the field has linear polarization, and when $\delta = (2n + 1)\pi/2$ and $E_\theta = E_\varphi$ [278] The polarization of an antenna field is characterized by the coefficient of polarization p and the angle of inclination α of the large axis of the ellipse relative to the horizontal angle φ .

The coefficient of polarization is equal to the ratio of the small semi-axis b of the ellipse to the large semi-axis a

$$p = \frac{b}{a} = \sqrt{\frac{1 - q^2 - \sqrt{(1 - q^2)^2 + 4q^2 \cos^2 \delta}}{1 + q^2 + \sqrt{(1 - q^2)^2 + 4q^2 \cos^2 \delta}}}, \quad (\text{IV.5})$$

in which $q = E_{\varphi} / E_{\theta}$.

The angle of inclination of the large axis of the ellipse is determined by the formula

$$\alpha = \text{arctg } q. \quad (\text{IV.6})$$

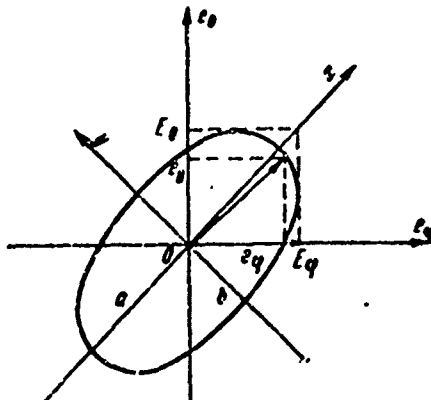


Fig. IV. 2. Ellipse of Polarization

Coefficient of Antenna Directivity

The coefficient of directivity is used for total evaluation of an antenna's directional properties. It shows how much greater is the power of the radio signal at a certain point in space radiated by a directional antenna than that of a signal radiated by an omnidirectional antenna at that same point with the same amount of power fed to the antennas.

The magnitude of the coefficient can be computed by the following formulas:

$$G(\varphi, \theta) = \frac{P_H(\varphi, \theta)}{P_0};$$

$$G(\varphi', \theta') = \frac{4\pi F^2(\varphi', \theta')}{\int_0^{2\pi} \int_0^\pi F^2(\varphi, \theta) \sin \theta d\theta d\varphi}, \quad (\text{IV.7})$$

in which $P_H(\varphi, \theta)$ is the power of radiation of a directional antenna; P_0 is the power of radiation of an omnidirectional antenna; $F(\varphi', \theta')$ is the value of the radiation pattern in the direction φ', θ' ; and $F(\varphi, \theta)$ is the standard field radiation pattern.

Sometimes, another parameter is used in technical literature to describe the directional properties of antennas -- the coefficient of directivity relative to the half-wave dipole $G_{\lambda/2}$ [279

$$G_{\lambda/2}(\varphi, \theta) = \frac{P_n(\varphi, \theta)}{P_{\lambda/2}(\varphi, \theta)}, \quad (\text{IV.8})$$

in which $P_{\lambda/2}(\varphi, \theta)$ is the radiating power of the half wave dipole.

If the coefficient of directivity of the dipole relative to the omnidirectional antenna (isotropic source) is equal to 1.64 it follows from expression (IV. 8) that

$$G(\varphi, \theta) = 1.64 G_{\lambda/2}(\varphi, \theta).$$

The magnitude of the coefficient of directivity depends only on the amplitude characteristic of antenna directivity, and its maximum value coincides with the maximum lobe of the radiation pattern

$$G_{\max} = \frac{4\pi}{\int_0^{\pi} \int_0^{2\pi} F^2(\varphi, \theta) \sin \theta d\theta d\varphi}. \quad (\text{IV. 9})$$

The coefficient of directivity of the antenna in any direction is found using the formula

$$G(\varphi, \theta) = G_{\max} F^2(\varphi, \theta). \quad (\text{IV. 10})$$

The graph-analytic method (cf Part I, Chap. 1) is frequently used to get an approximate value of the coefficient of directivity; it consists of approximations of the diagram of functions of $F(\varphi, \theta)$ which make it possible to compute the integral (IV. 7). In a case where it is difficult to select an approximating function the integral is resolved by the numerical integration method.

If the radiation pattern is approximated as an ellipsoid of rotation with semi-axes $a, b,$ and c the maximum coefficient of antenna directivity can be determined from the following formulas [4]:

if $t > 1$

$$G_{\max} \approx \frac{4(t^2 - 1)}{1 - \frac{1}{2t\sqrt{t^2 - 1}} \ln \frac{t + \sqrt{t^2 - 1}}{t - \sqrt{t^2 - 1}}};$$

if $t < 1$

$$G_{\max} \approx \frac{4(1 - t^2)}{1 - \frac{1}{t\sqrt{1 - t^2}} \operatorname{arctg} \frac{\sqrt{1 - t^2}}{t}};$$

where $t = \sqrt{p_1 p_2}$, $p_1 = a/b$, $p_2 = a/c$.

Input Impedance and Antenna Radiation Resistance

[280

The concept "antenna radiation resistance" is used in determining the radiation power of antennas consisting of thin leads with a current of I_a . As far as the transmitter is concerned the antenna of a radar set is considered a complex load whose resistance $Z_{EX} = R_{EX} + jX_{EX}$ is termed the input impedance of the antenna. The active component R_{EX} characterizes the

active power required (radiated) by the antenna, while the reactive component characterizes the reactive power of the field which oscillates between the antenna and the field of the antenna near zone.

The energy required by an antenna is expended for radiating and to overcome losses due to heating, ionization, and the like. Therefore, the active resistance of an antenna will be made up of radiation resistance R_z and loss resistances R_n . Radiation power is related to radiation resistances by the formula

$$P_z = \frac{I_a^2}{2} R_z. \quad (\text{IV. 11})$$

The power emitted by the antenna is determined by the expression

$$P_z = \frac{I_a^2}{240\pi} \int_0^{2\pi} \int_0^\pi f^2(\varphi, \theta) \sin \theta d\theta d\varphi. \quad (\text{IV. 12})$$

By substituting we get the following result:

$$R_z = \frac{1}{120\pi} \int_0^{2\pi} \int_0^\pi f^2(\varphi, \theta) \sin \theta d\theta d\varphi. \quad (\text{IV. 13})$$

In the case of a Hertz dipole of length l the field intensity amplitude is equal to

$$E = \frac{60\pi I_a l}{\lambda r} \sin \theta,$$

the amplitude function

$$f(\varphi, \theta) = \frac{60\pi I_a l}{\lambda} \sin \theta,$$

and the radiation resistance will be

$$R_z = 80\pi^2 \left(\frac{l}{\lambda}\right)^2. \quad (\text{IV. 14})$$

The maximum coefficient of directivity is related to the radiation resistance by an expression of the type

$$G_{\max} = \frac{f_{\max}^2}{30R_z}. \quad (\text{IV. 15})$$

Radiation Efficiency and Antenna Gain

[281

The efficiency of an antenna η_a is a term applied to the ratio of radiation power (useful power) to the power applied to the antenna (total power)

$$\eta_a = \frac{P_z}{P_z + P_n} = \frac{R_z}{R_z + R_n}. \quad (\text{IV. 16})$$

Antenna gain g is the product of the coefficient of directivity and the efficiency of the antenna

$$g = G\eta_a \quad (IV.17)$$

In the case of shipborne radar antennas $\eta_a \approx 1$ and, therefore, $g \approx G$.

Determination of gain is of special importance in the study of antennas. This parameter can be measured in three different ways.

The first method consists in comparing the power of the signal received P by the antenna under consideration with that received by a standard antenna P_0 whose gain g_0 is known,

$$g = \frac{P}{P_0} g_0.$$

The second method is based on the use of two similar antennas with unknown, though equal, coefficients of amplification. One antenna is used to transmit the signal and the other is used to receive. If the distance between the antennas is D the wavelength is λ , the power at the input to the receiving antenna is P_{np} , and the power at the output of the transmitting antenna is P , then

$$g = \frac{4\pi}{\lambda} D \sqrt{\frac{P_{np}}{P}} \quad (IV.18)$$

The third method is a modification of the second. One antenna is replaced by an ideal flat screen placed at a distance of $D = 8 \sqrt{A}$ from the antenna being examined, where A is the size of the antenna aperture. The cross section of the screen $h \gg 8 \sqrt{A}$. A metering line is connected into the waveguide circuit to measure the traveling wave coefficient k_G . Antenna gain is determined by the formula

$$g = \frac{4\pi}{\lambda} D \left(\frac{1 - k_G}{1 + k_G} \right) \quad (IV.19)$$

Antenna Passband

The radio signal radiated and received by the antenna of a shipborne radar unit is polychromatic, and, therefore, has a certain frequency spectrum. An antenna responds in different ways to the electromotive force effect of different frequencies, hence it can distort the incoming signal. The band of frequencies in which the electrical parameters of an antenna respond to certain requirements is termed the antenna passband or the operating band in which the electrical parameters of the antenna are responsive to the requirements set. Essentially, these parameters include the input impedance (or k_G), directional properties, and the polarization of the radiated wave.

The passband is determined by the frequency characteristic, i.e. by the relationship of the electrical parameters of the antenna to the frequency.

In the case of long wave antennas -- usually consisting of thin wires -- the frequency characteristic is the relationship of the current amplitude at antenna input to the frequency $I_{BX}(\omega)$ at constant input voltage. The passband is computed at the $0.707 I_{BX \text{ max}}$ level.

In the centimeter, decimeter and millimeter wave bands where the concept of antenna current loses its definiteness the operating range of the antenna is found by means of the functional relationship $k_{\sigma} = f(\omega)$.

Changes in the frequency of the feed voltage leads not only to changes in Z_{BX} but also results in a redistribution of current in the antenna, which, in turn, involves changes in the radiation pattern and the coefficient of directivity. Accordingly, we have the concept of a passband for the radiation pattern and for the coefficient of directivity.

Parameters of a Receiving Antenna

The parameters of receiving antennas include effective absorption area, coefficient of effectiveness, and noise temperature.

The receiving antenna may be regarded as an absorber of the energy of an incident wave, therefore we introduce the idea of an active or effective antenna absorbing surface, similar to the concept of effective length in linear antennas.

The effective area of a receiving antenna $A_{\Sigma\phi}$ (m^2) is determined by the ratio of the power received by the antenna P (watts) to the density of the electromagnetic field of the incident wave S (watts/ m^2).

Different portions of the antenna receive and transform the energy of an incident wave in different ways, consequently, the effective area $A_{\Sigma\phi}$ will not be equal to the geometrical area of antenna aperture A . The ratio $A_{\Sigma\phi}/A = \mu$ is referred to as the coefficient of utilization of an antenna surface. Antennas with flat radiating apertures are used in shipborne radar. For such antennas

$$A_{\Sigma\phi} = \frac{\left| \int_A \dot{E}(x, y) dx dy \right|^2}{\int_A |\dot{E}(x, y)|^2 dx dy}, \quad (\text{IV. 20})$$

and the coefficient of utilization of antenna surface is

$$\mu = \frac{\left| \int_A \dot{E}(x, y) dx dy \right|^2}{A \int_A |\dot{E}(x, y)|^2 dx dy}, \quad (\text{IV. 21})$$

in which $E(x, y)$ is the value of the field in the antenna aperture. It follows that $0 < \mu \leq 1$. The limiting value of the coefficient $\mu = 1$ occurs at a uniform, phased distribution of the field in the antenna aperture.

Since the efficiency of an antenna during reception η_a is not equal to 100% we introduce a parameter known as the coefficient of effectiveness for use in evaluating the receiving qualities of an antenna

$$q = \eta_a \mu. \quad (\text{IV. 22})$$

The relationship between the parameters of an operating antenna during reception and transmission is established by the formulas:

$$G_{\max} = \frac{4\pi}{\lambda^2} A_{\text{eff}} = \frac{4\pi}{\lambda^2} A_{\text{ap}}; \quad (\text{IV. 23})$$

$$G_{\max} = \frac{4\pi}{\lambda^2} A_{\text{ap}} \eta_a. \quad (\text{IV. 24})$$

Due to the employment of very sensitive receivers in radar work the range of operation of radar equipment -- and this includes radio sextants -- is restricted by the level of interior and exterior noises. The latter are due to the thermal movement of electrons in the conducting portions of the antenna.

The magnitude of thermal noises is determined by Boltzmann's equation

$$P_w = kT \Delta f,$$

in which P_w is the magnitude of the noise in watts; $k = 1.38 \cdot 10^{-23}$ joules/degree -- Boltzmann's constant; T is the temperature of the noise source; and Δf is the receiver passband.

It is therefore convenient to use the antenna noise temperature parameter T_a . It represents the mean temperature intensity of the surrounding space with respect to antenna directivity and is determined by the integral [5] [284]

$$T_a = \frac{1}{4\pi} \int_{4\pi} G(\varphi, \theta) T(\varphi, \theta) d\Omega, \quad (\text{IV. 25})$$

in which $T(\varphi, \theta)$ is the temperature of space in the φ, θ directions; $G(\varphi, \theta)$ is the coefficient of antenna directivity in the same direction.

If the antenna has inherent losses the useful signal and the noise level related to the propagation of radiowaves will decrease while the thermal noise of the antenna will increase.

The resulting noise temperature of the antenna with losses T_p is determined from the expression

Reproduced from
best available copy.

$$T_{p,a} = \eta_a T_a + (1 - \eta_a) T, \quad (\text{IV. 26})$$

in which T is the temperature of the space surrounding the antenna.

Because of the irregular distribution of the luminance temperature in space the temperature T_a depends to a considerable degree on the orientation of the antenna, the width of the main lobe, and the side lobe level of the antenna radiation pattern.

The surface temperature of the earth is $T \approx 300^\circ\text{K}$; in the ionized E-layer it is $300 - 400^\circ\text{K}$; in the F-layer it is $1000 - 2000^\circ\text{K}$; and the temperature of the sun and certain discrete sources of cosmic radiation is $10^4 - 10^6$ degrees Kelvin.

For sharply directional antennas with orientation toward the zenith on wavelengths of $\lambda < 1 \text{ m}$ $T_a \approx 10^{-4}$ with the antenna beam oriented along the surface of the earth the noise temperature of the antenna increases up to 40°K .

To lower the antenna noise temperature it is necessary to constrict the major lobe of the radiation pattern, lower the side lobe level, and increase the efficiency of the antenna-waveguide circuit.

Characteristics of Shipboard Antennas

Classification of Antennas

Antennas presently used on ships can be divided into six groups.

1. Doublet types whose elements consist of dipoles made of thin wire or tubing (in the first case the diameter of the wire is considerably less than the wavelength, and in the second case it is commensurable with the wavelength).
2. Slotted antennas.
3. Horn antennas consisting of metallic horns of various shapes.
4. Optical antennas, reflector and lens types. 285
5. Antennas with rotating (circular) polarization, both helical and horn.
6. Surface wave antennas -- dielectrical rod and flat antennas with ribbed structure or a dielectric covering.

Doublet Antennas

Included among doublet antennas are those made in the form of dipole arrays (multielement array antennas) and wave duct type antennas. Both types of systems are widely used in detection radar equipment and in television set in the decimeter and meter wave bands. They consist of a combination of discrete radiators in the form of a number of active and passive dipoles. In contrast to phased multielement array antennas "wave duct" antennas are excited with a shift in phase. Current amplitudes in the dipoles are not equal.

Slotted Antennas

Slotted antennas are used in detection radar sets and in navigation equipment. They are convenient to use because of their small size.

Slotted antennas are made in the form of waveguides, rectangular or circular in cross section, on the surfaces of which slots are cut of a width considerably less than the wavelength. Narrow slots of this type can be regarded as linear dipoles.

Horn and Optical Antennas

Antennas of this type are used in the centimeter and millimeter wave band and are peculiar in that their dimensions are considerably greater than the wavelength. In systems of this type the radiation field is formed not by discrete radiators, but by radiating surfaces -- by a wave front.

To compute the radiation field of antennas that produce a wavefront we can use methods borrowed from optics, as well as those employed in the audio wave band. The approximation method, which is based on the well-known Huygens Principle of optics, is widely used in designing reflector, horn, and other types of antennas. The chief advantages of reflector and horn antennas are their simplicity of design and the low side lobe level.

Dielectric Antennas

286

Because they are portable dielectric antennas can be used successfully on units in which the problem of decreasing antenna dimensions is important.

An electromagnetic wave propagated in a dielectric medium is subjected to considerable absorption, the losses being greater to this cause with higher frequency of oscillation and greater field strength. Taking this fact into account, it is most desirable to use dielectric antennas in the decimeter wave band. Furthermore, it is rather difficult to obtain narrow patterns of radiation in dielectric antennas. For that reason they are generally used in search and navigation types of radar equipment.

The electromagnetic field in dielectric antennas is excited by a source like a stub or the open end of a waveguide, and it is propagated along a dielectric rod penetrating through the open surface into outer space.

Surface Wave Antennas

Surface wave antennas consist of two elements -- the exciter and director. The exciter in surface antennas can be horns, linear dipoles, or a series of slots fed by a waveguide. The director is a metallic sheet covered with a dielectric of certain thickness or a ribbed surface. The directing surface with dielectric layer can be regarded as a dielectric rod of rectangular section disposed on a metallic surface. Insofar as the nature of their action

is concerned the projections of the ribbed surface are similar to a flat metal-dielectric lens. The ribbed structure can be regarded as a layer of a synthetic dielectric.

Surface wave antennas are similar to multi-dipole antennas with axial radiation; they differ only in that the entire directing surface of the antenna serves as the radiator and not its individual elements. Thus, conversion of the electromagnetic radiations of the exciter into a surface wave aids in improving the directivity of radiation compared with the directivity of a single exciter.

Due to retardation of the wave in the dielectric layer the main portion of the energy transmitted by the wave is concentrated in the immediate vicinity of the antenna surface, and it increases exponentially as one increases the distance perpendicularly from the surface. In the process, the energy from the directing surface is continuously scattered; in other words, a diffraction of the electromagnetic wave takes place on the surface of the director.

Directivity of radiation is determined by the length of the wave and the structural parameters of the antenna, i.e. the length, width, thickness and dielectric penetrance of the layer or the dimensions of the ribbed structure in the case of the ribbed surface.

Because of the spread out design and comparatively good frequency band characteristics, surface wave antennas can be used as low profile shipborne antennas, especially in decimeter band equipment. /287

Helical Antennas

Axially radiating antennas with rotating polarization are made in the form of metallic helices with high conductance. This kind of radiating system can be fed by a coaxial cable or waveguide. In the former, the helical conductor is connected to the central core of the cable. Given the specific ratio between the dimensions of the helix and the length of the wave (when the length of a helical coil is approximately equal to the length of the wave) the helix becomes a longitudinally radiating antenna and its field will have rotating polarization. The direction of rotation of polarization is governed by the direction of the winding in the helix. If the antenna radiates a levorotatory field of polarization it will not receive a dextrorotatory field and vice versa.

The radiation pattern of a helical antenna depends on the number of coils, the diameter and pitch of the coil, as well as the frequency. Helical antennas are broad-banded: their input impedance and width of radiation pattern remain stable in a broad band of frequencies.

The advantages listed in the foregoing adapt helical antennas for use in search radar equipment in which it is most important that the antenna systems operate within a broad band of frequencies with rotating polarization. Because of considerations of design helical antennas are used in decimeter waves and in that portion of the centimeter band contiguous with the decimeter band.

Multiple-Unit Phased Antennas

With the development of electrical methods for controlling the phase and amplitude of the antenna radiation field (reference is made to the use of ferrite and semiconductor devices) it is now possible to make antennas in the form of a system of phased discrete sources. By way of elementary sources we can use low directivity antennas of the following types: half-wave doublets, slotted, open end waveguide, dielectric rod, and other kinds of antennas.

The chief advantages of multiple element phased antennas include:

1. The possibility of forming in the same system of sources radiation patterns which can be controlled in space with regard to shape and position.
2. Convenience of placement and installation on vessels in that the antenna can readily be adapted into the ship's architecture due to its design. [288]

#4. Broadly Directional Antennas

Linear Dipoles

In the meter and decimeter band of radar sets symmetrical (half wave) and non symmetrical (quarter wave) linear dipoles are widely used as independent antennas and as elements of complex antennas.

The intensity of an electrical field of radiation of a symmetrical dipole (volts/meter) is determined in accordance with the following formula

$$\dot{E} = j \frac{60 I_0 l}{\lambda D} e^{-jkD} \frac{\cos(kl \cos \theta) - \cos kl}{\sin \theta}, \quad (\text{IV. 27})$$

in which D is the distance from the antenna to the point of reception in meters; I_0 is the current on the dipole terminals in amperes; l is the length of the dipole arm in meters; θ is the angle measured from the dipole axis; and $k = 2\pi/\lambda$ is the wave number.

For a half wave dipole ($2l = 0.5\lambda$) the standardized radiation pattern is determined by the expression

$$F(\theta) = \frac{I(\theta)}{60} = \left| \frac{\cos\left(\frac{\pi}{2} \cos \theta\right)}{\sin \theta} \right|, \quad (\text{IV. 28})$$

In the magnetic plane (the plane perpendicular to the dipole axis) the dipole does not have directional properties, i.e. $F(\varphi) = 1$ owing to axial symmetry.

The field phase of a symmetrical dipole is not a function of direction; the phase center is located in the center of the dipole. The current in the dipole flows in a straight line and for that reason the dipole has linear field polarization.

The phase of the field in a symmetrical dipole is not a function of direction; the phase center is located in the center of the dipole. The current in the dipole flows in a straight line, and for that reason the dipole has linear field polarization.

The effective length of a half-wave dipole is equal to

$$l_{\text{eff}} = \frac{\lambda}{2}$$

The resistance of a radiator of a symmetrical dipole relative to the current antinode is determined by the following formula [15]

$$R_{\Sigma} = 30 \left[2(0,577 - \ln 2kl - C_1 2kl) + (0,577 + \ln kl + C_1 4kl - 2C_1 2kl) \cos 2kl + (S_1 4kl - 2S_1 2kl) \sin 2kl \right]$$

For a half-wave dipole $R_{\Sigma} = 73.1$ ohms.

The coefficient of directivity of any wire antenna in the direction of maximum radiation is computed by the expression [289]

$$G_{\text{max}} = \frac{I_{\text{max}}^2}{3R_{\Sigma}}$$

For a half wave-wave dipole $G_{\text{max}} = 1.64$.

The input impedance of a symmetrical dipole can be computed using the following approximation formula:

$$Z_{\text{in}} = \frac{R_{\Sigma}}{\left(\frac{R_{\Sigma}}{W}\right)^2 + \sin^2 kl} - j \frac{W}{2} \frac{\sin 2kl}{\left(\frac{R_{\Sigma}}{W}\right)^2 + \sin^2 kl} \quad (\text{IV. 29})$$

The reactive component of the input impedance of a dipole is equal to zero at $2l = 0.5\lambda$. However, due to the mutual influence of one section of the dipole on the other the reactive component of the input impedance is equal to zero when the length of the dipole is somewhat less than that given by the approximation theory. When the length $l = 0.25\lambda$, $X_{\text{BX}} = 42.5$ ohms and $Z_{\text{BX}} = (73.1 + j42.5)$ ohms).

The amount of shortening of the dipole Δl which compensates for the reactance when $\Delta l \ll l$ is equal to

$$\Delta l \approx l \frac{27}{W^2} \quad (\text{IV. 30})$$

Ordinarily, the amount by which it is shortened is only a few percentage points, the figure increasing as the dipole gets thicker.

A non-symmetrical dipole can be represented as a symmetrical dipole one arm of which is replaced by a planar, ideally conducting surface of infinite length. Hence, the field of a non-symmetrical dipole will have the same structure as the field of a symmetrical dipole. Consequently, the radiation pattern of a non-symmetrical dipole in one semi-sphere corresponds to the radiation pattern of a symmetrical dipole. The voltage at the input of the non-symmetrical dipole is half as great as it is at the input to the symmetrical dipole, and, therefore, the input impedance and radiation impedance of a non-symmetrical dipole is half as great as it is in the symmetrical dipole.

The characteristic impedance of a dipole (in ohms) is determined from its length $2l$ and the thickness a by the formula

$$W = 120 \left(\ln \frac{2l}{a} - 1 \right). \quad (\text{IV.31})$$

The non-symmetrical quarter wave dipole has a characteristic impedance half as great as the half-wave dipole. The coefficient of directivity of a non-symmetrical dipole is twice as great as that of a symmetrical dipole. This is explained by the shielding effect of the conducting surface. [290

The pass band of a dipole is computed from the expression

$$\Delta f = f_0 \frac{2}{\pi} \frac{R_{\text{act}}}{W}. \quad (\text{IV. 32})$$

It follows from the formula that the pass band increases as the characteristic impedance decreases and as the active component of the input impedance increases. The band characteristics of the dipole are determined by the relationship of the reactive component of the input impedance to the frequency.

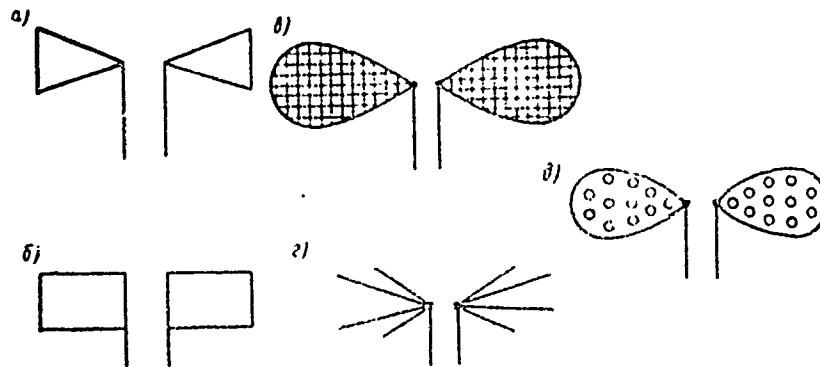


Fig. IV. 3. Plate dipoles: a - triangular; b - rectangular; c - grid type; d - fan-shaped; e - perforated type.

Three methods are used to improve the band characteristics of a dipole:

1. Increasing the characteristic impedance; 2. Increasing the active component of the input impedance; 3. Compensating the reactance of the input impedance.

The characteristic impedance of a dipole is lowered by increasing the lateral dimensions.

Each arm of the dipole may be cylindrical, spheroidal, or conical in shape. In the radar band of frequencies flat types of wide band dipoles are widely used (Fig. IV. 3).

Increasing the active portion of the input impedance is achieved by imparting a loop-shaped design to the dipole. The first person to propose such a design was A. A. Pistol'kors (Fig. IV. 4). It consists of a short-circuited twin wire line so shaped that the direction of the currents in the

upper and lower conductors coincides as a result of which the dipole will radiate and receive radio signals. Since the radiating power is directly proportional to the square of the current, and the current of the twin loop dipole is twice as great as the current of a simple dipole, the radiation resistance of a twin loop dipole will be approximately four times greater than the radiation resistance of an ordinary dipole [291

$$R_{\Sigma n} = 4R_{\Sigma} \approx 300 \text{ om.}$$

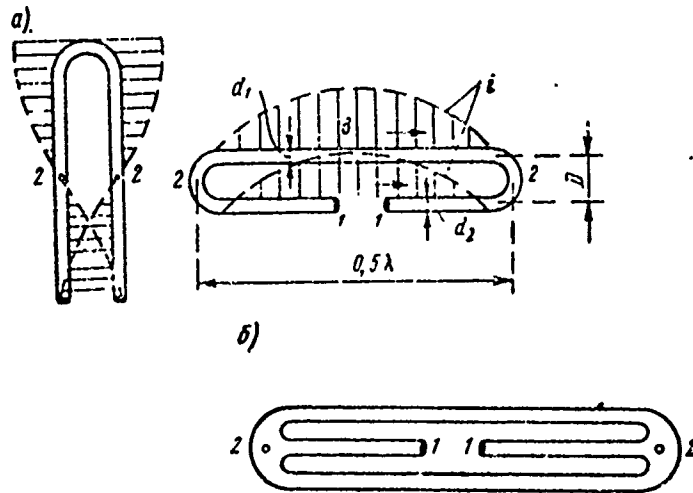


Fig. IV. 4. Looped dipole suggested by Pistol'kors: a - forming a loop dipole; b. twin loop dipole.

For a dipole with N parallel arms $R_{\Sigma n} \approx N^2 R$

Since the voltage node is at point 3 (cf Fig. IV. 4), the loop dipoles can be attached to masts at these points without the use of insulators.

The reactive portion of the input impedance of the dipole is compensated for by connecting a short-circuited reactive stub whose impedance value at the points of contact in a particular band of frequencies is equal but opposite in sign

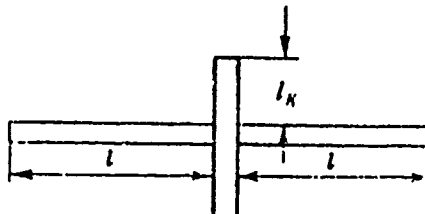


Fig. IV. 5. Dipole with compensator

The length of the compensator l_k (fig. IV. 5) is determined when the wavelength is close to resonance from the condition

$$W \operatorname{ctg} kl = W_k \operatorname{tg} kl_k \quad (\text{IV. 33})$$

in which W and W_k are the characteristic impedances of the dipole and compensator; and l , l_k are the lengths of the dipole and compensator arms.

The above methods of extending the frequency coverage insure a band coverage coefficient of

$$K_n = \frac{f_{\max}}{f_{\min}} \approx 3 - 4.$$

In many cases this kind of dipole is not adequate to the situation.

So-called logarithmic antennas, i.e. dipoles with arms whose curvature conforms to logarithmic law or with dipole elements arranged according to logarithmic periodicity have the best band characteristics. Antennas of this kind may be planar or spatial (flat or three dimensional) (Fig. IV. 6). They have a 20-30 coefficient of overlap. The broad band coverage of logarithmic antennas is explained by the fact that the projections and troughs represent dipoles whose coefficient of reflection are approximately equal in magnitude and opposite in sign; this situation insures their being compensated properly at the points of feed. [292]

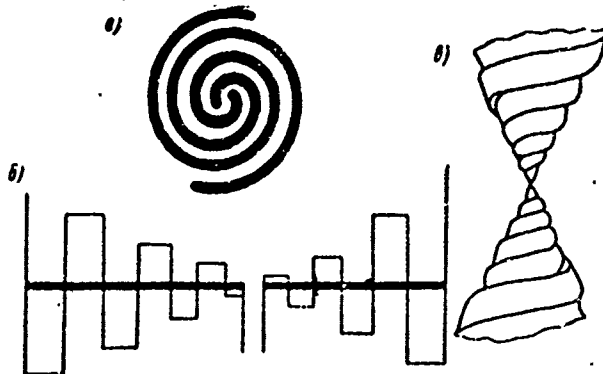


Fig. IV. 6. Logarithmic antennas: a, b -- planar; c - spatial.

Slot Antennas

The slot antenna consists of a slot made in a metallic surface such as screen, the side of a waveguide, or the side of a resonator. If such a surface has a current component that flows laterally with respect to the slot a voltage will appear at the edges of the latter; beyond the limits of the slot surface currents will be induced, resulting in the radiation of radio waves into outer space.

Serving as a basis in designing slot antennas is the theory involving an ideal slot, i.e. a slot cut into an infinite, ideally-conducting planar screen. It is assumed that the slot is narrow, i.e. the width is considerably smaller than the length and much shorter than the length of the radio wave. The field of an ideal slot antenna is determined from the field of an equidimensional linear dipole $[\frac{11}{7}]$. [293]

A comparison of the slot field structure with that of a corresponding type of dipole shows their similarity. This similarity is expressed by

the following equalities:

within the limits of the openings and the surface of the dipole

$$E_{\tau_0} = 0; \quad H_{\tau_{01}} = 0,$$

outside the limits of the openings and the surface of the dipole

$$H_{\tau_0} = 0; \quad E_{\tau_{01}} = 0.$$

Between the current in the center of the dipole I_{D0} and the voltage on the rim of the slot $U_{\mu 0}$ the following relationship holds true:

$$I_{D0} 60\pi = U_{\mu 0}. \quad (\text{IV. 34})$$

The similarly oriented slot and dipole have differing polarizations. Whereas the vertical dipole is vertically polarized, the vertical slot is horizontally polarized. As a practical rule, use is made of antennas with half-wave slots whose radiation pattern repeats the radiation pattern of a half-wave dipole, i.e. in the \bar{H} plane

$$F_{\mu}(\theta) = \left| \frac{\cos\left(\frac{\pi}{2} \cos \theta\right)}{\sin \theta} \right|,$$

and in the \bar{E} plane

$$F_{\mu}(\varphi) = 1.$$

The radiation conductance of a slot can be determined by the radiation resistance of the dipole

$$G_{\mu} = \frac{R_z}{(60\pi)^2}. \quad (\text{IV. 35})$$

From formulae (IV. 34) and (IV. 35) it is apparent that one ampere of dipole current is equivalent in radiation power to 60 volts at the slot.

The relationship between the input conductance of the slot and the input impedance of the dipole is as follows:

$$Y_{\text{ex. } \mu} = \frac{Z_{\text{ex. } D}}{(60\pi)^2}. \quad (\text{IV. 36})$$

For a slot whose length $L \approx 0.5\lambda$

$$Y_{\text{ex. } \mu} \approx \frac{1}{(60\pi)^2} \left[R_{z_0} + j \left(42.5 - W \operatorname{ctg} \frac{hL}{2} \right) \right], \quad (\text{IV. 37})$$

in which $W = 120 \left(\ln \frac{4\lambda}{\pi d} - 0.577 \right)$ is the characteristic impedance; and d is the width of the slot. [294]

It is apparent that the half-wave slot has a reactive input conductance that is capacitive in character.

In order that the input conductance of the slot be purely active, the slot should be shortened. The amount of shortening ΔL is determined from the formula

$$\Delta L \approx \frac{0,225}{\ln \frac{2L}{\pi d}} L. \quad (\text{IV. 38})$$

The narrower the slot the less it should be shortened. For a shortened slot radiating in both hemispheres

$$G_{\text{ex. m}} \approx \frac{73,1}{(69,7)^2} \approx 2 \cdot 10^{-3} \text{ mo.} \quad R_{\text{ex. m}} \approx 500 \text{ ohms}$$

In the case of single sided radiation it can be assumed that the power of radiation is decreased by one-half, and, therefore,

$$G_{\text{ex. m}} \approx 10^{-3} \text{ mhos}$$

$$R_{\text{ex. m}} \approx 10^3 \text{ ohms}$$

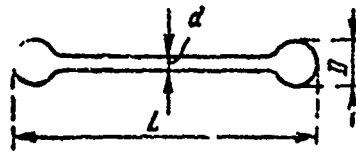


Fig. IV. 7. Dumbbell shaped slot

Affecting the conductance of the slot is its width d which in actual conditions is selected out of consideration to electrical durability

$$d \approx k_{\text{np}} \frac{U_{\text{max}}}{E_{\text{np}}}, \quad (\text{IV. 39})$$

in which U_{max} is the maximum voltage in the slot; E_{np} is the penetrating voltage of the slot (for air the figure is 30 kw/ohm); k_{np} is the coefficient of durability reserve (usually equal to 2 - 4).

The width of the slot affects the active and reactive components of input impedance. As we can see from formula (IV.38) when the width of the slot is increased its resonant length L , which corresponds to zero reactive component, decreases, while the active component increases.

In some instances it is necessary to increase the length of the slot L considerably for structural considerations. In such case so-called dumbbell slots may be incised (Fig. IV. 7.). The circular openings at the ends of the slot are equivalent to concentrated inductances. The relationship of the resonant length of the dumbbell slot to the diameter of the holes at the end D with a relative slot width $d/L \approx 0.03$ is shown in Fig. IV. 8.

The above relationships hold true for a slot cut into a screen of infinite length. In the slotted antennas generally used the slots are made in metal surfaces of finite dimensions (plane surfaces or cylinders). Because of the interferences of the slot field and the current field on a screen -- a metallic surface -- the resulting field in the far zone intensifies in some directions and attenuates in others. Therefore, the major lobe in the radiation pattern appears somewhat dissected.

The results of an approximation computation of the directivity pattern (in the \bar{E} plane) of a half-wave slot cut in the center of a rectangular plate (Fig. IV. 9) are shown in Fig. IV. 10 [8]. These results coincide satisfactorily with experimental results.

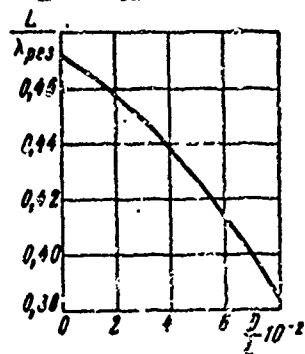


Fig. IV. 8. Curve showing the relationship between resonant length of dumbbell slot and the diameter of the terminal openings.

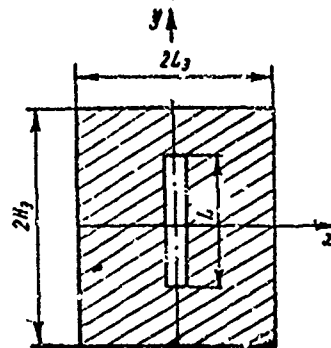


Fig. IV. 9. Slot on a rectangular screen.

The radiation pattern of a slot cut out on the surface of a cylinder depends, to a very considerable extent, on its diameter $2a$. The larger the electrical diameter of the cylinder $2a/\lambda$ the weaker the diffracted field.

The directional characteristics of a slot cut into a circular cylinder (Fig. IV. 11) are computed as follows in accordance with formulas [13]: for a longitudinal slot in the electrical plane

$$f_E(\varphi) = \left| \sum_{m=0}^{\infty} e_m j^m \frac{\cos m\varphi}{H_m^{(2)}(ka)} \right|;$$

for a lateral slot in the magnetic plane

$$f_H(\varphi) = \left| \sum_{m=0}^{\infty} e_m j^{m+1} \frac{\cos \frac{m\pi}{2} \cos m\varphi}{\left[1 - \left(\frac{m}{ka}\right)^2\right] H_m^{(2)}(ka)} \right|.$$

in which

$$e_m = \begin{cases} 2 & \text{if } m \neq 0; \\ 1 & \text{if } m = 0; \end{cases}$$

$H_m^{(2)}(ka)$ is a second degree Hankel function.

For engineering computations it is sufficient to take $m \gg 3ka$ from the sum of the first members. [296]

The radiation pattern of a slotted source in the vertical plane (in the plane of angles θ) given a long cylinder can be computed from the formulas for an ideal slotted antenna.

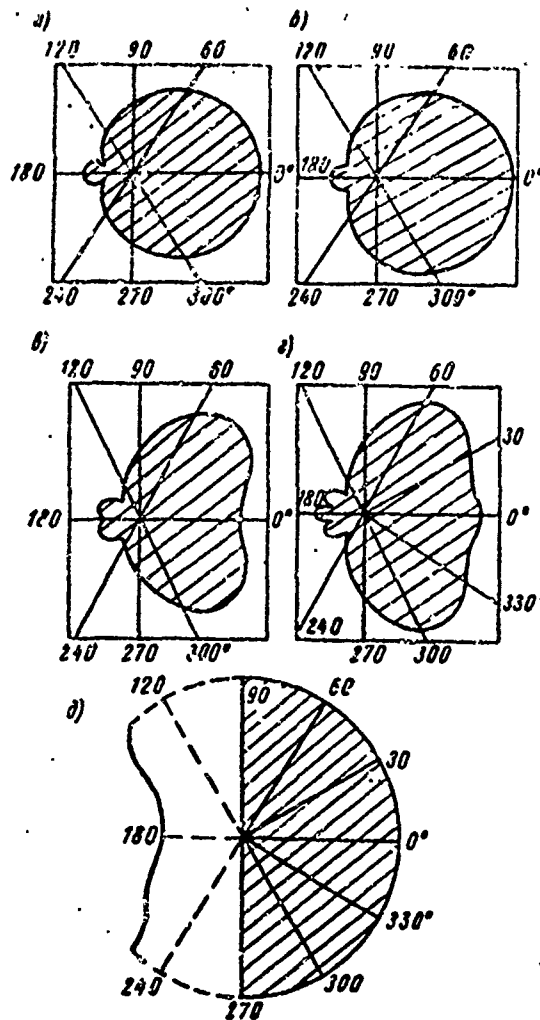


Fig. IV. 10. Radiation patterns of a slot on a rectangular screen:

$$\begin{aligned}
 H_0 = 0,25\lambda; & \quad a - L_0 = 0,5\lambda, H_0 = 0,5\lambda, G - L_0 = 0,5\lambda, \\
 & \quad s - L_0 = H_0 = \lambda; \quad z - L_0 = 1,5\lambda, \\
 H_0 = 2,25\lambda; & \quad \theta - L_0/\lambda = \infty, H_0/\lambda = \infty.
 \end{aligned}$$

The slot source is an antenna with a low order of directivity. To increase the directivity slot sources are combined into linear arrays [297] (multiple slot antennas). The system of slots changes the energy rate of feeding waveguide which substantially determines the power that is fed to the slot antenna and the nature of the amplitude-phase distribution of the field along the array.

The power radiated by a slot antenna depends on the dimensions of the slot, its location on the side of the waveguide, the shape and dimensions of the feeding waveguide, as well as the power and frequency of the excitation wave. The slot will radiate when it cuts across the surface current lines i.e. when it is located along the magnetic lines of force.

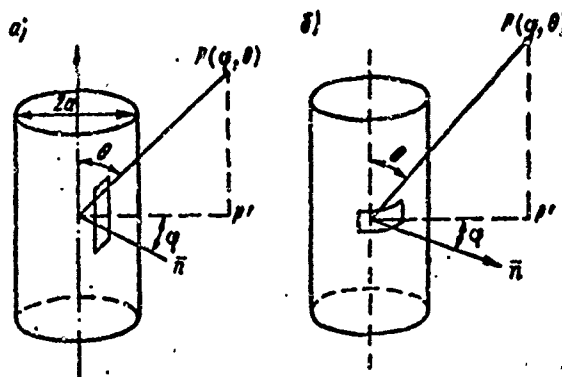


Fig. IV. 11. Slot incised in a cylinder: a - longitudinal; b. lateral.

Occasionally, when matching polarizations for structural or other considerations, it is necessary to cut out slot sources across the magnetic lines of force as well. In such case, use is made of stub type oscillators which produce a field distortion such that a longitudinal component of the magnetic field appears. Three types of slots are usually dealt with in the construction of slot antennas (Fig. IV. 12).

For a longitudinal slot on the broad side of a rectangular waveguide

$$g_1 = \frac{2a}{\pi^2 \beta b W_0} \cos^2 \left(\frac{\pi \beta}{2} \right) \sin^2 \left(\frac{\pi x_1}{a} \right);$$

$$g_2 = \frac{R_2}{2 (60\pi)^2}$$

in which g_1 is the unilateral internal radiation conductance of the slot; a, b are the dimensions of the wide and narrow sides of the waveguide; [298

$\beta = \sqrt{1 - (\lambda/\lambda_{cp})^2}$ is the retardation of the main wave;

$$W_0 = \sqrt{\mu/c} \quad 120\pi \text{ ohms}$$

$$\lambda_{cp} = 2a;$$

x_1 is the displacement of the slot relative to the axial line of the wide side of the waveguide; g_2 is the radiation conductance of the slot into outer space; R_2 is the radiation impedance of the dipole.

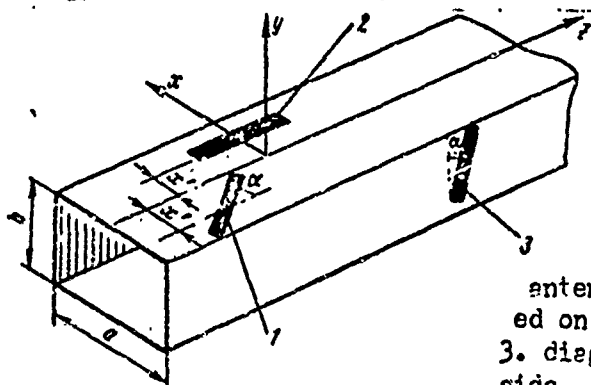


Fig. IV. 12. Types of slot antennas: 1 - diagonally positioned on broad side; 2. longitudinal; 3. diagonally positioned on narrow side.

The conductance referred to is equal to

$$g' = \frac{153}{R_z} \frac{a}{b\beta} \cos^2\left(\frac{\pi\beta}{2}\right) \sin^2\left(\frac{\pi x_1}{a}\right).$$

From this expression it is apparent that the longitudinal slot does not radiate on the axial line of the waveguide because the lateral component of the surface current is absent at that point.

Maximum conductance occurs at the slot that is cut out at the edge of the wall. When $x_1 = a/2$

$$g'_{\max} = \frac{153a}{b\beta R_z} \cos^2\left(\frac{\pi\beta}{2}\right).$$

The conductance of a diagonal slot on the narrow wall of a rectangular waveguide as referred to in the foregoing is computed in accordance with formula [2]

$$g' = \frac{9.6}{R_z} \frac{\lambda^4}{a^2 b \beta} \left[\frac{\sin \alpha \cos\left(\frac{\pi\beta}{2} \sin \alpha\right)}{1 - (\beta \sin \alpha)^2} \right]^2.$$

When the slot angle of inclination $\alpha < 30^\circ$ we can use the following approximation expression [299]

$$g' \approx \frac{153a}{bR_z} \left(\frac{\lambda}{2a}\right)^4 \beta \sin \alpha.$$

The diagonally biased slot on the broad side of the waveguide is excited by both longitudinal and lateral currents, and, therefore, it is most difficult to compute its conductance.

The input admittance of a diagonally biased slot (when the waveguide is matched with the slot even at resonant slot length) is complex in nature. However, after selecting appropriate values of x_1 and α we can obtain a phase displacement θ_1 such that the slot will be fully matched by the reactive element disposed in the central section of the slot. Diaphragms and rods are used as the reactive elements.

The case of a slot antenna in an infinite waveguide is realized in practice by disposing in the end of the waveguide an absorbing load for which the reflection factor in the operating band of frequencies is equal to zero. It is not desirable to use this kind of antenna because the slot will not radiate over 50% of the power supplied. To decrease losses a short circuiting piston is placed at the end of the waveguide instead of the absorbing load with the aid of which the nature of the incident and reflected waves changes in the desired direction.

In contrast to infinite and semi-infinite waveguides a slot antenna can be totally matched (coefficient of reflection is equal to zero, $k_{\rho} = 1$). Complete matching occurs when there is equality of piston and slot reactance (short-circuited stub) and the signs are opposite.

When the antenna slot is tuned this is achieved by placing the slot in the antinode area of the exciting surface current or in the magnetic field antinode; this, in turn, occurs when the following conditions are fulfilled:

for a longitudinal slot $l_1 = (2n + 1) \frac{\lambda_g}{4}$, $n = 0, 1, 2, \dots$;

for a lateral slot $l_1 = n \frac{\lambda_g}{2}$, $n = 0, 1, 2, \dots$.

in which l_1 is the length of the short-circuited portion of the waveguide; and λ is the length of the wave in the waveguide.

Loop Antenna

A loop or frame antenna is essentially a flat coil of arbitrary cross section circular, quadrangular and the like in form. As a rule, the leads in a loop antenna are much shorter than the length of the wave. The chief versions of loop antennas are shown in Fig. IV. 13. [300

The intensity of the electric field in a loop antenna in the plane perpendicular to the plane of the antenna can be computed from the formula [9]

$$E = 120\pi^2 \frac{InS}{r\lambda^2} \cos\varphi,$$

in which E is the voltage component of the field parallel to the plane of the antenna in volts/meter; I is the current in the frame in amperes; n is the number of coils; S is the area encompassed by the loop in m^2 ; r is the distance to the point of reception, meters; λ is the length of the wave in meters; φ is the angle with the plane of the frame.

If the dimensions of the frame are considerably less than the length of the wave and the current I is constant throughout the entire perimeter of the frame the radiation pattern will not be a function of the form of the cross section of the frame, and it will have the shape described in Fig. IV. 14. The radiation pattern of the frame repeats the radiation pattern of the half-wave dipole whose axis is perpendicular to the plane of the frame. The polarization of the frame is determined by its position.

If the frame antenna is receiving the signal the voltage on its terminals will be equal to

$$U(b) = \frac{2\pi}{\lambda} nSE \cos\varphi.$$

Reproduced from
best available copy.

The radiation impedance of a frame antenna is obtained from the formula

$$R_r(\omega) \approx 3 \cdot 10^3 \frac{n^2 S^2}{\lambda^3} = 197 \eta^2 \left(\frac{P}{\lambda}\right)^4, \quad (\text{IV. 40})$$

in which S is the area encompassed by the frame; P is the perimeter of the frame. [301

When $nL < 0.1\lambda$ the radiation impedance of a frame antenna is low and is measured in hundredths of an ohm, therefore, with the unavoidable losses in the antenna being present its efficiency is extremely low. For this

reason, loops are used only as receiving antennas. Increasing the frame perimeter provides greater gain than increasing the number of loops. The radiation pattern of a frame antenna in the plane of the loop is approximately circular in shape.

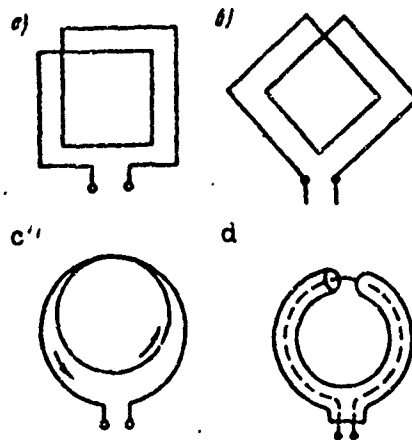


Fig. IV. 13. Versions of loop antennas: a. rectangular; b. rhombic; c. loop; d. shielded.

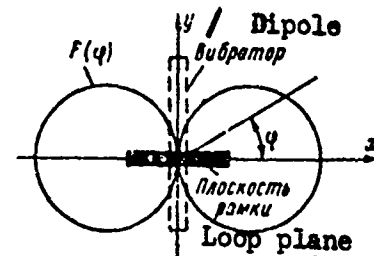


Fig. IV. 14. Radiation pattern of frame antenna: a. dipole; b. loop plane

Waveguide Radiator

The open end of a waveguide is known as a waveguide radiator. It is the simplest kind of antenna in the centimeter, millimeter and decimeter wave bands.

The waveguide radiator has weak directional properties, therefore in radar work it is used for illuminating reflector and lens antennas. The phase center of a waveguide radiator is approximately in the center of the radiating aperture.

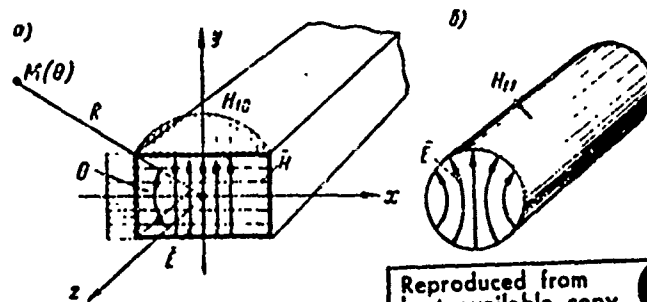


Fig. IV. 15. Open end waveguide radiators: a. rectangular; b. circular.

Most frequently used are radiators consisting of open ended rectangular waveguides with a basic H_{10} wave and a circular waveguide with H_{11} type wave (Fig. IV. 15). Waveguide sources of this kind create linearly polarized radiation.

A strict solution of the problem of radiation by an open end of a waveguide was accomplished in 1948 by L. A. Vaynshteyn [3]. However, such a solution is characterized by complexities. Therefore, in engineering practices this problem is resolved as an approximation on the basis of the Huygens-Kirchoff method. The essence of approximation consists in disregarding the higher type waves and surface currents on the exterior surfaces of the waveguide. Experience has shown that these approximations are within acceptable limits. [302

The intensity of field radiation at the open end of a rectangular waveguide at a distance D in the E and H planes, respectively, is determined by the formulas:

$$|E|_E \approx \frac{E_0 ab}{\pi \lambda D} \left| (1 - \Gamma_1) \left(1 + \frac{1 - \Gamma_1}{1 + \Gamma_1} \frac{\lambda}{\lambda_n} + \cos \theta \right) \frac{\sin \psi_E}{\psi_E} \right|;$$

$$|E|_H \approx \frac{E_0 ab}{\pi \lambda D} \left| (1 + \Gamma_1) \left(1 - \frac{1 - \Gamma_1}{1 + \Gamma_1} \frac{\lambda}{\lambda_n} + \cos \theta \right) \frac{\cos \psi_H}{1 - \left(\frac{2}{\pi} \psi_H \right)^2} \right|;$$

in which E_0 is the field amplitude in the center of the waveguide aperture; a and b are the dimensions of the waveguide aperture; λ_0 is the length of the wave in the waveguide; Γ_1 is the reflectance factor of the wave from the end of the waveguide; θ is the angle measured from the longitudinal axis of the waveguide;

$$\psi_E = \pi \frac{b}{\lambda} \sin \theta, \quad \psi_H = \pi \frac{a}{\lambda} \sin \theta.$$

The maximum coefficient of directivity of a rectangular waveguide is determined by the expression

$$G_{\max} \approx \frac{4\pi ab}{\lambda^2} \left[\frac{2}{\pi} \frac{\lambda_n}{\lambda} \left(1 + \frac{\lambda}{\lambda_n} \right) \right]^2. \quad (\text{IV. 41})$$

Ordinarily, on an operating wave $\lambda/\lambda_P \approx 0.71$, therefore

$$G_{\max} \approx 0.84 \frac{4\pi}{\lambda^2} ab. \quad (\text{IV. 42})$$

For a waveguide of standard dimensions $a = 0.72 \lambda$, $b = 0.32 \lambda$, and $G_{\max} = 2.4$.

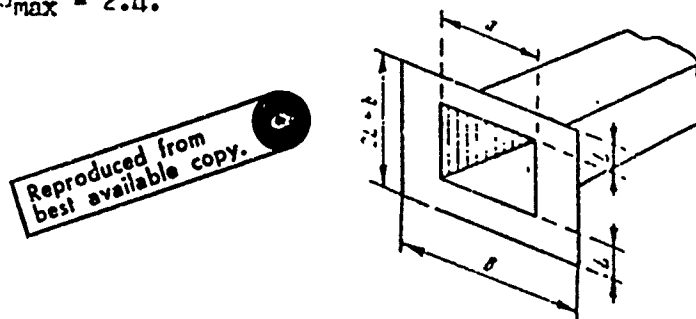


Fig. IV. 14. Open end of waveguide with E and H flanges

In order to change the form of the radiation pattern of the waveguide use is made of E and H plane flanges (Fig. IV. 16) and wedge-shaped sections with pins (Fig. IV. 17).

Increasing the electrical length of the flange L/λ results in lowering the level of the rear lobes and in changing the shape of the major lobe. For example, when $L = 0.25 \lambda$ the width of the major lobe is reduced by one-half compared with the pattern of a simple open ended waveguide; when $L = 0.75 \lambda$ the radiation pattern becomes bifurcated; and when $L \gg \lambda$ the major lobe expands considerably, acquiring a multi-lobed structure with small troughs [21].

The relationship of the width of the waveguide radiation pattern with a wedge-shaped section to shear angle is shown in Fig. IV. 18. [303]

The radiation field of a circular waveguide with a basic type H_{11} wave in the two principal E and H planes is determined according to these formulas:

$$|E|_E = \frac{E_0}{2\lambda D} \pi a^2 \left| \left(1 + \frac{1-\Gamma_1}{1+\Gamma_2} \frac{\lambda}{\lambda_n} \cos \theta \right) \Lambda_1(\psi) \right|;$$

$$|E|_H = \frac{E_0}{2\lambda D} \pi a^2 \left| \left(\frac{1-\Gamma_1}{1+\Gamma_2} \frac{\lambda}{\lambda_n} + \cos \theta \right) \frac{J_1(\psi)}{1 - \left(\frac{\psi}{\beta_{H_1}} \right)^2} \right|,$$

in which E_0 is the initial value of the field; Γ is the reflectance factor; a is the radius of the waveguide; λ is the length of the type H_{11} wave in the waveguide; θ is the angle measured from the longitudinal axis of the waveguide; $\Lambda_1(\psi)$ is the λ -function of the first degree; ψ is equal to $ka \sin \theta$, $\beta_{H_1} = 1.84$

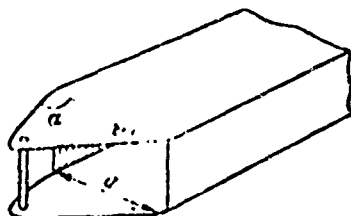


Fig. IV. 17. Wedge shaped waveguide radiates with pin.

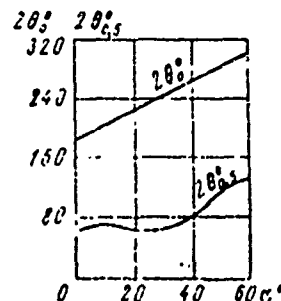


Fig. IV. 18. Relation of width of major lobe of wedge-shaped waveguide to shear angle.

The condition for excitation in a circular waveguide with radius a and wave type H_{11} will be:

Reproduced from best available copy.

$$0.588 < \frac{2a}{\lambda} < 0.766.$$

The width of the main lobe in the radiation pattern in a circular waveguide is determined from the formula

$$\theta_{0.5} \approx (50 + 75^\circ) \frac{\lambda}{2a}. \quad (\text{IV. 43})$$

The coefficient of directivity of a circular waveguide radiator upon matching the waveguide with external space can be computed from the formula

$$G_{\max} \approx 0,9\pi \frac{4\pi}{\lambda^2} a^2. \quad (\text{IV. 44})$$

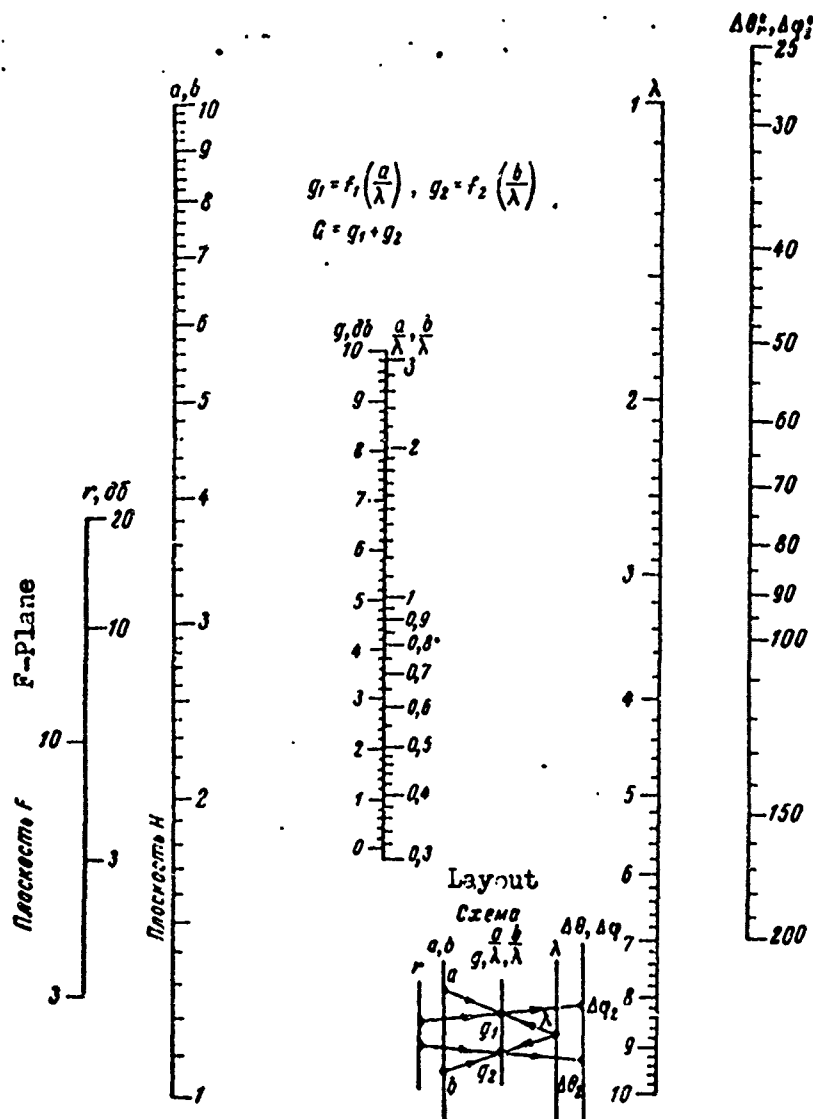


Fig. IV. 19. Nomogram for determining the principal parameters of a rectangular waveguide radiator

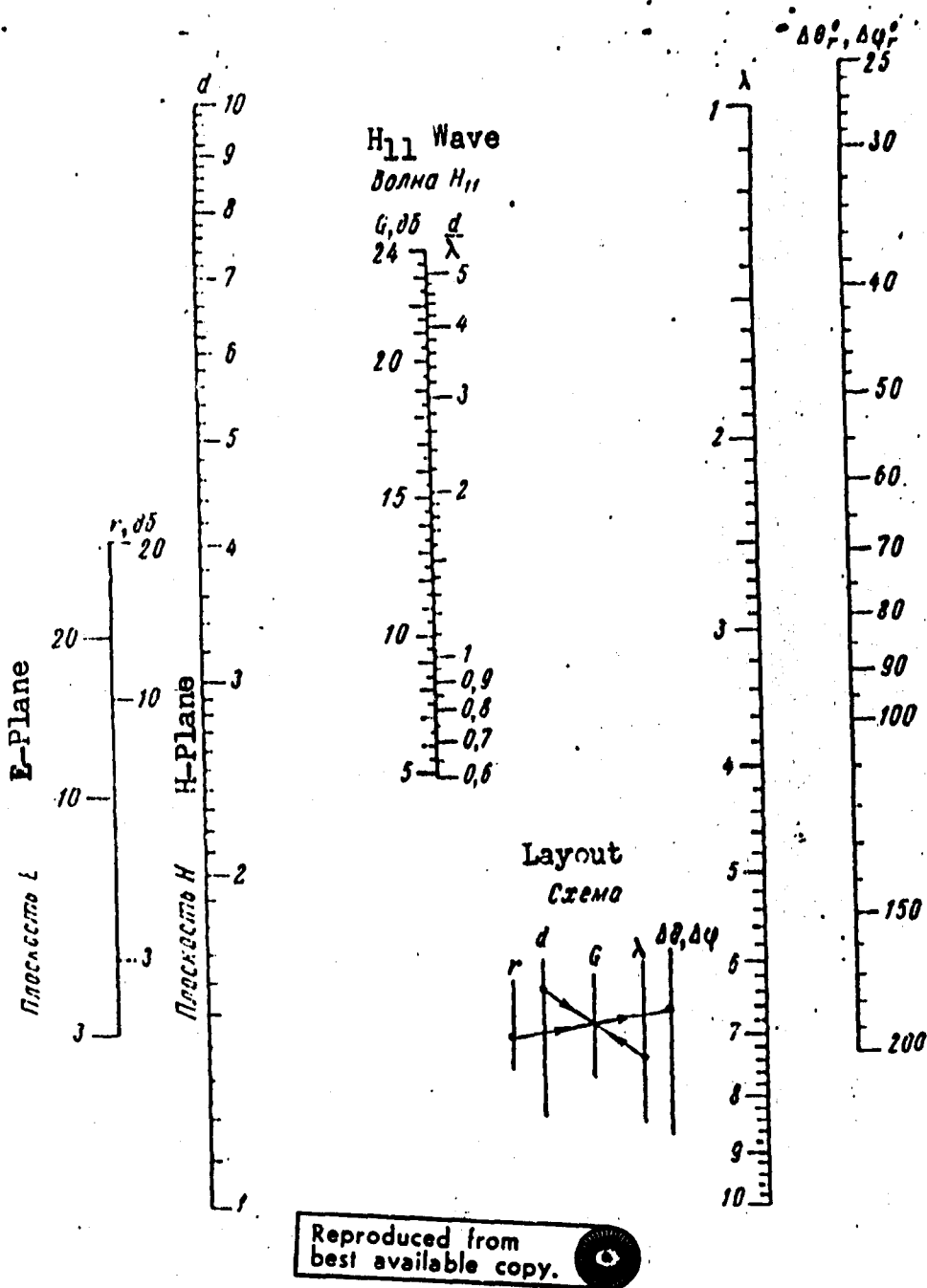


Fig. IV. 20. Nomogram for determining the principal parameters of a circular waveguide radiator.

The principal parameters of waveguide radiators (directivity factor and width of radiation pattern) are obtained from nomograms [16] described in Fig. IV. 19 and Fig. IV. 20.

The magnitude of the coefficient of directivity of a rectangular waveguide is determined by adding together the auxiliary parameters g_1 and g_2 which are obtained from the nomogram through the dimensions a and b and the length of the wave. The width of the radiation pattern of a rectangular waveguide in the E and H planes ($\Delta\theta_r, \Delta\phi_r$) is determined from the ratios a/λ and b/λ (Fig. IV. 19) and the level of the pattern r .

The initial data for determining the parameters of radiation of an open end circular waveguide (Fig. IV. 20) are the diameter d , the length of the wave λ , and the level of r in decibels.

5. Antennas as a System of Discrete Sources

Classification of Systems of Discrete Sources

The antenna as a system of discrete sources represents the sum of individual radiators or elements located in space and fed in a specific manner. Any concentrated group of antennas or sources can be used as such elements, especially half-wave dipoles, slots, open end waveguides, and the like.

Antennas as a system of discrete sources are used for the purpose of obtaining greater directivity and a higher level of radiated power than can be achieved with individual elementary antennas. The use in antenna-waveguide circuits of electrically controlled phase inverters, attenuators, and changeover switches in the form of ferrites and semiconductors opens up great opportunities for controlling the shape and position of the antenna radiation pattern in space.

The following are the most commonly used alternatives in the arrangement of discrete sources:

- linear arrangement along a straight line or in a circle;
- surface arrangement on a plane or on the surface of a cylinder, cone, or sphere;
- volumetric arrangement in a parallelepiped or cylinder.

The intervals between discrete sources in an antenna system can be the same or they may differ. In the first case the system is termed equidistant, and in the second -- non-equidistant.

Equidistant systems of discrete sources are also known or referred to as antenna arrays. Depending on the manner in which discrete sources are fed we differentiate between uniform and non-uniform systems, whether the current amplitudes in the sources are the same or different, and whether they are phased or non-phased, whether the phases of the feeding currents are equal or unequal.

In practice, one most often encounters equidistant systems with constant "bvertaking" $\left[\text{nbeg} \right]$ of phase (phase difference) between adjacent sources. For convenience in constructing a system of discrete sources they are made up of monotypical elementary antennas whose radiation patterns are the same. In such case, the radiation pattern of the system will be determined by the product $f(\varphi, \theta) = f_0(\varphi, \theta) f_{\text{syst}}(\varphi, \theta)$ in which $f_0(\varphi, \theta)$ is the radiation pattern of the elementary antenna; $f_{\text{syst}}(\varphi, \theta)$ is the multiplier in the system.

Reproduced from
best available copy.

Linear System of Discrete Sources

The resulting field of radiation in a system of discrete sources at a far point $M(D, \theta)$ (Fig. IV. 21) is obtained by taking the sum of the fields of all N sources.

For an equidistant linear system with interval d the radiation pattern is determined by the expression:

$$f(\theta) = f_0(\theta) \times \sum_{i=1}^N A_i e^{j\psi_i} e^{jkd(i-1)\cos\theta}, \quad (\text{IV. 45})$$

in which $A_i = I_i/I_1$ is a coefficient characterizing the relative value of the current of the i -th source; and Φ_i is the phase of that source.

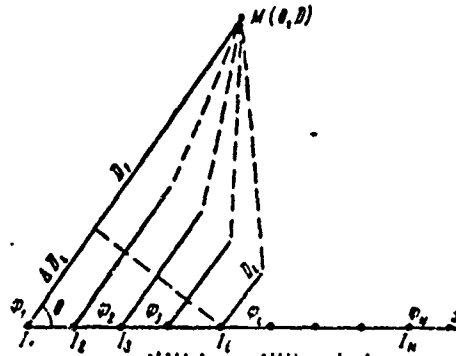


Fig. IV. 21. Linear system of discrete sources

In the case of a uniform and linearly non-phased system of sources $A_i = 1$, $\Phi_i = -(i-1)\Delta\Phi$ ($\Delta\Phi$ - the advance along a series of sources) the multiplier of the system will be

$$f_{\text{mult}}(\theta) = \left| \frac{\sin \left[\frac{N}{2} (kd \cos \theta - \Delta\Phi) \right]}{\sin \frac{1}{2} (kd \cos \theta - \Delta\Phi)} \right|. \quad (\text{IV. 46})$$

Denoting

$$\psi' = \frac{N}{2} kd \cos \theta - \frac{N}{2} \Delta\Phi = \psi - \psi_0$$

we will get

$$f_{\text{mult}}(\theta) = \left| \frac{\sin \psi'}{\sin \frac{\psi'}{N}} \right|. \quad (\text{IV. 47})$$

The maximum value of the function $f_{\text{mult}}(\theta)$ occurs when $\psi' = Nn\pi$ $= 0, \pm 1, \pm 2, \dots$; $f_{\text{mult}}(\theta)_{\text{max}} = N$, hence the fixed multiplier of the system is equal to

$$F_{\text{mult}}(\theta) = \frac{1}{N} \left| \frac{\sin \psi'}{\sin \frac{\psi'}{N}} \right|. \quad (\text{IV. 48})$$

The direction of the main lobe of the radiation pattern θ_{max} is determined by the following equality

$$\cos \theta_{\text{max}} = \frac{n\lambda}{d} + \frac{\Delta\Phi}{kd}, \quad (\text{IV. 49})$$

in which $n = 0, \pm 1, \pm 2, \dots$

Considering the multiplier of the system within the limits $0 \leq \theta \leq \pi$ it is necessary to take into account the condition

$$|\cos \theta_{\max}| \leq 1,$$

which can be fulfilled with several values of n . Hence, the radiation of the system can have several major lobes.

An unambiguous determination of the direction to the object is possible when the radiation pattern of the antenna has one major lobe. A condition for a single maximum of a main lobe is the inequality [1]

$$\frac{d}{\lambda} < \frac{1}{1 + |\cos \theta_{\max}|}. \quad (\text{IV. 50})$$

Specifically, for a phased antenna, when $\theta_{\max} = \lambda/2$, the condition for a single major lobe will be $d < \lambda$, and for an antenna with axial radiation (traveling wave) it will be $d \leq \lambda/2$ when $\theta_{\max} = 0$.

Given a large number of radiators ($N > 10$) and fulfilling the conditions for a single main lobe, the radiation pattern of a system of discrete sources is similar to the radiation pattern of an antenna with an uninterrupted distribution of sources of length $L = Nd$. Consequently, upon analyzing the radiation pattern of multielement antennas we can make use of relationships obtained for continuous antennas.

Occasionally, in certain special kinds of equipment (for example, radio-interferometers) it is necessary to utilize multi-beam radiation patterns. Such patterns are formed on discrete systems with interval $d > \lambda$. The number of main maximums in this case is determined by the inequality

$$2 \frac{d}{\lambda} - 1 \leq n_{\max} \leq \frac{2d}{\lambda} + 1.$$

Changing the position of the main lobe of the radiation pattern θ_m can be achieved by changing (deviating) the frequency of the signal at which a phase shift of $\Delta \varphi$ will occur at the source system. [309]

When evaluating the possibilities of the method of frequency deviation from the point of view of beam scanning in space, use is made of a special character -- the angular frequency sensitivity of the antenna. By angular frequency sensitivity of a system of discrete sources we mean changing the angle of inclination of the radiation pattern major lobe θ_m in degrees by the percent of change in the frequency of the oscillator f

$$\theta'_f = \frac{0.573}{\sin \theta_{\max}} \left(\frac{\Delta \varphi}{kd} + f \frac{d \left(\frac{\Delta \varphi}{kd} \right)}{df} - \cos \theta_{\max} \right). \quad (\text{IV. 51})$$

It follows from this that antennas with powerfully dispersing waves have the greatest angular frequency sensitivity, that is, those systems in which changes in the phase of the wave depends greatly upon the frequency.

The direction of zero radiation of a system of discrete sources, as well as the direction and level of the maximums of its side lobes are computed from the following formulas:

$$\cos \theta_0 = \frac{n\lambda}{Nd} - \frac{\Delta q}{kd}, \quad (\text{IV. 52})$$

in which $|n| = 1, 2, 3, \dots$; $|n| \neq mN$; $|m| = 0, 1, 2, \dots$

$$\cos \theta_{0, \max} \approx \left(n + \frac{1}{2}\right) \frac{\lambda}{Nd} + \frac{\Delta q}{kd};$$

$$F_{0, m} \approx \frac{1}{N \sin \left[\left(n + \frac{1}{2}\right) \frac{\pi}{n} \right]},$$

$$\text{with } |n| = 1, 2, 3, \dots; |n| \neq \begin{cases} mN \\ mN - 1 \end{cases}; |m| = 0, 1, 2, \dots$$

It is apparent that the number of side lobes increases with an increase in the electrical length of the system Nd/λ . The level of side lobes with similar amplitude is greater than the side lobe level of an antenna with irregular distribution. When $N \gg 10$ the levels of side lobes of continuous and discrete systems are practically the same.

Non-uniform systems of discrete sources have a lesser level of side lobes but a wider major lobe in the radiation pattern.

Most commonly used in practice are systems of discrete sources with an amplitude distribution sloping symmetrically toward the edges

$$A_i = \Delta + (1 - \Delta) \sin^p \left(\frac{i-1}{N-1} \pi \right),$$

in which Δ is the magnitude of the drop in the field on the edge of the system.

For such a distribution the coefficient of the system is determined as follows:

when $p = 1$

$$f_{\text{coef}}(\psi') = \left| \Delta \frac{\sin \psi'}{\sin \frac{\psi'}{N}} + \frac{1-\Delta}{2} \left\{ \frac{\sin \left(\psi' + \frac{N}{N-1} \frac{\pi}{2} \right)}{\sin \left[\frac{1}{N} \left(\psi' + \frac{N}{N-1} \frac{\pi}{2} \right) \right]} + \frac{\sin \left(\psi' - \frac{N}{N-1} \frac{\pi}{2} \right)}{\sin \left[\frac{1}{N} \left(\psi' - \frac{N}{N-1} \frac{\pi}{2} \right) \right]} \right\} \right|; \quad (\text{IV. 53})$$

when $p = 2$

$$f_{\text{coef}}(\psi') = \left| \frac{1+\Delta}{2} \frac{\sin \psi'}{\sin \frac{\psi'}{N}} + \frac{1-\Delta}{4} \left\{ \frac{\sin \left(\psi' + \frac{N}{N-1} \pi \right)}{\sin \left[\frac{1}{N} \left(\psi' + \frac{N}{N-1} \pi \right) \right]} + \frac{\sin \left(\psi' - \frac{N}{N-1} \pi \right)}{\sin \left[\frac{1}{N} \left(\psi' - \frac{N}{N-1} \pi \right) \right]} \right\} \right|. \quad (\text{IV. 54})$$

Spatial System of Discrete Sources

Spatial systems of discrete sources are used in the formation of narrow radiation patterns in the two principal planes.

If the combination of sources forms a spatial grid the main parameters of which are:

a_1, a_2, a_3 -- the intervals between the sources disposed, correspondingly, along the ox, oy and oz axes;

$\alpha_1, \alpha_2, \alpha_3$ -- "nabegi" [advances] of the phase along the linear systems on the ox, oy and oz axes;

q_1, q_2, q_3 -- the number of sources in the system along the $ox, oy,$ and oz directions;

λ -- the length of the wave;

$F_0(\varphi, \theta)$ -- the radiation pattern of the source, then the radiation pattern of the system is determined by formula

$$F_c(\varphi, \theta) = F_0(\varphi, \theta) F_1(\varphi, \theta) F_2(\varphi, \theta) F_3(\varphi, \theta),$$

in which

$$F_1(\varphi, \theta) = \frac{\sin \frac{q_1 \gamma_1}{2}}{\sin \frac{\gamma_1}{2}};$$

$$F_2(\varphi, \theta) = \frac{\sin \frac{q_2 \gamma_2}{2}}{\sin \frac{\gamma_2}{2}}; \quad F_3(\varphi, \theta) = \frac{\sin q_3 \frac{\gamma_3}{2}}{\sin \frac{\gamma_3}{2}};$$

$$\gamma_1 = -\frac{2\pi}{\lambda} a_1 \sin \varphi \cos \theta + \alpha_1;$$

$$\gamma_2 = \frac{2\pi}{\lambda} a_2 \sin \varphi \sin \theta + \alpha_2;$$

$$\gamma_3 = -\frac{2\pi}{\lambda} a_3 \cos \theta + \alpha_3.$$

Reproduced from
best available copy. 

Analysis of the formulas indicated will demonstrate that control over the directional properties of antennas in a system of discrete sources can be achieved by the following methods: phasing the sources; regulating the amplitude factors of the sources; changing the number of sources; selecting mutual disposition of sources; changing the operating frequency of the system. 311

"Wave Front" Type Antennas

Characteristics

"Wave front" type of antennas include the horn, reflector and lens varieties. Formed in the output openings (apertures) of these antennas is a field (the current is on the antenna surface) with a continuous distribution, or, as is commonly said, a "wave front" is created.

The parameters of this antenna include the following: field (current) amplitude distribution law in the radiating opening; field (current) phase distribution law in the aperture; length of wave or frequency of the field; dimension of the wave front; shape of the wave front.

The "wave front" type of antenna consists of the primary radiating element and the radiator which forms the antenna radiation pattern. Sources with poor directional characteristics serve as exciters for reflector and lens antennas. They include the open end of a waveguide, a dipole, a slot, and others. The reflector and radio lens, respectively, form the radiation pattern in these antennas. In the case of horn antennas the waveguide serves as the exciter, and the horn adapter is the shaping element.

The nature of the distribution of amplitudes and phases of the field on the wave front of the antenna is a function of the radiation pattern of the exciter, its position relative to the focal point of the shaping element, and the dimensions of the latter. /312

The chief advantage of "wave front" antennas is the simplicity of their design. However, such antennas have limited possibilities in changing the parameters of the "wave front" and, therefore, the shape and position of the antenna beam in space.

The radiation pattern of a "wave front" type of antenna is computed in conformity with the two principal planes -- horizontal and vertical or the E and H planes with respect to the field amplitude and phase distribution in the respective planes.

The volumetric radiation pattern of the antenna is equal to the product of the planar radiation patterns

$$F(\varphi, \theta) = F(\varphi) F(\theta).$$

The radiation pattern of $F(\varphi)$ is determined by the law of distribution of field amplitudes $A(x)$ and field phases $\phi(x)$, while the pattern for $F(\theta)$ is determined by the $A(z)$ and $\phi(z)$ laws of distribution.

Directional Properties of Linear Phased Antennas With Continuous Field (Current) Distribution

The radiation pattern of a continuous linear system $a/2, -a/2$ as a special case of a planar system (Fig. IV. 22) is determined by the integral

$$F(\theta) = \int_{-a/2}^{a/2} A(z) e^{j\phi(z)} e^{jkz \cos \theta} dz. \quad (\text{IV. 55})$$

or $F(\theta) = \int_{-a/2}^{a/2} A(z) e^{j\phi(z)} e^{jkz \cos \theta} dz$, for $\phi(z) = 0$ and its generalized radiation pattern becomes:

$$F(\nu) = \frac{1}{2} \int_{-1}^1 A(\xi) e^{j\nu\xi} d\xi. \quad (\text{IV. 56})$$

in which $v = \frac{\pi a}{\lambda} \cos \theta$ is the generalized angular coordinate; a is the length of the linear radiator; λ is the length of the wave; θ is the angle measured in the zoy plane from the Oz axis; and $\xi = 2z/a$ is the standardized linear coordinate.

The coefficient of directivity of the antenna can be computed from the formula

$$G = \frac{2\pi a}{\lambda} \frac{1}{\int_{-\pi a/\lambda}^{\pi a/\lambda} F^2(v) dv} \quad (\text{IV. 57})$$

If the utilization factor of an antenna surface equal to the ratio of the coefficient of directivity of a given antenna and an antenna with uniform amplitude and phase distribution is determined by the expression

$$\mu = \frac{\pi}{\int_{-\pi a/\lambda}^{\pi a/\lambda} F^2(v) dv} \quad (\text{IV. 58})$$

then $G = 2\mu \frac{a}{\lambda}$.

For specific laws of field distribution integration gives us the following expression / 1 /:

Uniform distribution, i.e. $A(\xi) = 1, |\xi| \leq 1$:

$$F(v) = \frac{\sin v}{v}; \quad \mu = 1 \quad G = 2 \frac{a}{\lambda}$$

The distribution $A(\xi) = \cos^n x - \frac{n\xi}{2}, |\xi| \leq 1$:
when n is an odd number

$$F(v) = \frac{n! \cos v}{\prod_{k=0}^{(n-1)/2} \left[(2k+1)^2 - \frac{4v^2}{n^2} \right]} \frac{2}{\pi};$$

$$\mu = \frac{4}{n^2} \left[\frac{2 \cdot 4 \cdot 6 \cdots (n-1)}{1 \cdot 3 \cdot 5 \cdots n} \right]^2 \left(\frac{2 \cdot 4 \cdot 6 \cdots (2n)}{1 \cdot 3 \cdot 5 \cdots n} \right);$$

when n is an even number

$$F(v) = \frac{n! \frac{\sin v}{v}}{\prod_{k=1}^{n/2} \left[(2k)^2 - \frac{4v^2}{n^2} \right]};$$

$$\mu = \left[\frac{1 \cdot 3 \cdot 5 \cdots (n-1)}{2 \cdot 4 \cdot 6 \cdots n} \right] \left[\frac{(n+2)(n+4) \cdots 2n}{(n+1)(n+3) \cdots (2n-1)} \right];$$

The distribution

$$A(\xi) = 1 - (1 - \Delta) \xi^2, \quad |\xi| \leq 1:$$

$$F(v) = \left[\frac{\sin v}{v} + (1 - \Delta) \frac{v^2}{v^3} \left(\frac{\sin v}{v} \right) \right];$$

$$\mu = \frac{(2 + \Delta)^2}{9 \left[1 - \frac{2}{3} (1 - \Delta) + \frac{1}{5} (1 - \Delta)^2 \right]}.$$

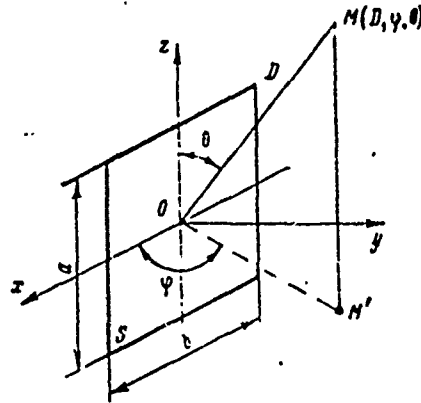


Fig. IV. 22. Rectangular wave front

Of practical importance are the so-called "optimal" antennas, i.e. antennas with a minimal side lobe level at a given magnitude of width of the major lobe. Optimal antennas require a field distribution at which infinitely great field surges occur on the rim of the aperture. It is apparent that such a distribution is not practically realizable. Antennas with distribution $A(\xi)$ which coincide with the optimum, but having undershoots of the field or current are referred to as "quasi-optimal."

The standard radiation pattern for quasi-optimal antennas is determined by the formula [18]

$$F(\nu) = \frac{\text{ch} \sqrt{\text{Arch}^2 r - \nu^2} - \cos \nu}{r - 1}, \quad (\text{IV. 59})$$

in which r is the side lobe level.

Amplitude distribution is in accordance with

$$A(\xi) = \frac{2}{\pi D(r-1)} \int_0^{\pi} \text{ch} \sqrt{\text{Arch}^2 r - \nu^2} - \cos \nu \cos \nu \xi \, d\nu. \quad (\text{IV. 60})$$

Corresponding to it are the relative drops of the field or current on the edges

$$\frac{A(\xi = 1)}{A(\xi = 0)} = \frac{\pi}{2} \frac{\text{Arch}^2 r}{\int_{-\pi}^{\pi} (\text{ch} \sqrt{\text{Arch}^2 r - \nu^2} - \cos \nu) \, d\nu}$$

Calculations [15] show that for a side lobe level of $r_1 = 20$ db and $r_2 = 40$ db, $\mu_1 = 0.95$ and $\mu_2 = 0.74$, while the differences in current on the aperture rim are equal, respectively, to 0.37 and 0.082.

The parameters of quasi-optimal antennas can be determined from the nomogram (Fig. IV. 23).

The formulas cited in #8 can be used for computing radiation patterns and determining the efficiency of a rectangular wave front.

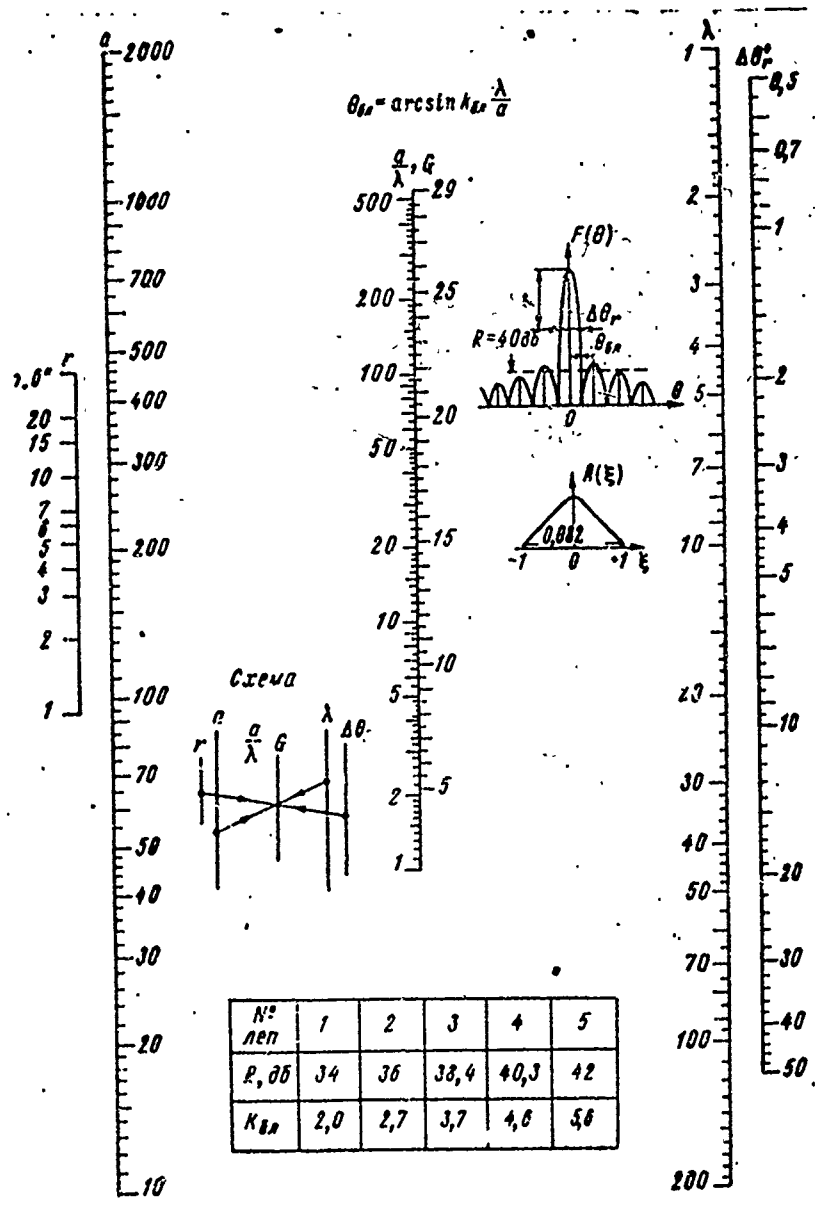


Fig. IV. 23. Nomogram for determining the parameters of "quasi-optimal" antennas

Phased Antennas With Circular Apertures

The radiation pattern of a circular, phased wave front with an amplitude distribution $A(\xi)$ along the radius $D/2$ is determined by the integral

$$F(v) = \int_0^1 A(\xi) J_0(v\xi) \xi d\xi. \quad (IV . 61)$$

in which $\xi = 2\rho/D$ is the standardized coordinate in the aperture; ρ is the polar coordinate in the aperture; $J_0(v\xi)$ is a zero order Bessel function; $v = \pi D/\lambda \sin \theta$ is the generalized spatial angular coordinate; and θ is the angle measured from the normal to the wave front. [316]

The coefficient of directivity of a circular wave front is equal to

$$G = \left(\frac{\pi D}{\lambda} \right)^2 \mu, \quad (\text{IV. 62})$$

in which

$$\mu = \frac{\left| \int_0^1 A(\xi) d\xi \right|^2}{\int_0^1 |A(\xi)|^2 d\xi}$$

For distributions $A_1(\xi) = 1$, $A_2(\xi) = 1 - \xi^2$ и $A_3(\xi) = (1 - \xi)^2$ the pattern, the surface utilization factor, and the coefficient of directivity are determined by the following formulas:

$$F_1(v) = \frac{J_1(v)}{v}, \quad \mu_1 = 1.0, \quad G_1 = \pi^2 \left(\frac{D}{\lambda} \right)^2;$$

$$F_2(v) = \frac{J_2(v)}{v^2}, \quad \mu_2 = 0.75, \quad G_2 = 7.4 \left(\frac{D}{\lambda} \right)^2;$$

$$F_3(v) = \frac{J_3(v)}{v^3}, \quad \mu_3 = 0.53, \quad G_3 = 5.53 \left(\frac{D}{\lambda} \right)^2,$$

in which $J_1(v)$, $J_2(v)$, and $J_3(v)$ are Bessel functions of the first, second, and third orders.

Effect of Phase Distribution on the Radiation Pattern of a Wave Front

The radiation pattern of a wave front with a field phase distribution $\Phi(\xi)$ is determined by an integral of the following form

$$F(v) = \frac{1}{2} \int_{-1}^1 A(\xi) e^{i(v\xi - \Phi(\xi))} d\xi. \quad (\text{IV. 63})$$

Analysis of this expression shows that phase distribution substantially affects the form of the radiation pattern and, therefore, the value of the antenna coefficient of directivity.

In general, phase distribution is a non-linear function which can be approximated by the following series: [317]

$$\Phi(z) = \beta_0 + \beta_1 z + \beta_2 z^2 + \beta_3 z^3 + \dots = \sum_{n=0}^{\infty} \beta_n z^n. \quad (\text{IV. 64})$$

As a rule, the specific value of members of the fourth order and higher orders is low, hence in practical computations only the first four terms are taken into account. The first term β_0 corresponds to a case of phase uniformity along the aperture. No change in the radiation pattern is produced. The second term characterizes the linear phase distribution. The magnitude β_1 expresses the maximum deviation of phase on the aperture edge.

in which $\xi = 2\rho/D$ is the standardized coordinate in the aperture; ρ is the polar coordinate in the aperture; $J_0(v\xi)$ is a zero order Bessel function; $v = \pi D/\lambda \sin \theta$ is the generalized spatial angular coordinate; and θ is the angle measured from the normal to the wave front. 316

The coefficient of directivity of a circular wave front is equal to

$$G = \left(\frac{\pi D}{\lambda}\right)^2 \mu, \quad (\text{IV. 62})$$

in which

$$\mu = \frac{\left| \int_0^1 A(\xi) d\xi \right|^2}{\int_0^1 |A(\xi)|^2 d\xi}.$$

For distributions $A_1(\xi) = 1$, $A_2(\xi) = 1 - \xi^2$ and $A_3(\xi) = (1 - \xi)^2$ the pattern, the surface utilization factor, and the coefficient of directivity are determined by the following formulas:

$$F_1(v) = \frac{J_1(v)}{v}, \quad \mu_1 = 1.0, \quad G_1 = \pi^2 \left(\frac{D}{\lambda}\right)^2;$$

$$F_2(v) = \frac{J_2(v)}{v^2}, \quad \mu_2 = 0.75, \quad G_2 = 7.4 \left(\frac{D}{\lambda}\right)^2;$$

$$F_3(v) = \frac{J_3(v)}{v^3}, \quad \mu_3 = 0.55, \quad G_3 = 5.53 \left(\frac{D}{\lambda}\right)^2,$$

in which $J_1(v)$, $J_2(v)$, and $J_3(v)$ are Bessel functions of the first, second, and third orders.

Effect of Phase Distribution on the Radiation Pattern of a Wave Front

The radiation pattern of a wave front with a field phase distribution $\Phi(\xi)$ is determined by an integral of the following form

$$F(v) = \frac{1}{2} \int_{-1}^1 A(\xi) e^{i(v\xi - \Phi(\xi))} d\xi. \quad (\text{IV. 63})$$

Analysis of this expression shows that phase distribution substantially affects the form of the radiation pattern and, therefore, the value of the antenna coefficient of directivity.

In general, phase distribution is a non-linear function which can be approximated by the following series: 317

$$\Phi(z) = \beta_0 + \beta_1 z + \beta_2 z^2 + \beta_3 z^3 + \dots = \sum_{n=0}^{\infty} \beta_n z^n. \quad (\text{IV. 64})$$

As a rule, the specific value of members of the fourth order and higher orders is low, hence in practical computations only the first four terms are taken into account. The first term β_0 corresponds to a case of phase uniformity along the aperture. No change in the radiation pattern is produced. The second term characterizes the linear phase distribution. The magnitude β_1 expresses the maximum deviation of phase on the aperture edge.

The radiation pattern of a wave front, given linear phase distribution, is determined by the integral

$$F(\theta) = \int_{-a/2}^{a/2} A(z) e^{i(kz \cos \theta - \beta_1 z)} dz,$$

solution of which, with $A(z) = 1$ gives the expression

$$F(\theta) = a \left| \frac{\sin \left[\frac{\pi a}{\lambda} \left(\cos \theta + \frac{\beta_1}{k} \right) \right]}{\frac{\pi a}{\lambda} \left(\cos \theta + \frac{\beta_1}{k} \right)} \right|. \quad (\text{IV. 65})$$

From formula (VII. 65) it is apparent that the direction of maximum radiation of the radiation pattern is oriented at an angle of $\theta_m = \arccos - \left(-\frac{\beta_1}{k} \right)$ to its aperture. The shape of the radiation pattern remains the same.

The third term in the formula (IV. 64) $\beta_2 z^2$ determines the magnitude of the quadratic phase error which appears either as a result of inaccuracy of performance (shifting of the exciter from the focal point along the axis of the reflector) or because of shortcomings in the very design of the antenna itself, for example, as in a horn antenna.

In a uniform amplitude distribution
$$F(\theta) = \int_{-a/2}^{a/2} e^{i(kz \cos \theta - \beta_1 z - \beta_2 z^2)} dz,$$

which, after applying the following substitution

$$t = \sqrt{\frac{2}{\pi}} \left(\frac{k \cos \theta}{2\beta_2} - z \right).$$

becomes

$$F(\theta) = \frac{1}{\beta_2} \sqrt{\frac{\pi}{2}} \left| \int_{t_1}^{t_2} e^{-i \frac{\pi}{2} t^2} dt \right|, \quad (\text{IV. 66})$$

in which

$$t_{1,2} = \sqrt{\frac{2}{\pi}} \frac{1}{\beta_2 a} \left(\frac{\pi a}{\lambda} \cos \theta \pm \frac{\beta_2 a^2}{2} \right).$$

The integral (IV. 66) is computed through the Fresnel integrals $C(t)$ and $S(t)$ by the formula 318

$$F(\theta) = \frac{1}{\beta_2} \sqrt{\frac{\pi}{2}} \left| \sqrt{[C(t_1) - C(t_2)]^2 + [S(t_1) - S(t_2)]^2} \right|.$$

The square error produces a symmetrical distortion in the radiation pattern.

It is apparent from computation that non-uniformity of the wave front weakens the effect of the square phase error. The generalized radiation patterns of the wave front with square phase error are shown in Fig. IV. 24.

The fourth member of the series (IV. 64) $\beta_3 z^3$ is called the cubic phase error. This phase error appears when there is a marked lateral shifting of the primary radiation elements in reflector and lens type antennas away from their focuses in a plane perpendicular to the focal axis. Here, the

deflection in the radiation pattern is accompanied by a distortion in the shape of the major lobe and by an increase in the side lobe level.

Formulas for the computation of the radiation pattern of a wave front with cubical phase distribution are given in [12].

The integral

$$F(\theta) = \int_{-a/2}^{a/2} A(z) e^{i(kz \cos \theta - \beta z^3)} dz$$

is computed in accordance with the following formulas:

$$\text{when } v < 2\beta - \sqrt[3]{3\beta}$$

$$F(\theta) = \frac{C_0 a \sqrt{\pi}}{2 \sqrt[3]{3\beta}} \left[U(t_1) + U(t_2) - \frac{\sqrt{\pi} \sqrt[3]{3\beta} \cos \frac{1}{2} (a\beta - ka \cos \theta + 2\beta)}{\left(\frac{a\beta}{2} - \frac{ka}{2} \cos \theta + 3\beta\right)^2 - \frac{\pi^2}{4}} \right];$$

$$\text{when } v > 3\beta + \sqrt[3]{3\beta}$$

$$F(\theta) = \frac{C_0 a}{2} \frac{\cos \frac{1}{2} (a\beta - ka \cos \theta + 2\beta)}{\left(\frac{a\beta}{2} - \frac{ka}{2} \cos \theta + 3\beta\right)^2 - \frac{\pi^2}{4}};$$

$$\text{when } 2\beta - \sqrt[3]{3\beta} < v < 3\beta + \sqrt[3]{3\beta}$$

$$F(\theta) = \sum_{l=1}^2 \sqrt{\frac{2\pi}{v-l}} \left\{ \left[C \left(\sqrt{\frac{2}{\pi}} (\beta - v_l + \frac{2}{3}) \sqrt{-l^3} \right) \sqrt{-l^3} - \right. \right. \\ \left. \left. - C \left(\sqrt{\frac{4}{3\pi}} \sqrt{-l^3} \right) \right] \cos \left(\frac{2}{3} \sqrt{-l^3} \right) + \left[S \left(\sqrt{\frac{4}{3\pi}} \sqrt{-l^3} \right) - \right. \right. \\ \left. \left. - S \left(\sqrt{\frac{2}{\pi}} (\beta - v_l + \frac{2}{3}) \sqrt{-l^3} \right) \right] \times \right. \\ \left. \times \sin \left(-\frac{2}{3} \sqrt{-l^3} \right) \right\} + \frac{1}{2l} \sin(\beta - v_l),$$

in which

$$A(z) = C_0 \cos \frac{\pi z}{a}; \quad v_{1,2} = \frac{1}{2} (ka \cos \theta + \beta a \pm \pi);$$

$\beta = \beta_0 \frac{a^3}{8}$, $U(t_l)$ is the Airy's integral whose magnitude is determined from tables for the argument $t_l = v_l / \sqrt[3]{3\beta}$. [320]

The relationship of the general radiation pattern to the magnitude of the cubic phase error with different amplitude distributions is shown in Fig. IV. 25.

In actual practice we often deal with complex amplitude-phase distributions which do not lend themselves to accurate approximations. In such circumstances computation of the integral (IV. 55) can be achieved by the numerical integration or "stationary phase" methods [4, 12].

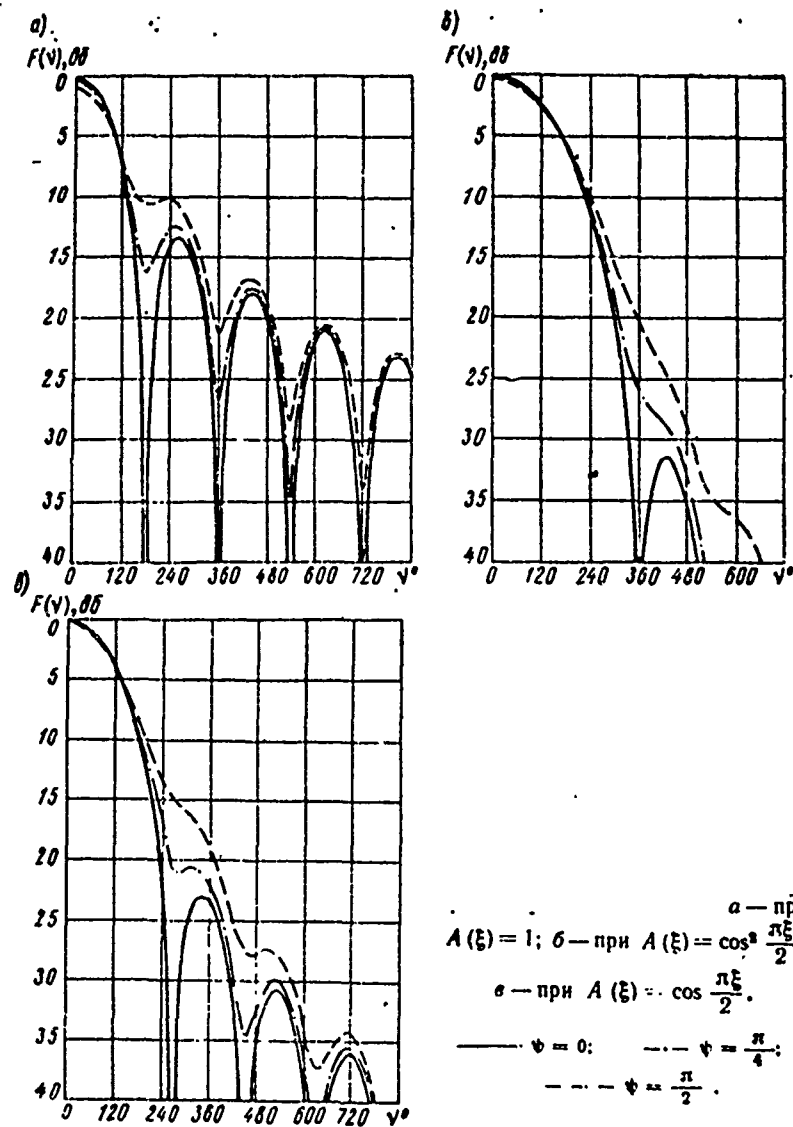


Fig. IV. 24. Radiation pattern of a wave front with square phase errors:

а — when $A(\xi) = 1$; б — when $A(\xi) = \cos^2 \frac{\pi\xi}{2}$;
 в — when $A(\xi) = \cos \frac{\pi\xi}{2}$.

In the first case the complex integral is the sum of two integrals to each of which is applied one of the formulas of numerical integration, as, for example, the Simpson formula

$$F(0) = \int_{-a/2}^{a/2} A(z) e^{ik\psi(z)} dz = \int_{-a/2}^{a/2} A(z) \cos k\psi(z) dz + j \int_{-a/2}^{a/2} A(z) \sin k\psi(z) dz = J_1 + jJ_2;$$

$$J_1 = \frac{a}{3n} (\eta_0 + 4\eta_1 + 2\eta_2 + 4\eta_3 + \dots + 4\eta_{n-1} + \eta_n);$$

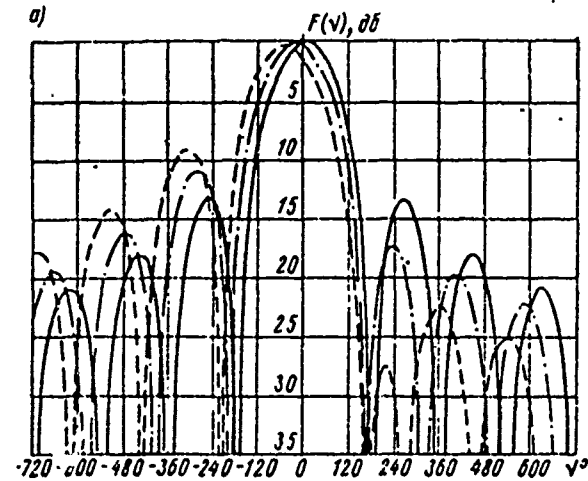
$$J_2 = \frac{a}{3n} (\xi_0 + 4\xi_1 + 2\xi_2 + \dots + 4\xi_{n-1} + \xi_n),$$

in which

$$k\psi(z_i) = kz_i \cos \theta + \Phi(z_i);$$

$$\eta_i = A(z_i) \cos k\psi(z_i); \quad \xi_i = A(z_i) \sin k\psi(z_i),$$

n is the number of segments of the interval $[-a/2, a/2]$.



[321

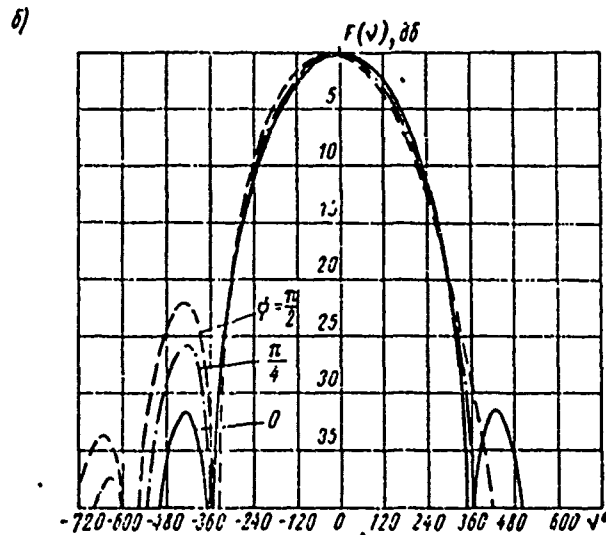


Fig. IV. 25. Radiation pattern of wavefront with cubic error;
a - when $A(\xi) = 1$; b - when $A(\xi) = \cos^2 \frac{\pi}{2} \xi$

The "stationary phase" method gives the following asymptotic expansion of the integral (IV. 55) $\sqrt{17}$: 322

$$\int_{-a/2}^{a/2} A(z) e^{ik\psi(z)} dz = \sqrt{\frac{2\pi}{k\psi''(c)}} e^{i\left[k\psi(c) + \frac{\pi}{4}\right]} \left\{ A(c) + \frac{1}{ik} \times \right. \\ \times \left[\frac{A(c)\psi^{IV}(c) + A'(c)\psi'''(c) + A''(c)\psi''(c)}{2[\psi''(c)]^2} \right] \left. + \right. \\ \left. + \frac{1}{ik} \left[\frac{A\left(\frac{a}{2}\right)}{\psi'\left(\frac{a}{2}\right)} e^{ik\psi\left(\frac{a}{2}\right)} - \frac{A\left(-\frac{a}{2}\right)}{\psi'\left(-\frac{a}{2}\right)} e^{-ik\psi\left(-\frac{a}{2}\right)} \right] \right\},$$

in which c is the value of a point of the stationary phase determined from the equation

$$\frac{d[k\psi(z)]}{dz} = 0.$$

Horn Antennas

The horn antenna is a waveguide equipped with a horn adapter in the form of a sector, pyramid or cone. The uniform change in the cross section of the horn virtually excludes the formation of higher type waves in the antenna.

We distinguish between the following kinds of horn antennas (Fig. IV. 26): sectoral (H plane and E plane) types formed by expanding the waveguide in one of the planes; pyramidal; conical; and biconical (one-sided and two-sided).

A uniform transformation of the waveguide field to free space occurs in the horns. Increasing the horn aperture a has the effect of narrowing the radiation pattern. Attempts to match the waveguide with free space and to decrease phase errors has the following effect: as the horn aperture is increased there is a corresponding increase in the length of its l value.

If an H_{10} type wave is excited in a waveguide feeding the horn, the phase error on the edges of the aperture whose angle does not exceed 60° is equal to:

for an H-plane horn

$$\Phi_m = \pi \frac{a^2}{4\lambda l};$$

for an E-plane horn

$$\Phi_m = \pi \frac{b^2}{4\lambda l}.$$

The amplitude and phase distribution for the H- and E-planes of horns, respectively, is: 323

along the a dimension

$$A(\xi) = \cos \frac{\pi\xi}{2}, \quad \Phi(\xi) = \Phi_m \xi^2, \quad \xi = \frac{2x}{a};$$

$$A(\xi) = \frac{\cos \pi\xi}{2}, \quad \Phi(\xi) = 0;$$

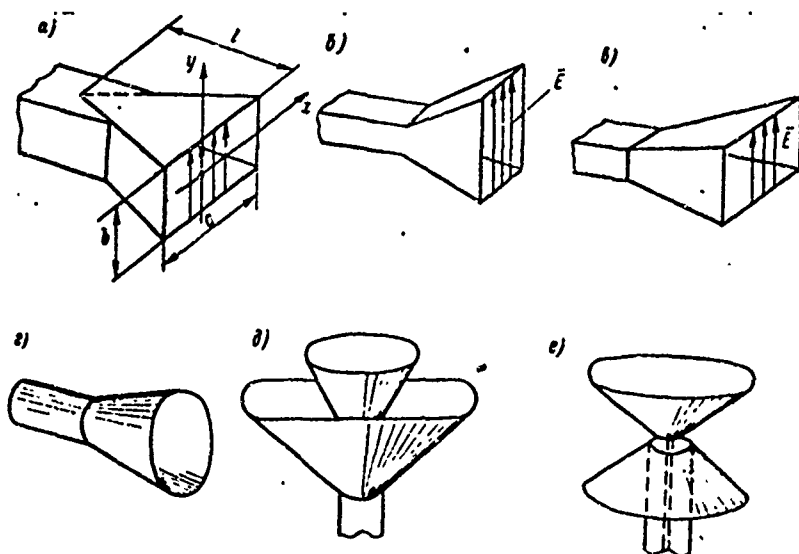


Fig. IV. 26. Horn antennas: a - H-plane; b - E'-plane; c - pyramidal; d - conical; e - one-sided biconical; f. two-sided biconical.

along the b dimension

$$A(\xi) = 1, \quad \Phi(\xi) = 0, \quad \xi = \frac{2y}{b};$$

$$A(\xi) = 1, \quad \Phi(\xi) = \Phi_m \xi^2.$$

The radiation pattern of sectoral horns is derived using the following formulas [16]

$$F(\theta) = \frac{\sin\left(\frac{\pi b}{\lambda} \sin \theta\right)}{\frac{\pi b}{\lambda} \sin \theta}; \quad (\text{IV. 67})$$

in the H plane

[324

$$F(\theta) = \left\{ [C(\alpha_1) + C(\alpha_2) - jS(\alpha_1) - jS(\alpha_2)] e^{j\frac{v}{4n}} + [C(\beta_1) + C(\beta_2) - jS(\beta_1) - jS(\beta_2)] e^{-j\frac{v}{4n}} \right\}; \quad (\text{IV. 68})$$

in which

$$v = \frac{\pi a}{\lambda} \sin \theta, \quad n = \Phi_m / \pi, \quad \Phi_m = \pi a^2 / 4l;$$

$$\alpha_1 = \sqrt{2n} - \frac{v_1}{\pi \sqrt{2n}}, \quad \alpha_2 = \sqrt{2n} + \frac{v_1}{\pi \sqrt{2n}}, \quad v_1 = v - \frac{\pi}{2};$$

$$\beta_1 = \sqrt{2n} - \frac{v_2}{\pi \sqrt{2n}}, \quad \beta_2 = \sqrt{2n} + \frac{v_2}{\pi \sqrt{2n}}, \quad v_2 = v + \frac{\pi}{2}.$$

For the E-plane horn:
in the H plane

$$F(\theta) = \frac{\cos\left(\pi \frac{a}{\lambda} \sin \theta\right)}{1 - \left(2 \frac{a}{\lambda} \sin \theta\right)^2}; \quad (\text{IV. 69})$$

in the E plane

$$F(\theta) = \{ [C(\gamma_1) + C(\gamma_2)] - j[S(\gamma_1) + S(\gamma_2)] \}, \quad (\text{IV. 70})$$

in which

$$\gamma_1 = \sqrt{2n} - \frac{u}{\pi\sqrt{2n}}, \quad \gamma_2 = \sqrt{2n} + \frac{u}{\pi\sqrt{2n}};$$

$$u = \frac{\pi b}{\lambda} \sin \theta, \quad n = \Phi_{\max}/\pi, \quad \Phi_{\max} = \pi b^2/4\lambda.$$

Formulas (IV. 68) and (IV. 70) make it possible to compute the radiation patterns of pyramidal and biconical horns. In the case of the latter they are applicable to the vertical plane [formula (IV. 68) in horizontal polarization and formula (IV. 70) in the vertical system of polarization]

The optimal construction dimensions of a horn (L - length of horn i.e. the distance from the peak of the horn to its aperture, and θ_0 , the horn aperture angle) are determined by the following expressions:

for the H-plane horn

$$L_H = \frac{a^2}{3\lambda} - \frac{3\lambda}{16}, \quad \frac{\theta_0}{2} = \arccos \frac{8L_H}{8L_H - 3\lambda}; \quad (\text{IV. 71})$$

for the E-plane horn

$$L_E = \frac{b^2}{2\lambda} - \frac{\lambda}{4}, \quad \frac{\theta_0}{2} = \arccos \frac{4L_E}{4L_E - \lambda}; \quad (\text{IV. 72})$$

for the conical horn

$$L = \frac{a^2}{2.4\lambda} - 0.15\lambda, \quad \frac{\theta_0}{2} = \arccos \frac{L}{L + 0.3\lambda}. \quad (\text{IV. 73})$$

The coefficient of directivity depends on the magnitude of the surface utilization factor of the wave front.

$$G = \frac{4\pi}{\lambda^2} ab\mu. \quad (\text{IV. 74})$$

For sectoral H- and E-plane horns the utilization factor is determined from the expressions:

$$\left. \begin{aligned} \mu_H &= \frac{\lambda l}{b^2} \{ [C(u) - C(v)]^2 + [S(u) - S(v)]^2 \}; \\ \mu_E &= \frac{16\lambda l}{\pi^2 a^2} \{ [C(w)]^2 + [S(w)]^2 \}, \end{aligned} \right\} \quad (\text{IV. 75})$$

in which

$$u = \frac{1}{\sqrt{2}} \left[\sqrt{\left(\frac{\lambda}{a}\right)^2 \frac{l}{\lambda}} + \sqrt{\left(\frac{a}{\lambda}\right)^2 \frac{\lambda}{l}} \right];$$

$$v = \frac{1}{\sqrt{2}} \left[\sqrt{\left(\frac{\lambda}{a}\right)^2 \frac{l}{\lambda}} - \sqrt{\left(\frac{a}{\lambda}\right)^2 \frac{\lambda}{l}} \right];$$

$$w = \sqrt{\left(\frac{b}{\lambda}\right)^2 \frac{\lambda}{2l}}.$$

For optimal E- and H- plane horns $b_{opt} = \sqrt{2\lambda l}$, $a_{opt} = \sqrt{3\lambda l}$, therefore, $\mu_E = 0.64$, and $\mu_H = 0.63$.

The surface utilization factor of a pyramidal horn antenna is found from the formula

$$\mu = \frac{2\lambda^2 L_E L_H}{a^2 b^2} \{ [C(u) - C(v)]^2 + [S(u) - S(v)]^2 \} \times \{ [C(w)]^2 + [S(w)]^2 \}, \quad (IV. 76)$$

in which L_E and L_H represent the length of the horn from its peak to the aperture in the E- and H-planes.

Fig. IV. 27 is a nomogram used for determining the coefficient of directivity of a pyramidal horn. The values G_H and G_E are found from the construction parameters and then from the formula

$$G = \frac{\pi}{32} G_H G_E \quad (IV. 77)$$

the required coefficient of directivity is obtained.

The diameter of an optimal conical horn is equal to

$$d = \sqrt{3\lambda l}, \quad (IV. 78)$$

and the coefficient of directivity corresponding to it is determined from the expression [19] [327]

$$G = (20 \lg \pi \frac{d}{\lambda} - 2.82). \quad (IV. 79)$$

The coefficient of directivity of biconical horns can be computed from the value of the coefficient of directivity of sectoral horns [16]. Thus, for a biconical horn with vertical polarization

$$G_{bmk}^v = G_E \frac{\pi \lambda}{16b}, \quad (IV. 80)$$

and for a beconical horn with horizontal polarization

$$G_{bmk}^h = G_H \frac{\lambda}{2\pi b}. \quad (IV. 81)$$

To improve the balancing conditions of the horn antenna and to improve the coefficient of directivity use is made of exponential or smooth transitions from the waveguide to the horn, phase-correcting lens inserts, lengthening and shortening the horn inserts, and replacing one long horn with a grid made up of short horn antennas.

Lens Antennas

The lens antenna consists of an exciter with poor directivity and a lens (Fig. IV. 28). The lens consists of a radio permittive body with one or two surfaces of a secondary order (quadric surfaces). Its principal dimensions are D and d . It is designed to convert the spherical or cylindrical waves of the exciter into the planar wave front of the antenna aperture which forms the narrow radiation pattern. Such a transformation of the radio wave in the lens is possible when its index of refraction $n \neq 1$,

or when $n = 1$ due to the difference in beam travel.

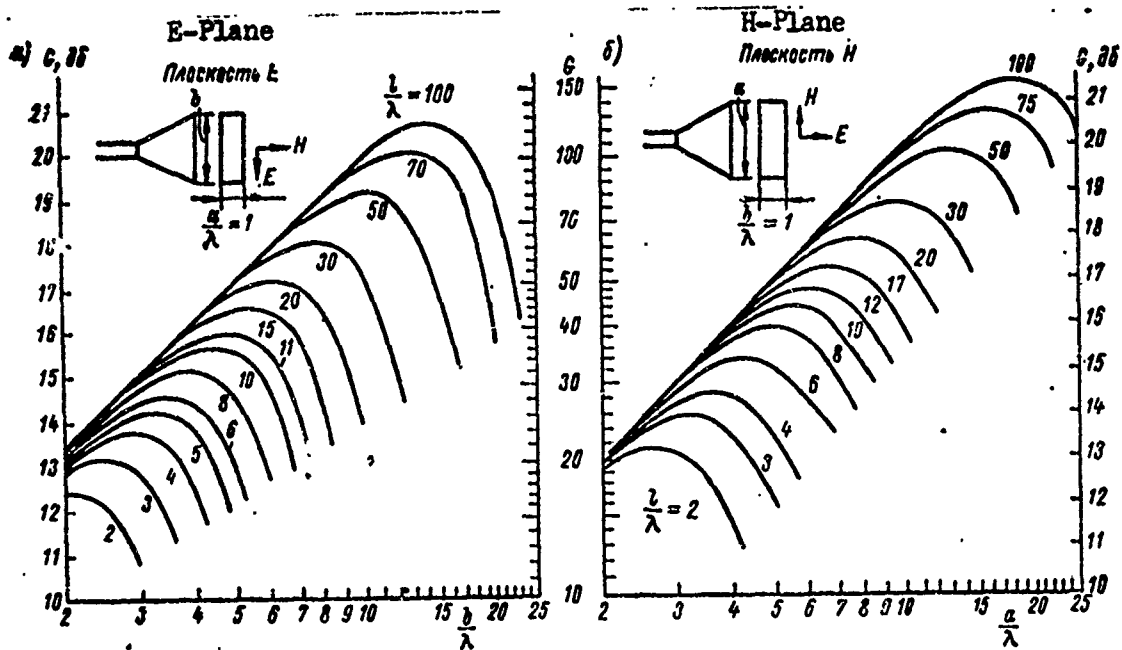


Fig. IV. 27. Nomogram for determining the coefficient of directivity of a pyramidal horn. 326

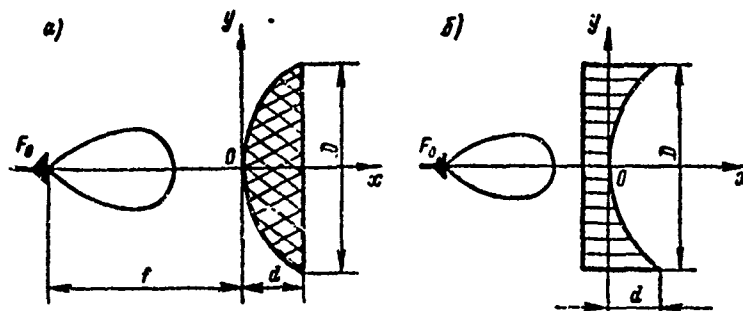


Fig. IV. 28. Lens antennas: a - retarding type; b - accelerating type.

Lens antennas are classed according to the method by which they perform their basic function. One differentiates between the following kinds of lenses: delaying ($v_{\phi} < c$); accelerating ($v_{\phi} > c$); and lenses which delay owing to changes in the difference of beam travel ($v_{\phi} = c$). 328

From the structural standpoint lenses may be dielectrical, metal-dielectric, metal-elastic, and metal-air.

The cross section of a delaying lens is a hyperbola described by the equation

$$x^2(n^2 - 1) + 2fx(n - 1) - y^2 = 0, \quad (\text{IV. 82})$$

in which $n = c/v = \sqrt{\epsilon'} > 1$; ϵ' is the relative dielectric permeance of the lens material.

The cross section of accelerating lenses is described by the equation for an ellipse

$$x^2(1-n) + 2fx(1-n) + y^2 = 0, \quad (\text{IV. 83})$$

in which $n = c/v = \sqrt{1 - (f/2a)^2} < 1$; a is the distance between the parallel plates of the lens ($a > 0.5\lambda$); and f is the focal distance of the lens.

The relationship between the dimensions of the plano-convex lens of the antenna, D , F , d , and the coefficient n is established by the following expression:

$$\frac{d}{D} = \sqrt{\frac{f^2}{(n+1)^2 D^2} + \frac{1}{4(n^2-1)}} - \frac{f}{D(n+1)}. \quad (\text{IV. 84})$$

It is apparent, therefore, that the thickness of the lens decreases as f increases and the focal distance f increases. Consequently, the weight of the lens can be decreased by lowering the efficiency and increasing antenna dimensions. In designing antennas with retarding lenses D is usually taken as equal to f and $n = 1.5 - 1.7$, and the thickness of the lens $d = (0.15 - 0.20) D$.

To decrease the weight of the antenna the lens is zoned (Fig. IV. 29). The idea behind zoning is to exclude those areas of the lens body within whose limits the field phases change by a whole number of 2π radians. In contrast to the non-zoned delaying lens, the zoned lenses have a narrower frequency band.

Delaying lenses are made of dielectrics with $\epsilon' = 2-3$; have low loss, and possess high mechanical strength and thermostability. Satisfying these requirements are materials like polystyrene ($\epsilon' = 2.3 - 2.6$, $\text{tg}\delta = 10^{-4} - 10^{-3}$), polytetrafluoroethylene-4 ($\epsilon' = 2.0$, $\text{tg}\delta = 10^{-4}$) and artificial dielectrics (metal-dielectrics). Metal dielectrics consist of metallic elements (balls, plates, discs) disposed in a definite way in the body of the dielectric lens [7].

The refractive index of a metal-dielectric can be computed from the formula

$$n = \sqrt{\epsilon_1 \mu_1} \sqrt{\left(1 + \frac{N\alpha}{\epsilon_1}\right) \left(1 + \frac{N\chi}{\mu_1}\right)}, \quad (\text{IV. 85})$$

in which ϵ_1, μ_1 are the dielectric and magnetic penetrances of the medium in which the metallic elements are suspended; α and χ are the electrical and magnetic susceptibilities of the elements; N is the number of elements per unit volume of the lens.

The parameters α and χ depend on the form and dimension of the elements.

The relationship between the dimensions of the plano-concave accelerating lens D , f , and d and its index of refraction n is determined by the equation [19]

$$\frac{d}{D} = \frac{f}{D(1+n)} - \sqrt{\frac{f^2}{(1+n)^2 D^2} - \frac{1}{4(1-n^2)}}. \quad (\text{IV. 86})$$

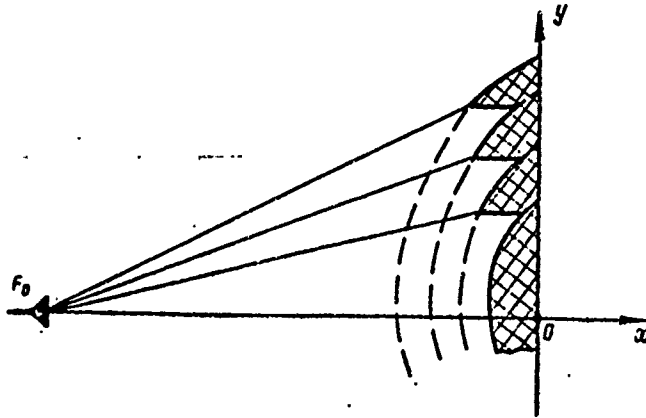


Fig. IV. 29. Zoned retarding lens

The radicand in formula (IV. 86) has real value in the condition

$$\frac{l}{D} > \sqrt{\frac{1+n}{1-n}},$$

therefore the focal distance of the accelerating lens should be $f \gg 0.5D$.

The metal-air lens antenna consists of a system of two metallic plates between which TEM or TE_1 type wave are propagated. The medium inside the antenna is uniform. To increase the electrical strength the interior space is sometimes filled with a high quality dielectric.

The optical paths are balanced to obtain a phased wave front in a metal-air lens by equalizing the geometric paths from the radiator to the different points of the aperture. Structurally, this is achieved by curving the metallic surfaces of the antenna. Shown in Fig. IV. 30a is an antenna with a "humped" lens. The height of the hump in the center portion is greatest, decreasing to zero on the edges.

Because of the large dimensions of the plates the metal-air lens can be considered a flat waveguide in which TEM (Fig. IV. 30 b), TH , and TE (Fig. IV. 30, b) waves can be generated. For TEM waves the critical wave is equal to infinity, hence such lenses have good broadband characteristics.

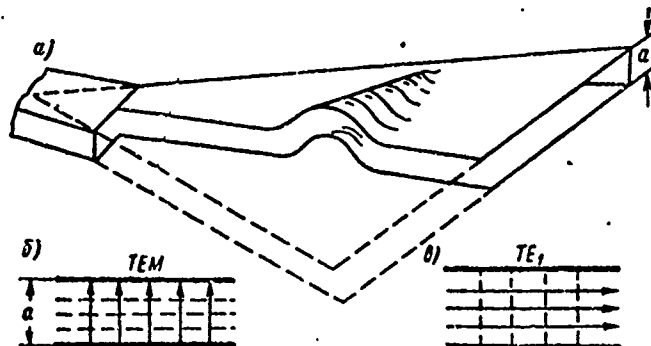


Fig. IV. 30. Metal-air lens: a - general view of antenna; b - structure of TEM wave field; c - structure of TE_1 field.

To suppress higher type waves the distance between the plates is selected from the condition

$$a < \frac{\lambda_0}{2\sqrt{\epsilon_1}}, \quad (\text{IV. 87})$$

in which ϵ_1 is the relative dielectric penetrance of the medium that fills the interior space of the lens.

When the TE_1 is excited the critical wave is finite $\lambda_{\text{KP}} = 2a$ and the index of refraction will be equal to

$$n = \sqrt{\epsilon' - \left(\frac{\lambda_0}{2a}\right)^2}. \quad (\text{IV. 88})$$

The distance between the plates for this kind of wave should be selected from the condition

$$\frac{\lambda_0}{2\sqrt{\epsilon'}} < a < \frac{\lambda_0}{\sqrt{\epsilon'}}. \quad (\text{IV. 89})$$

From expression (IV. 88) it is apparent that the metal-air lens with TE_1 wave has dispersive properties and, therefore, it has a lesser frequency band. However, a lens of this type is capable of transmitting a great amount of power; its metallic surfaces can be secured together by means of metallic rods because they are perpendicular to the E vector.

Metallic surfaces in the form of conic sections, circular cylinders, condensers, and the like may be used in the construction of metal-air lenses.

In many instances it is convenient to have a lens with flat surfaces of refraction (Fig. IV. 31); the focusing is done by changing the index of refraction from the center of the lens to the periphery. If the index of refraction decreases from the center toward the edges a phased wave front will form at the lens output.

The index of refraction can be a function of the distance r from the exciter to the lens

$$n(r) = \frac{n_0}{1 + \left(\frac{r}{d}\right)^2} \quad (\text{IV. 90})$$

or a function of the distance x from the focal axis [10]

$$n(x) = \frac{n_0}{\cosh \frac{\pi x}{2d}}, \quad (\text{IV. 91})$$

in which n_0 is the index of refraction in the center of the lens.

A variable coefficient of refraction can readily be made in metal-plastic and metal-dielectric lenses.

The discontinuous Luneberg / 23 / lens presents a special interest in connection with the resolution of the problem of undistorted, circular scanning. This lens is shaped like a cylinder or sphere whose index of refraction is a function of the radial coordinate ρ

$$n(\rho) = \sqrt{2 - \left(\frac{\rho}{R}\right)^2}, \quad (\text{IV. 92})$$

in which R is the radius of the lens.

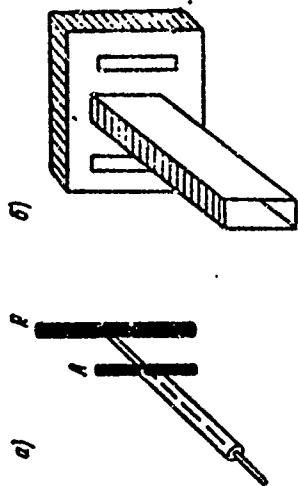


Fig. 33. Exciters: a - dipole; b. dual slot.

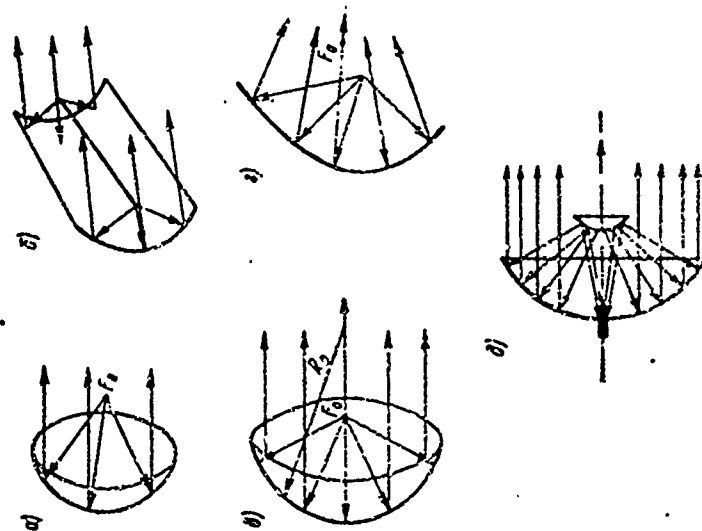


Fig. IV. 32. Types of reflector antennas: a. Paraboloid of rotation; b. parabolic cylinder; c. spherical reflector; d. special shape reflector; e. dual reflector system.

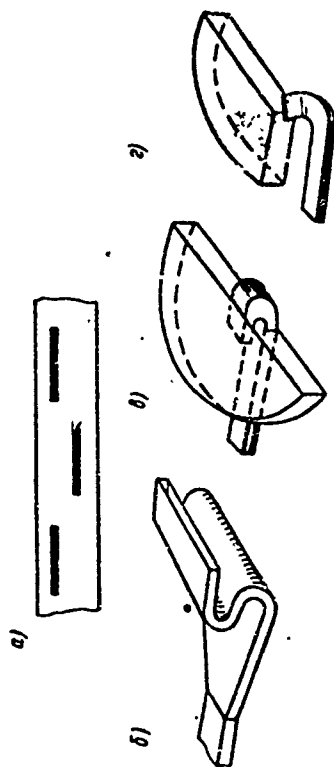


Fig. IV. 34. Parabolic cylinder exciters: a. waveguide-slot; b. horn-lens; c. segment; d. half-segment paraboloid.

332

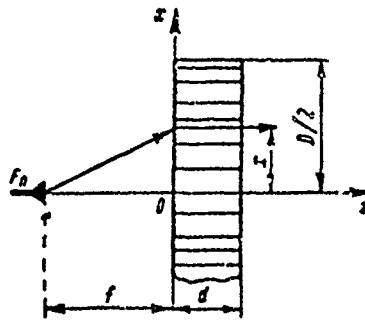


Fig. IV. 31. Metal-plastic lens with variable index of refraction

Reflector Antennas

Reflector antennas are deemed the best UHF antennas insofar as radio engineering characteristics are concerned, and for that reason they are used in most shipborne radar units. The basic elements of these antennas are the mirror or reflector, and the exciter, a low directivity type antenna.

The most common reflector type antennas include the following (Fig. IV 32): parabolic (paraboloid of rotation and parabolic cylinder); spherical and sphero-parabolic; special profile (to form cosecant radiation patterns); and multiple reflector

[333

Spherical or cylindrical waves from the exciter are converted to plane waves in the reflector antenna. The reflector, which is in the form of a paraboloid of rotation or a sphere, is used to produce a needle-shaped radiation pattern, and the parabolic cylinder is used to create a fan-shaped radiation pattern. The latter can be formed, also, by a truncated paraboloid of rotation.

The following may serve as the primary radiating element in a parabolic or spherical reflector: dipole with counter-reflector (Fig. IV. 33a), a double slot source (Fig. IV. 33,b), the open end of a waveguide and a horn.

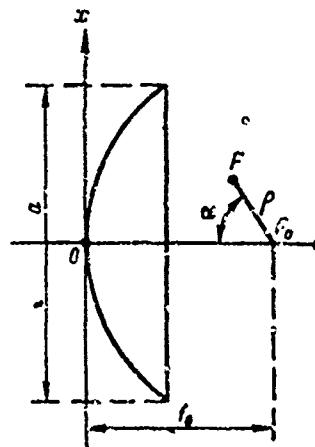


Fig. IV. 35. Reflector antenna at other than the focal point.

The following linear radiators are used as reflectors in the form of a parabolic cylinder: waveguide-slot, horn-lens, segmented and semi-segmented paraboloid (Fig. IV. 34).

In engineering practice approximation methods are used for computing the field of radiation of reflector antennas. These include the method of surface currents and the aperture method. The first makes it possible to solve the radiation problem somewhat more accurately, but the most common is the aperture method because of the simpler mathematics involved.

The radiation patterns of a reflector antenna in the two principal planes are determined from formulas cited above in the discussion on the linear phased antenna with uniform field distribution through appropriate amplitude-phase distribution. The latter is computed by the known aperture a , the focal distance f_0 , the radiation pattern of the exciter, and its position relative to the reflector focus.

Generally, when the exciter is moved away from the focal point F_0 to a point with the coordinates p, a (Fig. IV. 35), the distribution functions of field amplitudes and phases in the aperture are determined by formulas [5] as follows: [334]

$$A(x) = \frac{\sqrt{A_0(x)}}{\rho}; \quad (\text{IV. 93})$$

$$\rho = \sqrt{(Mu - N \sin \alpha)^2 + \left[1 - \left(\frac{Mu}{2}\right)^2 - N \cos \alpha\right]^2}; \quad (\text{IV. 94})$$

$$\Phi(x) = \frac{\pi a}{M\lambda} \frac{N \left\{ Mu \sin \alpha + \left[1 - \left(\frac{Mu}{2}\right)^2\right] \cos \alpha \right\} - \frac{N^2}{2}}{1 + \left(\frac{Mu}{2}\right)^2},$$

in which $A_0(x)$ is the amplitude distribution with the exciter located at the focal point of the reflector;

$$u = \frac{2x}{a}; \quad N = \frac{p}{f_0}; \quad M = \frac{a}{2f_0}.$$

The coefficient of directivity of a reflector antenna is determined by the expression

$$G = \frac{4\pi S}{\lambda^2} \mu_1 \mu_2 \mu_3, \quad (\text{IV. 95})$$

in which S is the reflector aperture area; μ_1 is the multiplier which takes into account the discontinuity of the wave front and the fact that it is out of phase

Reproduced from
best available copy.

$$\mu_1 = \frac{\left| \int_S A(S) e^{j\Phi(S)} dS \right|^2}{S \int_S A^2(S) dS};$$

μ_2 is a multiplier which takes into account the "spillage" of exciter energy beyond the edges of the reflector,

$$\mu_2 = \frac{\int_{4\pi} F_0^2(\gamma, \theta) \sin \theta d\theta d\varphi}{\int_{4\pi} F_0^2(\gamma, \theta) \sin \theta d\theta d\varphi};$$

Ω is the solid angle bounded by the periphery of the reflector; $F_0(\varphi, \theta)$ is the radiation pattern of the exciter; μ_3 is a factor which takes into account the shielding effect of the reflector aperture by the exciter

$$\mu_3 = \frac{\int_S A^2(S) dS - \int_{S_{\text{shd}}} A^2(S) dS}{\int_S A^2(S) dS};$$

S_{shd} is the shielding area of the exciter.

To eliminate the undesirable phenomenon of "spillage" of energy outside the edges of the reflector it is advisable to increase the aperture of the latter, decrease the focal distance, or utilize an exciter with greater directivity. The latter method of increasing the coefficient μ_3 results in increasing the dimensions of the exciter (S_{shd}). This brings about greater shielding of the reflector aperture, reducing the value μ_3 and intensifying the reaction of the reflector on the exciter, as a result of which the conditions for matching the antenna and the oscillator in the set are less favorable. [335

Reflector reaction on the exciter can be eliminated by several technical procedures. The most common of these are the following: compensation for reflection by means of quarter wave plates; utilizing non-symmetrical reflectors; use of cross polarization.

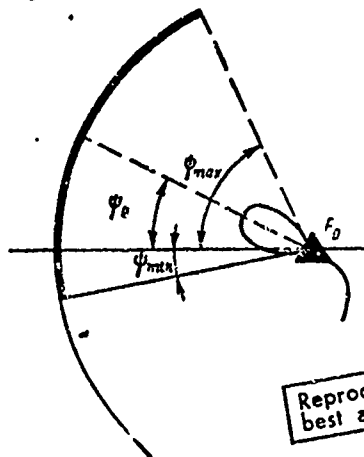


Fig. IV. 36. Antenna with non-symmetrical reflector

The compensating plate is inserted at the vertex of the reflector on its illuminated side. The thickness of the plate should be a multiple of an odd number of quarter waves. The diameter d and the thickness of the plate t , taking into account the parabolic form of the reflector, should be equal to

$$d = 2 \sqrt{\frac{f_0 \lambda}{\pi}}, \quad t = \frac{\lambda}{4} (2n + 1) - \frac{\lambda}{4\pi}, \quad (\text{IV. 96})$$

in which f_0 is the focal distance; λ is the length of the wave; and $n = 0, 1, 2, 3, \dots$

If we use for the reflector a portion of a parabolic reflector lying above the focal axis (Fig. IV. 36) and the exciter at the focal point F_0 so placed that the maximum lobe of its radiation pattern be oriented approximately toward the center of the non-symmetrical reflector, the reflected signal will be propagated, by-passing the exciter. The reflector angles should be approximately equal to $\Psi_{\min} \approx 2-10^\circ$, $\Psi_0 \approx 0.5\Psi_{\max}$.

The antenna with cross polarization should have a second semi-transparent reflector or a semi-transparent shield Ξ (Fig. IV. 37). The shield is a dielectric disc with built-in parallel conductors. The linearly polarized wave of the exciter \vec{E}_0 is totally reflected from the shield, striking the reflector \mathfrak{Z} with the dielectric layer deposited upon it 0.25λ in thickness. This layer is also reinforced with an application of conducting material. Due to the difference in amount of travel of the reflected waves E_{\parallel} and E_{\perp} the reflected signal \vec{E}'_{OTP} will be horizontally polarized. Under these conditions the energy will pass freely through the shield Ξ . The distance between the conductors of the reflector and the shield is selected from the condition

$$\Delta \leq \frac{\lambda}{8}. \quad (\text{IV. 97})$$

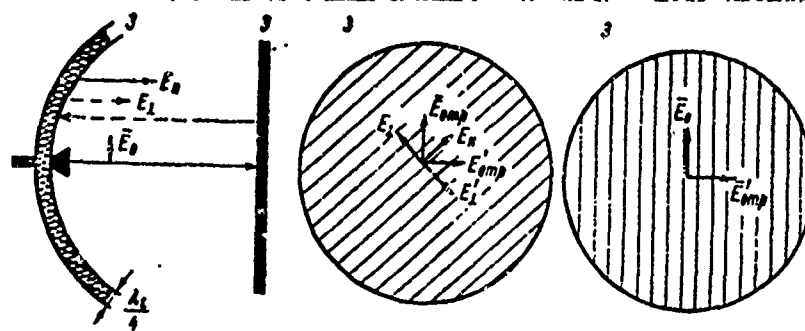


Fig. IV. 37. Antenna with cross polarization.

To lighten the construction, decrease the weight, and lessen the sail effect antenna reflectors are made in the form of metallic grids and arrays; they are also made in perforated form. The distance between grid elements or the diameters of the holes of a perforated reflector should be such that the portion of the energy passing through the reflector should not exceed 1%.

For arrays consisting of parallel rods the leakage factor τ (ratio of leakage power to incident power) is equal [2] to

$$\tau = \frac{1}{1 + \left(\frac{\lambda}{2\Delta \ln \frac{d}{\Delta} \pi} \right)^2}, \quad (\text{IV. 98})$$

in which λ is the wave length; Δ is the distance between their centers; and d is the diameter of the rods in the array.

For example, in the case of an array with $\Delta/\lambda = 0.04$ and $\Delta/d = 10$, the factor $\tau \approx 8 \cdot 10^{-3}$.

7. Beam Scanning in "Wave Front" Antennas

Characteristics of Scanning Devices

Electrical and mechanical devices are used to scan beams in a certain sector α_s in reflector and lens antennas. These devices can periodically shift the exciter in a certain trajectory that passes through the antenna focus.

The major lobe is deflected in a direction opposite that taken by the exciter F_1 (Fig. IV. 38). When the deflections are small $\alpha_s \approx \alpha$. In the case of vertical antennas when the exciter is shifted away from the focal point in a plane perpendicular to the focal axis by the amount p a non-phased wave front is formed in the aperture

$$\Phi(x) = -\frac{k_p}{l_0} x + \Delta(x). \quad (\text{IV. 99})$$

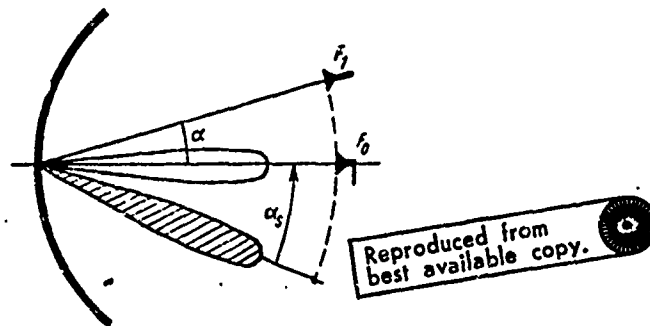


Fig. IV. 38. Reflector antenna with scanning beam.

The second term of this expression represents the cubic phase error which decreases the deflection of the maximum of the pattern and produces a distortion in the major lobe. Therefore, the scanning angle will be less than the angle of deflection of the exciter α , i.e.

$$\alpha_s = k_p \alpha, \quad (\text{IV. 100})$$

in which $k_p < 1$ is the reduction factor due to the existence of phase errors.

As an average it can be said that

$$k_p \approx 1 - 0.33 \text{tg}^2 \frac{\psi_0}{2}, \quad (\text{IV. 101})$$

in which $2\psi_0$ is the aperture angle of the reflector.

Therefore, to scan a beam in the sector $2\alpha_s$ it is necessary that the exciter be capable to perform a reciprocating motion within the limits of angle 2α .

To reduce phase errors during scanning use is made of a focusing system with two refracting (aplanatic lenses) or two reflecting surfaces (dual reflecting systems). In the case of double reflector antennas it is more convenient to scan the beam by rocking the second (small) reflector.

To increase the scanning sector spherical and sphero-parabolic reflectors are not infrequently used. The exciter in these antennas is shifted along the circular arc of a concentric sphere of the reflector. The radius of the arc is approximately equal to $0.5R$ of the sphere. One of the drawbacks of a spherical reflector is the fact that a wave front with a square phase error is formed in the aperture. [338

In the customary parabolic antenna when the reflector is wobbled relative to the fixed exciter to get the same angle α_s the required angle α need be one-half as great as that required when wobbling the exciter.

The curve along which the exciter moves should satisfy the following contradictory requirements: the need for minimal phase errors; constant amplitude distribution on the reflector; the curve should be technically realizable by the electro-mechanical scanning devices at a given scanning frequency. In this connection the circle is the most convenient trajectory for the movement of the exciter.

Conical Scanning

Conical scanning on the axis of symmetrical reflectors (or lenses) is accomplished by rotating the exciter about the focal axis (Fig. IV. 39). Scanning the beam in space in this manner makes it possible to attain zones of equal strength in the two main planes; these are used in radar work for making precision measurements of two angular coordinates.

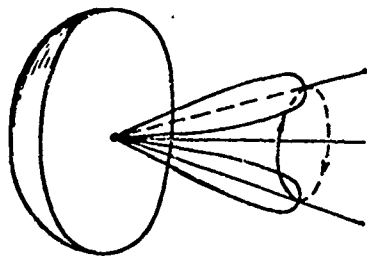


Fig. IV. 39. Antenna with conical scanning

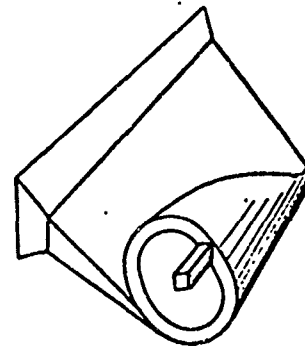
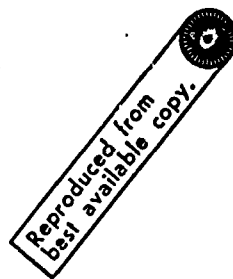


Fig. IV. 40. Antenna with a helical type of scanning device.

Helical Type Scanner

[339

This type of scanner is used in metal-air lenses (Fig. IV. 40). The flat part of the lens is equipped with a sloping, flat reflector and turns into a helix on the end portion of which the exciter describes a rotary motion.

The helical scanning device converts the circular movement of the exciter into the linear scanning of the antenna beam. The complete cycle of beam wobbling within the limits of $2\alpha_s$ is achieved in one complete turn of the exciter.

The helical scanner has sufficient broad band and permits beam scanning at a great frequency.

Rotary Scanner

The rotary scanner (Fig. IV. 41) consists of a fixed exciter, a fixed adapter of bent waveguides (stator) and a movable waveguide adapter (rotor). The radiating element 3 illuminates several adjacent waveguides of the rotor 2. Depending on the position of the rotor the energy is transmitted toward a specific group of waveguides of stator 1. This is equal to shifting the phase center of the reflector or the lens.

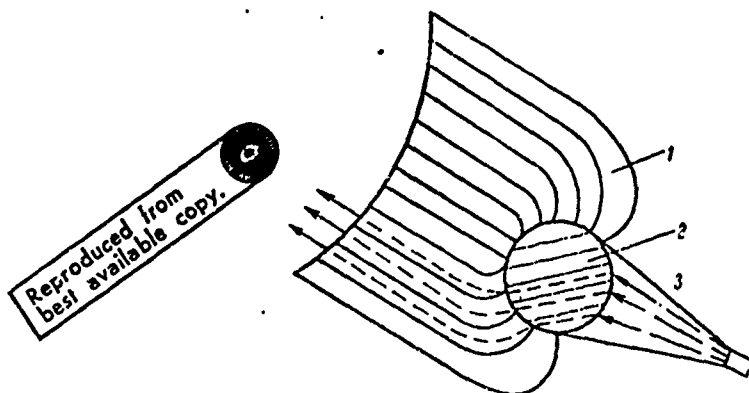


Fig. IV. 41. Rotary scanner. 1 - stator; 2 - rotor; 3 - exciter.

The rotary scanner does not require rotating articulation inasmuch as the exciter is rigid. Its speed of rotation compared with the helical scanner is half as great because of the fact that two rocking cycles occur in one turn of the rotor.

This scanner has less band coverage, however, and, because of wave reflections from the ends of the rotor and stator has lower efficiency.

Conical Scanners

In contrast to the other types discussed, conical scanners have a linear phased or direct phased rather than a point source exciter [22]. The device consists of a system of two coaxial metallic cones (Fig. IV. 42) of which the exterior one 3 is fixed and the interior one 2 rotates.

The linear exciter is connected via a slot cut lengthwise along the generatrix of one of the cones. The wave propagated in the inter-conal space is radiated through the linear aperture 1 of the fixed cone. Due to the dissimilar diameter of the bases of the truncated cone the paths of the

beams in the conical waveguide are different and a linear non-phased wave front will be formed in the aperture. When the rotor turns the slope of this front changes, thereby insuring beam scanning.

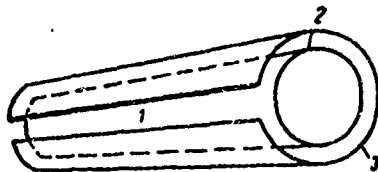


Fig. IV. 42. General view of a conical scanner.

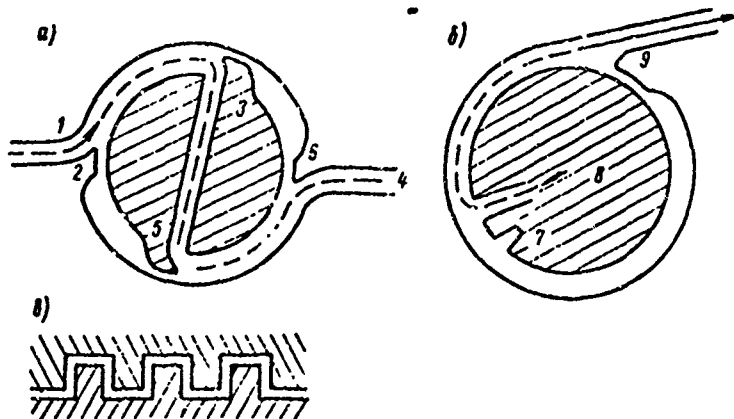


Fig. IV. 43. Cross section of conical scanning devices: a - feed through the stator; b. feed through the rotor; c. comb-shaped articulation.

Conical scanner can be made in two versions (Fig. IV. 43). The first version calls for switching in the linear exciter through a stator slot, and in the second version the exciter is switched in through a rotor slot. As we can see, in the first version the wave propagated from the longitudinal slot of the stator 1 travel between the cones after being reflected four times from the reflecting surfaces 2, 3, 5, and 6 and then reaches the structure 4. In this version the reflecting surfaces of the scanner are made in comb-shaped pattern. The reflecting surfaces of the second version are continuous. The stator reflector is made in the form of a sloping projection 9 and the rotor reflector is made in the form of a slot and loop 7 with zero input impedance. [34]

The first design requires extreme accuracy in fabrication, does not require rotating articulation, is broad banded, and makes two scans per turn of the rotor. The second design is simple but covers a narrower frequency band and requires a special rotation articulation which enables transmitting the energy from the fixed oscillator to the turning rotor. Only one scan is produced with each turn of the rotor in this case.

Aplanatic Lens and Reflecting Antennas

Non-distorting scanning of a beam in lens and reflector antennas is insured by meeting "sine conditions." By analogy with optical systems antennas in which this condition is met are known as aplanatic antennas.

Since aplanatic antennas have to meet "phased beam conditions" in addition to "sine conditions" they have two refracting or two reflecting surfaces.

In achieving "phasing conditions" the emerging beams are parallel to the antenna axis.

The sine condition is achieved if all the incident beams from the focal point and their corresponding emerging beams intersect on a circle the center of which lies in the focal point of the system. The radius of this circle will be equal to the focal distance of the antenna.

The shapes of the lens and reflecting, aplanatic antennas can be computed by the graphical and analytical methods using the procedure described in [11].

Reproduced from
best available copy.



Bibliography

1. Antenny santimetrovykh voln (Centimeter Wave Antennas), Parts 1 - 2, edited by Ya. N. Fel'd, Moscow, "Sovetskoye Radio," 1950.
2. Ayzenberg G. Z., Antenny ul'trakorotkikh voln (UHF Antennas), Part 1, Moscow, Svyaz'izdat, 1957.
3. Vaynshteyn, L. A., Difraktsiya elektromagnitnykh i zvukovykh voln na otkrytom kontse volnovoda (Diffraction of EM and Audio Waves in an Open End Waveguide), Moscow, "Sovetskoye Radio," 1948.
4. Vlasov, V. I., and Berman Ya. I., Proyektirovanniye vysokochastotnykh uzlov radiolokatsionnykh stantsiy, (Designing High Frequency Assemblies for Radar Sets), Leningrad, Sudpromgiz, 1961.
5. Gavelya, N. P. et al, Antenny (Antennas), Part 1, Leningrad VKAS Publishers, 1963.
6. King, D., Liniya peredachi s malymi poteryami i elementy volnovodnogo trakta dlya millimetrovogo diapazona (Transmission Lines With Small Losses and Millimeter Band Waveguide Circuit Elements), "Zarubezhnaya Radioelektronika," 1964, No. 11.
7. Kapitsov, N. A., Iskusstvennyye dielektriki (Artificial Dielectrics), Proceedings of the Third Session of the Russian Association of Physicists, 1923, No. 23.
8. Kocherzhevskiy, G. N., Diagrammy napravlenosti ploskikh shchelevykh anten (Radiation Patterns of Planar Slotted Antennas), "Radiotekhnika", 1953, Nos. 1, 2, 40.
9. Sankovskiy, G., and Gundlach, H., Radiotekhnicheskiy spravochnik (Radio Engineering Manual), Vol. 1-2, Moscow, Gosenergoizdat, 1960.

10. Mikheev, A. L., Linza s peremennym koefitsientom prelomleniy (Lens with Variable Coefficient of Refraction), DAN SSSR, 1952, Issues 5, 85, and 133.
11. Ponomarev, N. G., Graficheskiy metod postroyeniya profilye aplanaticheskikh anten (Graphic Method of Constructing Cross Sections of Aplanatic Antennas), "Radiotekhnika i Radioelektronika," Vol. 6, 2d Edition, 1961.
12. Peresada, V. P., O vychisleniy integralov v konchnykh predelakh (Integration in Finite Limits), "Radiotekhnika," 1957, No. 6.
13. Pistol'kors, A. A., Izlucheniye iz prodol'nykh shchelyev v krugovom tsilindre (Radiation From Longitudinal Slot in a Circular Cylinder), ZhTF, No. 3, 17, 315.
14. Pistol'kors, A. A., Izlucheniye shcheli na prymougol'nom volnovode (Radiation From a Slot on a Rectangular Waveguide), ZhTF, 1944, No. 12, 1, 693.
15. Pistol'kors, A. A., Antenny (Antennas), Moscow, Svyaz'izdat, 1947.
16. Ročionov, V. M., Linii peredachi i antenny SVCh (Transmission Lines and UHF Antennas), Svyaz'izdat, 1957.
17. Smirnov, V. A., Osnovy radiosvyazi na ul'trakorotkikh volnakh (Principles of Radio Communications on UHF), Moscow, Svyaz'izdat, 1957.
18. Sokolov, I. F., and Vakman, D. Ye., Optimal'nyye lineynyye sinfaznyye anteny s nepreryvnym rasporedeleniyem toka (Optimal Linear Phased Antennas With Continuous Current Distribution), "Radiotekhnika i Elektronika," 1958, No. 1.
19. Fradin, A. Z., Antenny sverkhvysokikh chastot (UHF Antennas), Moscow, "Sovetskoye Radio," 1957.
20. Gubarin, Yu. V., Antenny sverkhvysokikh chastot (UHF Antennas), Khar'kov, University of Kharkov Publishers, 1960.

Reproduced from
best available copy.

CHAPTER VI

AUTOMATIC TARGET TRACKING SYSTEMS

1. General Information

Types of Automatic Target Tracking Systems

/437

When reference is made to tracking a target it generally means the uninterrupted flow of information about a target's present coordinates in the form of voltages or currents or turns of shaft angles in pertinent indicators. For example, when conducting observations with a shipborne radar unit of a surface target the tracking process consists of developing data relative to its present range and any changes in its azimuth or course angle. When tracking an air target the procedure consists in making continuous measurements of three coordinates: the ~~slant~~ range, the azimuth, and the elevation.

In the case of non-automatic equipment tracking for range and angular coordinates is performed manually by one or several operators on the basis of data obtained from observing the positions of target markers on the plan position indicators. One advantage of manual tracking is that the operator can consciously differentiate between echoes given off by a tracked target and those by other targets. Another advantage is that the target can be tracked under conditions when the ratio of the useful signal to the interferences is equal or close to unity.

A disadvantage of this kind of tracking is its low level of accuracy in determining present coordinates, especially in the case of high speed targets, due to delayed response and fatigue on the part of the operator. For that reason, present day high precision radar sets generally have incorporated in them independent servo mechanisms for each of the coordinates being determined to insure automatic tracking of a target with a high degree of accuracy with a minimum amount of lag. Devices classed as discrete or continuous acting automatic control systems are used for making automatic measurements of present range, whereas analog servo systems are employed for tracking targets by angular coordinates.

A system of automatic target tracking by any coordinate can arbitrarily be considered as consisting of a direction finder and a servo unit.

A direction finder consists of all the elements in a radar set with the aid of which signals are received from a target and initially processed to provide information about a target's coordinates. The basic elements of a direction finder in an active radar system include the antenna, receiver, and transmitter; those of passive and semi-active radar systems include the antenna and receiver. /438

In radar systems for tracking targets in azimuth the antenna of the direction finder performs the function of a data unit for determining the

Reproduced from
best available copy.

target angle position relative to the equisignal direction. Depending on the principle involved in deriving equisignal directions and the method used for comparing signals received from a target, direction finders of automatic trackers in azimuth are divided into single and multiple channel systems.

In single channel direction finders the equisignal direction line is formed using conical or linear beam scanning in two mutually perpendicular planes and an antenna with a narrow radiation pattern. The method of comparing the amplitudes of signals received by a single channel receiver is used to determine the angular position of a target with respect to the equisignal line.

The chief disadvantage of single channel direction finders in automatic systems of tracking for azimuth lies in the fact that the method of amplitude comparison is applied to signals received at different times. Most radar targets however, produce signals whose intensity varies with time -- they are fluctuating signals. Accordingly, an error shows up in the measurement of angular coordinates. This error is continuous with time-random variations.

The effect of fluctuations can be decreased only by increasing the inertial properties of the system. However, increasing the inertial properties of an automatic system of tracking for azimuth involves increasing its dynamic errors, i.e. the system becomes incapable of tracking fast traveling targets with a high degree of accuracy.

Automatic systems of tracking for azimuth with multiple channel direction finders which employ the method of comparing simultaneously received signals are free of these shortcomings. The method of receiving signals from two points in space (by means of two antennas or two independent dipoles with a common reflector) located in the plane of the coordinate being measured and then amplifying them in independent receiving channels is used in these devices to determine one angular coordinate. With the direction finder so designed an equisignal plane is formed in space and the movement of a target along a particular angular coordinate is determined in relation to it.

To get the second coordinate the direction finder should have still another point of reception with an additional amplification channel. /439 However, in practice a second independent pair of points of reception and amplifier circuits are most often used; they form an equisignal plane in space that is perpendicular to the equisignal plane of the first two points of reception. As a result of the intersection of the two planes in space there is formed an equisignal direction whose position is determined by the condition of the elements in the direction finder receiver channels.

Accuracy in determining direction to the target in multiple channel direction finders is limited only by noises; it is much greater than that of single channel direction finders.

The drawbacks of the automatic tracking system with multiple channel direction finders is: comparatively great bulk of the apparatus and the high requirements to have the amplification channel characteristics identical and stable. Differences in the amplification channel parameters lead to angular displacements of the equisignal direction relative to the electrical axis of the antenna. Tracking the target by angular coordinates in this case will entail error.

Multiple channel direction finders can be used for pulsing or continuous operation. In multiple channel automatic systems of tracking for azimuth both the phase and amplitude method of comparison of received signals are used. The first method is based on the measurement of phase differences, while the second is based on the measurement of differences in amplitudes of signals picked up in separate points in space when the target is deflected from the equisignal direction.

The servo mechanism in an automatic target tracking system includes all the elements which insure automatic tracking of a target for a specific coordinate in complete accordance with the data output of the direction finder. In range tracking systems electronic servo devices are generally used, whereas in tracking targets by angular coordinates electromechanical servo mechanisms are employed.

General Principles of Automatic Tracking

The general operating principle in automatic tracking systems, regardless of which coordinate is being determined and the kind of servo mechanism used, consists in the following (Fig. VI. 1). The controlling action $x_{bx}(t)$ containing information about the actual rate of change of a particular target coordinate with respect to time goes from the output of the radar direction finder unit to the input of the error signal meter of the servo mechanism, and the signal $x_{pax}(t)$ developed by the servo mechanism proceeds from the output of the latter to the main feedback circuit.

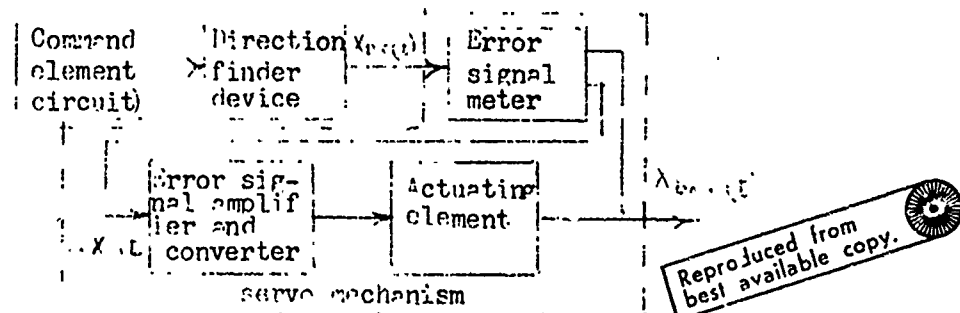


Fig. VI. 1. Block diagram of an automatic tracking system

These signals are compared in the error signal meter as a result of which an error signal is produced that is equal to their difference

$$\Delta x(t) = x_{\text{desired}}(t) - x_{\text{actual}}(t). \quad (\text{VI. 1})$$

After amplification and the necessary conversions the signal $\Delta x(t)$ acts on the actuating element of the system which changes its position or state and thereby develops the output signal $x_{\text{output}}(\tau)$

The work of the servo mechanism is such that the error signal constantly strives toward zero: $\Delta x(t) \rightarrow 0$. As a result, the output signal $x_{\text{output}}(t)$ of the system continuously reflects the true magnitude of the coordinate being measured with an accuracy determined by the quality of its operation. Thus, the process of automatically tracking a target by any coordinate is based on the constant measurement of the disagreement or difference between the input and the output signals of the system and reducing this error to zero.

2. Principle of Automatic Tracking for Range

Range Tracking in Pulsed Radar Systems

Automatic range tracking devices used in pulsing radar systems may arbitrarily be divided into those whose operation is associated with the requirement to get markers of the tracked target on the screen of the cathode ray tube of the system and those whose operation is not tied in with the need to get target markers on the range indicator. The latter, in turn, are divided into systems with a controlled delay circuit and systems with a variable frequency generator.

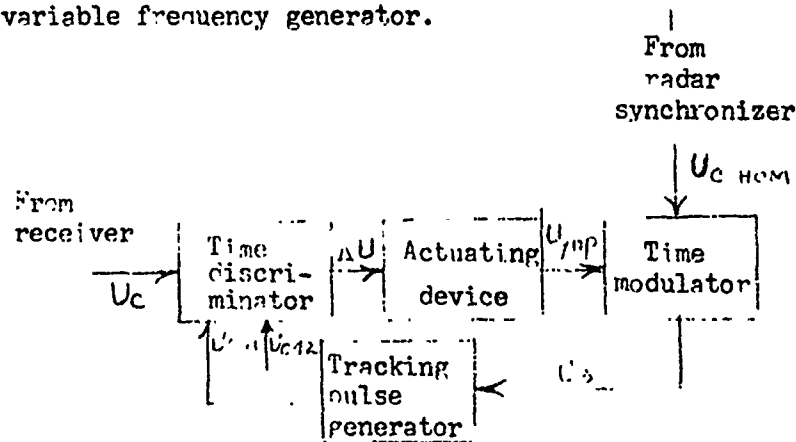


Fig. VI. 2. Block diagram of an automatic range tracking system with controlled delay circuit.

The former systems are electromechanical and the latter may be either electronic or electromechanical.

The block diagram of the automatic target tracking system for range with a controlled delay circuit and time-voltage diagrams which explain the

operation of the system are given in Figs. VI. 2 and VI. 3 [8, 9].

The operating principle of the system consists of the following. During each main pulse repetition period T_{Π} the pulse reflected from the tracked target goes to the time discriminator from the output of the radar receiver, and a pair of unipolar range tracking pulses enter from the tracking pulse generator output. The position of the center of the reflected pulse during the n -th repetition period relative to the leading edge of the synchronizing pulse is determined by the lag time t_3 , which is proportional to the actual range r_{μ} of the target during a particular period, while the line of contiguity of the pair of range tracking pulses is proportional to the lag time t'_3 . This lag time is proportional to the measured (actual) value of the range to the target during the n -th period, i.e. $t'_3 \equiv r_{\mu} T$. During this pulse repetition period, if $t_3 \neq t'_3$ an error signal appears at the output of the time discriminator whose mean value and polarity correspond to the magnitude and sign of the time difference $\Delta t = t - t'$ i.e.

$$\Delta U = K_{\Delta D} \Delta t, \quad (\text{VI. 2})$$

in which $K_{\Delta D}$ is the slope of the operating portion of the time discriminator characteristic curve in volts/second.

The error signal voltage goes to the controlling device where it is converted into the voltage U_{ynp} which controls the operation of the time modulator. Under the influence of this voltage and the synchronizing pulses the time modulator develops delay pulses U_3 whose duration is proportional to the controlling voltage

$$\tau_3 = K_3 U_{\text{ynp}}, \quad (\text{VI. 3})$$

in which K_3 is the delay control slope, sec/volts.

The range tracking pulse generator is triggered by the trailing edge of the delay pulse. In the process, time interval t_3 , which determines the position of the range pulses relative to the synchronizing pulses, changes in the following repetition periods in such a manner that the time difference Δt decreases, approaching a comparatively small value that equals the tracking error.

Since a specific value U_{ynp} corresponds to each position of the tracking pulses the present range to the target can be read from the value of the control voltage.

Automatic tracking begins when the tracking pulses first coincide with the pulse reflected by the target. This coinciding process, depending on the structural peculiarities of the radar system, can be accomplished "manually" by the operator by superposing the range marker on the target pip on the plan position indicator. Or it can be done automatically with the aid of the scanning circuit which periodically moves the tracking pulses along the time axis until the target is locked on.

The block diagram of an automatic range tracking system with a controlled generator is described in Fig. VI. 4 [8].

In contrast to circuits with a controlled delay circuit the operation of automatic range tracking systems with a tuned oscillator is not time-related to the elements forming the synchronizing pulses. Therefore, the magnitude of the controlling voltage in them is not proportional to the range of the target. These automatic tracking circuits find application in radar sets that are coupled to digital type computers for processing stable reference pulses that are time-matched with the echo signal from the tracked target. Measurement of the range is achieved by converting into binary code the time interval from the instant the radio pulse is beamed to the appearance of the reference pulse.

The circuit works as follows. When the center of the reflected pulse coincides with the limit of contiguity of the range tracking pulses the output voltage of the discriminator is equal to zero. In this case the oscillator being tuned generates middle frequency oscillations with an initial phase that determines the instant for starting the range pulse oscillator by triggering the pulse formation circuit. The mean frequency of the oscillations generated is a multiple of the repetition frequency of the transmitted pulses. If a difference appears subsequently in the time position of the tracking pulses and the reflected signal a controlling voltage is developed by the discriminator whose value is proportional to the error signal; the frequency of the tuned oscillator, therefore, departs from its mean value. Changing the frequency of the oscillator results in changing the phase of the oscillations it generates and, consequently, shifting the range pulses in a direction corresponding to a decrease in the initial error.

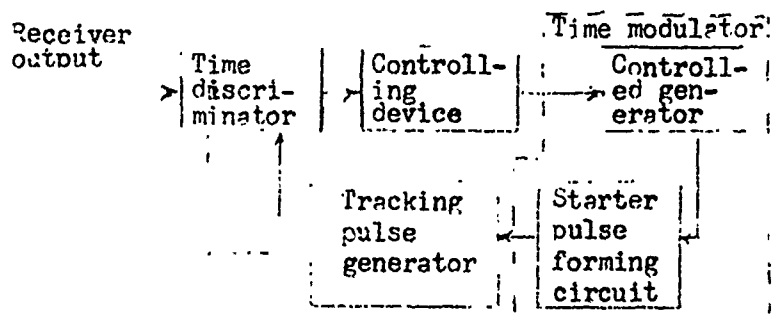


Fig. VI. 4. Block diagram of an automatic range tracking system with controlled oscillator

Range Tracking in Frequency Modulated Radar Systems

Forming the basis of automatic range tracking systems used in frequency modulated radar sets is the principle of maintaining continuous checks for changes in the beat frequency.

A simplified block diagram of a frequency modulated automatic range tracking system is shown in Fig. VI. 5 [9]. The tracker consists of an $\mu\mu\mu$ automatically controlled electromechanical system made up of the following tracking elements: the range selector, a narrow band filter tuned to a beat frequency corresponding to the range of the tracked target; the range metering circuit, including a beat pulse converter and integrator; and the comparator circuit and electric motor drive with range processing potentiometer. The automatic range tracking system also contains devices which are not directly involved in the automatic tracking process. They make it possible to conduct target scanning throughout the entire operating band of the system and change it from scanning to target tracking. These elements include: the scanning circuit, the lock on relay circuit, and the relay.

The target scan operation is accomplished by continuously retuning the center frequency of the selector transmittance band with an electric motor drive that is fed in this operation by the scanning circuit. The time of retuning the selector filter frequency throughout the full operating range of the automatic tracking system depends on its bandwidth. The narrower the transmittance band of the filter, the slower the buildup of voltage at its output and the slower the scanning rate.

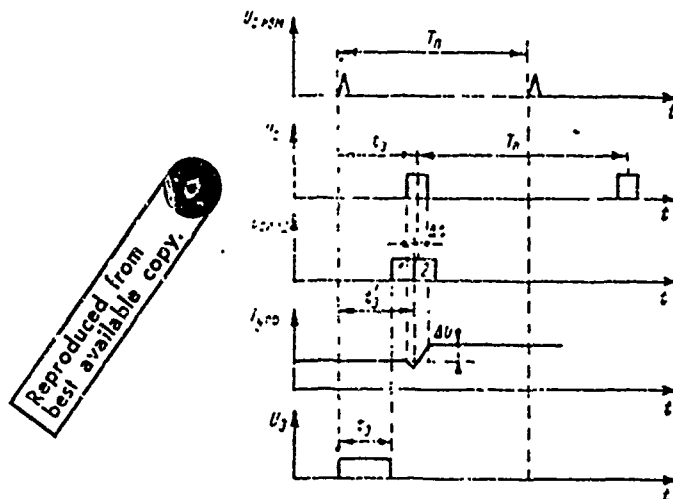


Fig. VI. 3. Voltage curves of circuit shown in Fig. VI. 2.

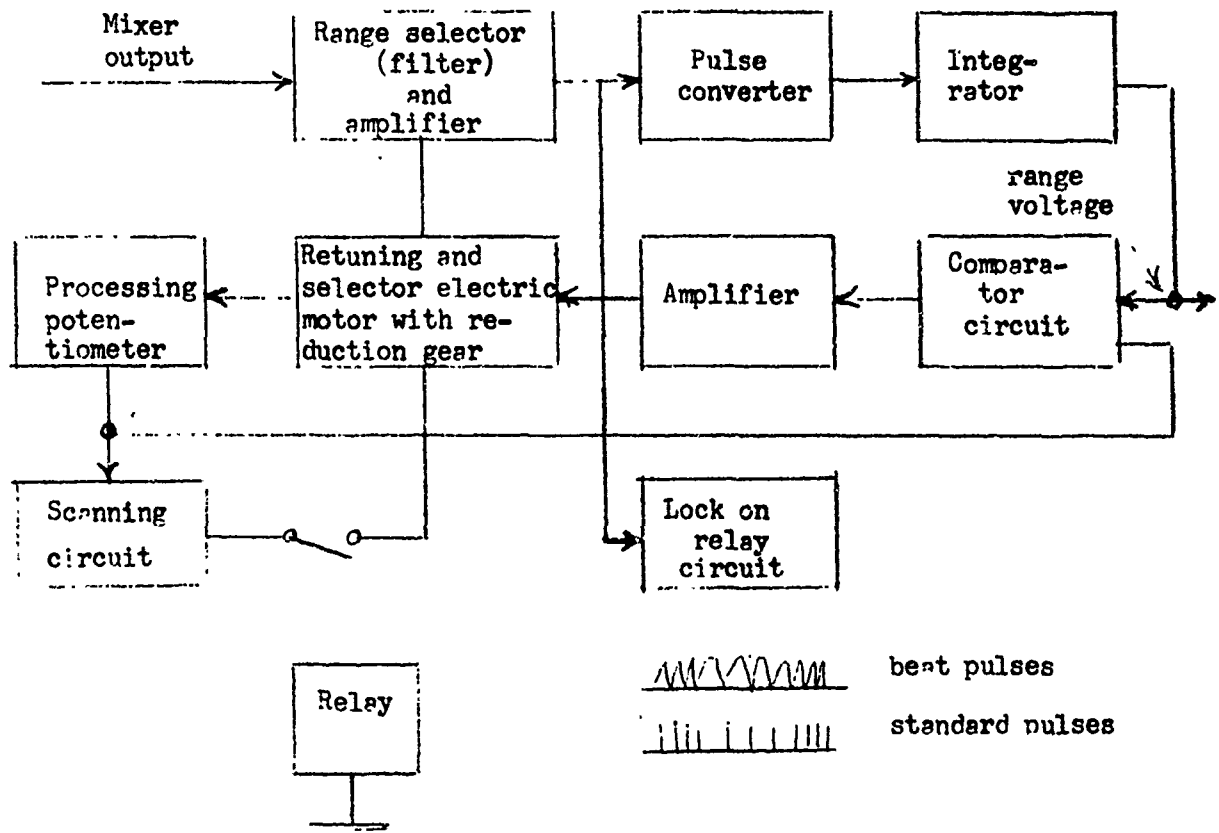


Fig. VI. 5. Block diagram of automatic system of tracking in range for frequency modulated radar

When the target appears at a certain range within the operating band of the system the selector filter becomes tuned at some moment in time to the beat frequency due to the continuous retuning of its frequency which corresponds to the range of the target. After amplification in the range selector these beats are fed to the lock on relay circuit. The latter triggers and disconnects the selector retuning electric motor from the scanning circuit. At this moment the system changes over to automatic tracking of target for range. In this mode of operation the beat pulses go from the range selector to the pulse converter input. The pulse converter changes pulses that differ in shape and duration into pulses of constant amplitude and duration. This conversion of beat pulses into standard pulses is necessary in order to eliminate the influence of shape, amplitude, and duration of beat pulses on the accuracy of range measurement. The pulse converter is an oscillator with forced starting that develops standard pulses with a frequency equal to the beat frequency.

The series of pulses with constant amplitude and duration goes from the converter output to the integrator which separates out the direct component; the latter is proportional to the measured range to the target. The range voltage is then compared with the processing potentiometer voltage opposite in sign, whose cursor is coupled to the selector retuning electric motor. If the absolute magnitude of the range voltage is not equal to the processing potentiometer voltage an error signal will appear at the output of the comparator circuit; it will be proportional to the difference between these voltages. After amplification the error signal is fed to the actuating electric motor which retunes the selector filter until the range voltage and processed voltages are the same. When these voltages are equal it means that the range selector is tuned to a sector in which the tracked target is located. As the target travels a continuous change in the range voltage takes place, and consequently the center frequency of the selector transmittance band is continuously retuned.

The automatic range tracking system discussed operates well enough only at comparatively low radial velocities of the target at which the Doppler frequency shift is confined to the transmittance band of the selector filter. Extension of the filter band is limited by deterioration of its interference killing features and by a reduction in the operating range of the system.

3. Basic Elements of Pulsed Automatic Range Tracking Systems

Time Discriminator

The time discriminator is an electronic device which converts the time difference between target pulses and tracking pulses into a constant voltage whose increase during the target pulse repetition period T_{Π} corresponds in magnitude and polarity to the magnitude and sign of the tracking error Δt . A variety of discriminator circuits are used, but despite the differences in circuitry the operating principle in most of them is the same [8]. It consists in that each pulse from a tracked 446

target is divided, with the aid of tracking pulses, into two parts. Portions of reflected pulses are compared and the error signal is developed from differences in their areas which are proportional to Δt .

The target pulse dividing operation in each repetition period T_{Π} is performed by two coincidence circuits which make up the time selector, while the operation of comparing portions of the reflected pulse is performed with a differential diode or triode detector [9].

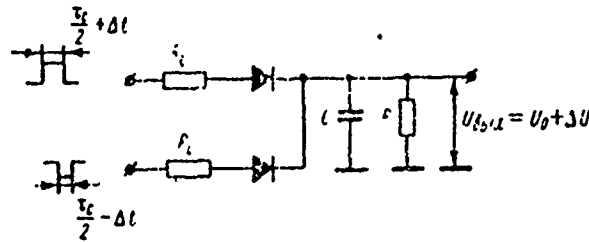


Fig. VI. 6. Time discriminator equivalent circuit.

The simplified equivalent circuit of a time discriminator is shown in Fig. VI. 6. The ratio of voltage increase ΔU at the discriminator output to the time difference Δt is referred to as the time discriminator characteristic. Shown in Fig. VI. 7 is a discriminator curve for rectangular target pulses and adjoining rectangular range tracking pulses. The operating part of the curve is the central linear portion limited by the values $\Delta t = \pm t_c/2$ and the overall length $\delta T_p = T_c$ in which T_c is the duration of the target pulse. For this portion of the curve the following [44] equation holds true

$$\Delta U = K_{u,d} \Delta t, \quad (\text{VI. 4})$$

in which $K_{u,d} = (d\Delta U/dt)_{\Delta t=0}$ — is the transfer coefficient or slope of the time discriminator curve, volts/second.

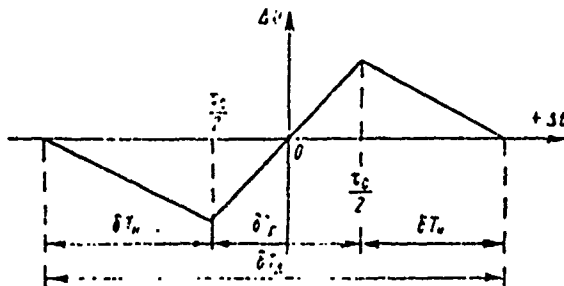


Fig. VI. 7. Idealized time discriminator curve.

Curve areas along the sector $\delta T_n = \tau_{cn}$, lying outside the limits of the operating section are known as unstable tracking areas. In these zones the signal from the target is partially covered by only one tracking pulse, and with an increase in the time difference the error signal voltage decreases; this may result in the stoppage of the automatic target tracking process. Stoppage of tracking will not occur if the error signal voltage at a particular initial difference is sufficient to move the tracking pulses at the rate of travel of the target pulses.

The entire area of the time discriminator curve designated δT_d determines the minimal interval between pulses reflected from two targets in which only the pulse from one of them will coincide with the tracking pulses. Therefore, this region is termed the time discriminator zone of sensitivity. The length of the sensitivity zone depends on the duration of the reflected and tracking pulses.

For idealized reflected and contiguous tracking pulses

$$\delta T_d = \delta T_p + 2\delta T_n = 2\tau_{cn} + \tau_c \quad (\text{VI. 5})$$

and if there is an interval t_n between the tracking pulses

$$\delta T_d = 2\tau_{cn} + \tau_c + t_n \quad (\text{VI. 6})$$

The interval between tracking pulses $t_n < \tau_c$ is generated to increase the slope of the discriminator curve.

The range resolution of a radar set with an automatic range tracking system, in contrast to sets with a manual tracking system, is determined not by the duration of the main pulses τ_c but by the extent of the discriminator aperture $\delta T_d > \tau_c$. Therefore, to increase the range resolution in such sets an attempt is made to decrease the duration of both the main and tracking pulses.

In any case, the time discriminator, as an element of the automatic control system, is an aperiodic element with the transfer function [8]

$$W(p) = \frac{K_{n,d}}{1 + pT_{B,d}} \quad (\text{VI. 7})$$

In expression (VI. 7) the time constant $T_{B,d}$ is a function of both the charging circuit time constant and the discharge time constant of the differential detector condenser

Reproduced from
best available copy.

$$T_{B,d} = \frac{T_n}{\frac{\tau_c}{T_{zap}} + \frac{T_n}{T_{pas}}}, \quad (\text{VI. 8})$$

in which T_{zap} is the charging circuit time constant of condenser C; $T_{pas} = RC$ is the time constant of the condenser discharge circuit through the load resistor R. If $T_{zap} \gg \tau_c$, $T_{zap} \gg T_{pas}$ and constancy of charging and discharging currents is insured, then regardless of the

magnitude of the voltage at the output of the gating circuit of the differential detector, the dynamic characteristics of the time discriminator are very close to the integrating member

$$W_{n,2}(p) = \frac{K_{n,2} F_{\Pi}}{p} = \frac{K_{\lambda}}{p}, \quad (\text{VI. 9})$$

in which $F_{\Pi} = 1/T_{\Pi}$.

The transfer coefficient of the time discriminator and, therefore, the dynamic properties of the whole automatic target tracking system depend substantially on the amplitude of the target pulse. Automatic gain control and amplitude limitation of target signals are utilized in receivers of radar sets with automatic systems of tracking in range to keep the discriminator transfer coefficient constant.

Controlling Device

In each repetition period of reflected pulses the controlling device forms a signal which changes the amount of delay of the tracking pulses t'_3 . Because the information about the present range of the target arrives in discrete form the time position of tracking pulses should be preserved during the time interval from the end of the reflected pulse to its beginning in the next repetition period. Therefore, integrating circuits are used as controlling devices in automatic pulsed systems of tracking in range.

The simplest integrator used in automatic range tracking systems is the condenser, a component element in the time discriminator. The discriminator condenser is used as an integrating element in a circuit when the input resistance of the following stage is of sufficient magnitude ($T_{sep} \ll T_{pas}$).

A second type of controlling device is the integrating (operational) amplifier with capacitive, negative feedback. An equivalent circuit of such an amplifier is shown in Fig. VI. 8.

From the standpoint of dynamic qualities this kind of amplifier represents an aperiodic element with a transfer function of [8]

$$W_A(p) = \frac{K}{(K+1)Tp + 1} \frac{k_{\Pi}}{p + \frac{1}{(K+1)T}}, \quad (\text{VI. 10})$$

in which K is the amplifier gain without feedback; $k_{\Pi} = 1/T$ is the transfer coefficient of the integrating amplifier; and $T = RC$.

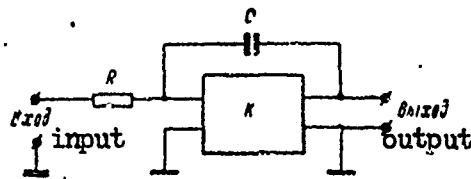


Fig. VI. 8. Equivalent circuit of an integrating amplifier

With sufficiently large values of K and assuming that the transient processes in the automatic range tracking system terminate within a time interval considerably less than the time constant T this amplifier can be regarded as an integrating member

$$W_y(p) = \frac{1}{Tp} = \frac{k_{ii}}{p}. \quad (\text{VI. 11})$$

The chief merit of integrating amplifiers consists in that the negative effect of the amplifier on the operation of the discriminator, especially a discriminator with differential detector on diodes, is K times less than that of the integrating capacitance.

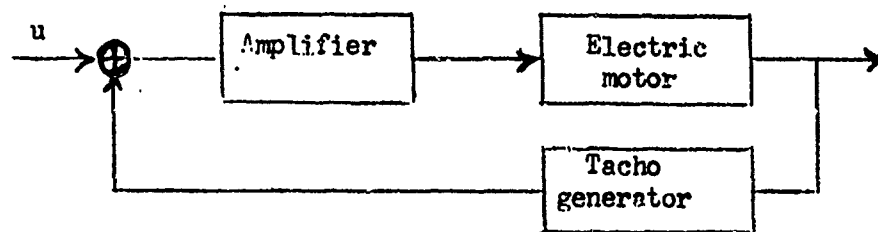


Fig. VI. 9. Block diagram of an electromechanical integrator.

Apart from electronic integrators automatic range tracking systems make use of electromechanical integrators, mainly when in order to control the time position of tracking pulses a mechanical rather than an electrical signal is required. This signal consists in a change in the shaft angle with a value that would be proportional to the integral from the voltage taken from the discriminator output. By way of example, electromechanical integrators are used in phase meter automatic tracking systems.

A block diagram of the most commonly used electromechanical integrator is shown in Fig. VI. 9. The integrating element of the circuit is an alternating or direct current motor. The angular velocity of the motor is proportional to the voltage applied to its armature (in a direct current motor) or to the control winding (in an asynchronous, two-phase motor), and the turn angle of the axis $\Delta\psi$ is proportional to the integral from the input voltage. The feedback circuit assembled on a tachometer generator of appropriate current differentiates the output signal, the resulting voltage compared to the input voltage, and their difference triggers /450 the electric motor. The processes continue until the output signal is

exactly proportional to the integral from the input signal and their difference becomes zero.

As an element of a closed circuit in automatic control this integrating drive is described by the transfer function

$$W_A(p) = \frac{K_y W_{дв}(p)}{1 + K_y W_{дв}(p) W_{тг}(p)} = \frac{K_y K_{дв}}{p(1 + T_{дв} p) + 1} \quad (\text{VI. 12})$$

in which $W_{дв}(p)$ is the transfer function of the electric motor, $W_{дв}(p) = K_{дв}/p(1 + T_{дв} p)$; $W_{тг}(p) = K_{тг}(p)$ is the transfer function of the tachometer generator; $T_{дв}$ is the electromechanical time constant of the motor; K_y , $K_{дв}$, and $K_{тг}$ respectively, are the transfer coefficients of the amplifier, electric motor, and the tachometer generator.

Electromechanical integrators are very precise, but have inertial qualities. For that reason they are not suited for use in quick response automatic range tracking systems. Other drawbacks of this kind of integrator include their bulkiness and a cost factor that is substantially greater than that of electronic integrators.

Time Modulators

Automatic range target tracking systems use as time modulators electronic circuits and devices which can generate either pulses of constant amplitude and variable duration or pulses with constant amplitude and duration but delayed, with respect to the synchronizing pulses, for a period determined by the magnitude of the controlling effect.

Time modulators may be based on the voltage comparison method or on the phase metering method. Modulators of the first group are more simple, while those of the second group offer a higher degree of accuracy. Modulators of the first type utilize phantastrons, senatrons, and other similar linearly charged and discharged condenser circuits operating together with comparator circuits.

Time modulators in which the phase metering method is used consist of a capacitive phase inverter and the pulse shaping circuit. The block diagram, which represents the operating basis of such modulators, with the voltage oscillograms pertaining to them, are shown in Figs. VI. 10 and 11. The time delay T_3 of pulses controlling the operation of the tracking pulse generator is accomplished by means of a capacitive phase inverter in which the phase shift of the output signal is proportional to rotor turn angle $\Delta\psi$.

The delay time T_3 is determined from the equation

$$T_3 = \frac{\psi}{2\pi} T_n \quad (\text{VI. 13})$$

in which ψ is the phase shift of phase inverter oscillations; T_{Π} is the period of sinusoidal oscillations from the generator that synchronizes the operation of the radar unit.

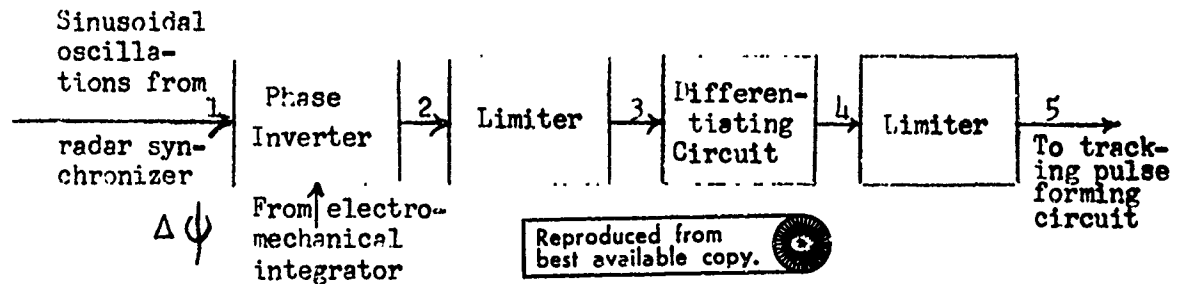


Fig. VI. 10. Block diagram of a phase metering time modulator.

During each repetition period T_{Π} of main pulses the phase inverter shaft is caused to turn through the angle ψ $\Delta\psi$ by the actuating electric motor in the electromechanical integrator. If the angle of turn of the phase inverter shaft $\Delta\psi$ be regarded as the input signal and the delay time as the input value, the phase meter time modulator can be considered, from the standpoint of the dynamics of control, as a non-inertial element with a transfer coefficient of $K_{n,u} = \tau/\Delta\psi$.

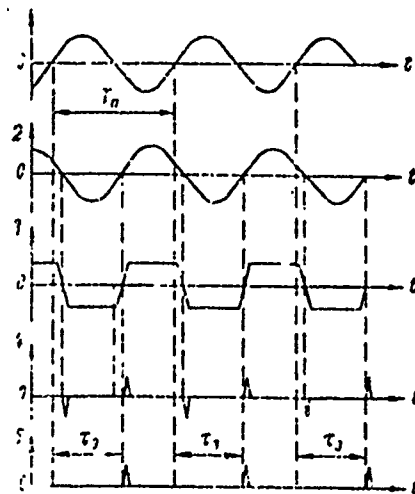


Fig. VI. 11. Voltage curves of circuits shown in Fig. VI. 10.

The time modulator of the frequency being subjected to change (cf Fig. VI-4) consists of the controlled generator of harmonic oscillations and the triggering pulse shaping circuit of the tracking pulse unit. For a controlled generator any frequency-tunable generator circuit can be used which insures a proportional relationship between the gain in frequency and changes in the controlling voltage

$$\Delta f(t) = K_n F_{n,u}(t), \quad (\text{VI. 14})$$

in which K_{η} is the frequency retuning factor; $F_{11} = 1/T_{11}$; $u(t)$ is the controlling voltage.

As an element of the closed automatic control circuit, the controlled oscillator is an ideal integrating unit with a transfer coefficient of $K_{yr} = K_{\eta} T_{\eta}$.

In automatic range tracking systems with a controlled oscillator ordinary pulsing circuits capable of converting harmonic oscillations into signals are used as starter pulse shaping circuits. Their time of appearance in each repetition period T_{η} is strictly related to a particular phase of such oscillations. The elemental structure of the circuit depends on both the changing frequency oscillator layout and the device which develops the tracking pulses. In the simplest case the triggering pulse shaping circuit will consist of a series connected limiter of sinusoidal oscillations and a differentiating element.

Tracking Pulse Generators

Circuits which produce tracking pulses are generators which can produce two pulses of similar amplitude and duration, paired or separated by a time interval. Ordinarily, these pulses are formed by a blocking oscillator with a section of artificially long line or with the aid of two delayed blocking oscillators; other similar types of pulsing devices may be used.

4. Dynamic Properties and Operating Characteristics of Pulsed Automatic Range Tracking Systems

The operating quality of an automatic range tracking system is determined by the stability of the system, its transient characteristics, the amount of steady state error, and its inherent fluctuating or random errors. These characteristics, and especially accuracy in the measurement of distances to object in the steady state, depend on the number of elements in the system capable of accumulating energy (integrators). The number of / 453 integrating elements used determines the order of astaticism of the system: systems with one integrator are first order astatic systems, those with two are second order astatic systems, etc. The higher the astatic order of the system the more accurately and precisely the objects are tracked in the steady operating state, the shorter the tracking pulses can be, and, consequently, the higher will be the range resolution of the system. However, automatic range tracking systems become more complex and sluggish with a larger number of integrating elements within them. Most commonly used in practice, therefore, are pulsed automatic range tracking systems with one or two integrators.

A thorough investigation of all the properties of automatic range tracking systems by analytical methods presents certain difficulties since it is associated with the solution of equations with finite differences.

Therefore, in the majority of cases when investigating pulsed tracking systems they are replaced by equivalent continuous operating systems and their characteristics are evaluated by a sophisticated automatic control apparatus based on the linear theory. Any pulsed tracking system can be represented with an adequate degree of accuracy, for all practical purposes, by an equivalent continuously operating system and, therefore, described by a linear or linearized differential equation of an appropriate order in those instances where the time for establishing transient processes in the system is several times greater than its time constant [12].

Automatic Range Tracking Systems With One Integrator

Block diagrams of continuous action tracking systems with one integrator [1, 5, 8] and equivalent automatic pulsed tracking systems are described in Fig. VI. 12.

The motion in a system with an integrating time discriminator (Fig VI-12a) is described by a linear, first order differential equation with a constant coefficient

$$\frac{dt_3'}{dt} + K_t t_3' = K_t t_3, \quad (\text{VI. 15})$$

in which $K_V = K_H K_Y$ is the speed conversion factor of the system, 1/sec; K_H is the coefficient characterizing the rate of change of the voltage on the integrating condenser of the time discriminator with an error per microsecond, volts/(microsecs·sec); K_Y is the transfer coefficient of the elements controlling the time delay of tracking pulses.

The transient characteristic in the system is

$$t_3' = t_{30} (1 - e^{-K_V t}), \quad (\text{VI. 16})$$

and the error signal changes in accordance with

$$\Delta t = \Delta t_0 e^{-K_V t} \quad /454 \quad (\text{VI. 17})$$

or

$$\Delta t = \Delta t_0 \left(1 - K_V t + \frac{1}{2!} K_V^2 t^2 - \dots \right) \approx \Delta t_0 (1 - K)^n, \quad (\text{VI. 18})$$

in which t_{30} , Δt_0 are respectively the input effect and the error signal corresponding to the initial moment of time; $K = K_V T_D$ is the dimensionless transfer coefficient of the system: $n = 0, 1, 2, \dots$

This type of automatic tracking system is stable if $0 < K < 2$. When $0 < K < 1$ an aperiodic transient process obtains, and when $1 < K < 2$ a damping, oscillatory, transient process prevails. When $K = 1$ the error is eliminated in one main pulse repetition period of main pulses.

The transfer function of the closed system is

$$\Phi(p) = \frac{t'_j(t)}{t_j(t)} = \frac{1}{1 + T_{ACD} p}, \quad (\text{VI. 19})$$

in which $T_{ACD} = 1/K_v$ is the time constant of the system.

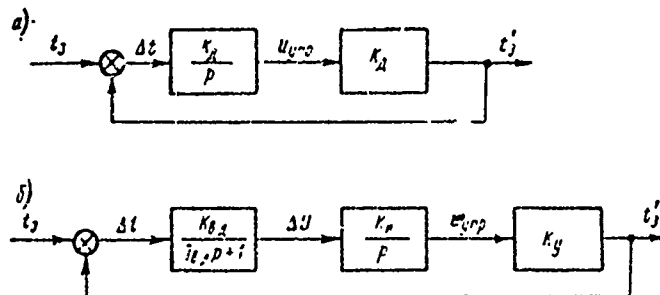


Fig. VI. 12. Block diagram of automatic tracking in range system with one integrator: a - with integrating time discriminator; b - with aperiodic time discriminator.

The basic characteristics of an automatic range tracking system with an aperiodic time discriminator (Fig. VI. 12b) are determined by the transfer functions of an open and closed systems

$$W(p) = \frac{K_v}{F(1 + T_{d.3} p)}, \quad (\text{VI.20})$$

Reproduced from best available copy. 
$$\Phi(p) = \frac{1}{T_{ACD}^2 p^2 + 2T_{ACD} \xi p + 1}, \quad (\text{VI.21})$$

in which $K_v = K_{d.3} K_u K_y$; $T_{ACD} = \sqrt{\frac{T_{d.3}}{K_v}}$; $\xi = \frac{1}{2\sqrt{K_v T_{ACD}}}$.

The steady state of the automatic range tracking system under consideration depends on the value of the parameter ξ . When $\xi > 1$ an aperiodic damping transient process obtains, and when $\xi < 1$ a damping oscillatory transient process occurs. The transient characteristics of the system for different values of parameter ξ are shown in Fig. VI. 13 [15].

In both the first and second systems the static error $\delta r_{CT} = 0$ is absent (the systems measure the range r to the stationary objects accurately) but there is a speed error of δr_{CK} . In the constant target velocity mode this error is equal to

$$\delta r_{CK} = -\frac{1}{v} \frac{dr}{dt}. \quad (\text{VI.22}) \quad (\text{VI. 22})$$

In contrast to automatic range tracking systems with integrating discriminators the second system has a speed "memory" that decreases with time. When the target pulses disappear, the tracking pulses do not stop but continue to move exponentially in the previous direction for a period of time approximately equal to $T_{d.3}$. The process of changing the delay time of tracking pulses here is described by the equation

$$t_s \approx t_{s0} + \frac{1}{2} \frac{dt_{s0}}{dt} T_{B.A} (1 - e^{-t/T_{B.A}}), \quad (\text{VI. 23})$$

in which t'_{s0} and dt'_{s0}/dt are respectively the tracking pulse delay time and the established speed of motion at the instant the pulses reflected from the target disappear.

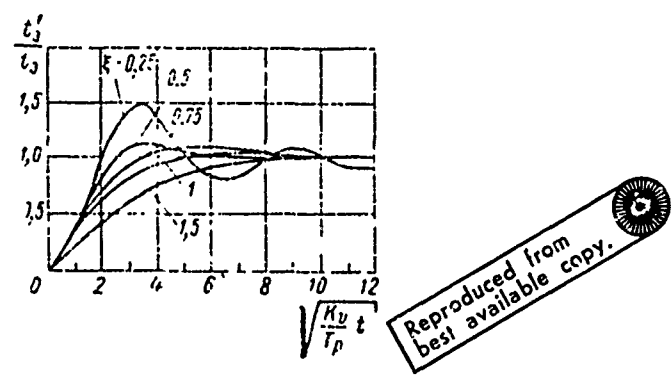


Fig. VI. 13. Transient characteristics of automatic range tracking systems with one integrator.

Automatic Range Tracking Systems With Two Integrators

Automatic tracking systems with two integrators are second order astatism controlling systems. Therefore, in the steady state with $dr/dt = \text{const}$ the speed dynamic error δ_{rck} is absent and there is no break in the tracking of the target with a temporary disappearance of target echoes. In addition, unlike systems with a single integrating element, these systems are capable of uninterrupted automatic tracking of a target not only in range but speed as well. The signal proportional to range is taken from the / 456 output of the second integrator, while that proportional to the radial velocity of the target is taken from the output of the first integrator.

Automatic range tracking systems with two series-connected integrators are structurally unstable. Therefore, in addition to the basic elements they have supplemental elements which stabilize the operation. Ordinarily, stabilization is achieved by the use of a boosting element in the loop which imparts the necessary dynamic characteristics to it. The circuits used in these correcting filters are shown in Fig. VI. 14.

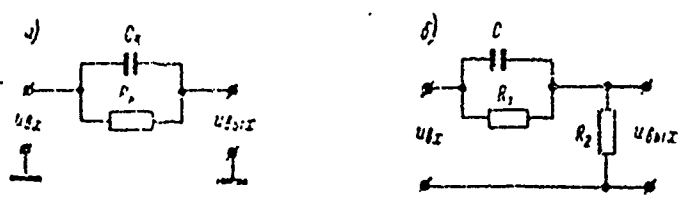


Fig. VI. 14. Circuits of correcting elements

The first element (Fig VI 14a) has a transfer function of

$$W_{k1}(p) = K_k (1 - T_k p), \quad (VI. 24)$$

in which $K_k = 1/R_k$; $T_k = R_k C_k$
while the second has a transfer function of

$$W_{k2}(p) = \frac{q(1 - T_k p)}{1 + T_k p}, \quad (VI. 25)$$

in which $q = R_2/(R_1 + R_2)$; $T_k = R_1 C_k$.

The element with the transfer function $W_{k1}(p)$ is mainly used in automatic range tracking systems with an aperiodic time discriminator, and those with a transfer function of $W_{k2}(p)$ are used in systems with integrating time discriminators.

Block diagrams of automatic range tracking systems with the correcting elements mentioned are given in Figs. VI. 15a and 15b.

Sometimes, another method of correcting the tuning error is used to provide stabilization. It consists in that the controlling action is made up of two signals, one of which is proportional to a single integral and the other to the double integral of the magnitude of error signal Δt (Fig. VI. 15b).

In automatic range tracking systems with two operating integrating amplifiers in order to produce a controlling action made up of voltages equal to single and double signal error integrals it is not essential to use an additional amplifier and a totalizing stage as shown in the block diagram of Fig. VI. 15b. This method of stabilization can be most simply achieved by coupling in the correcting resistance in the feedback circuit of the first integrating amplifier. / 457

The characteristics of the automatic range tracking system shown in Fig. VI. 15 are governed by the following transfer functions:

Reproduced from
best available copy.

$$W(p) = \frac{K_3(1 - T_k p)}{p^2(1 - T_{\theta} p)}, \quad (VI.26)$$

$$\Phi(p) = \frac{K_3(1 - T_k p)}{T_{\theta} p^3 + p^2 + K_3(T_k p + 1)}, \quad (VI.27)$$

in which $K_3 = K_{\theta} K_{\Delta} K_{\Sigma} K_{\Sigma} K_{\Sigma}$.

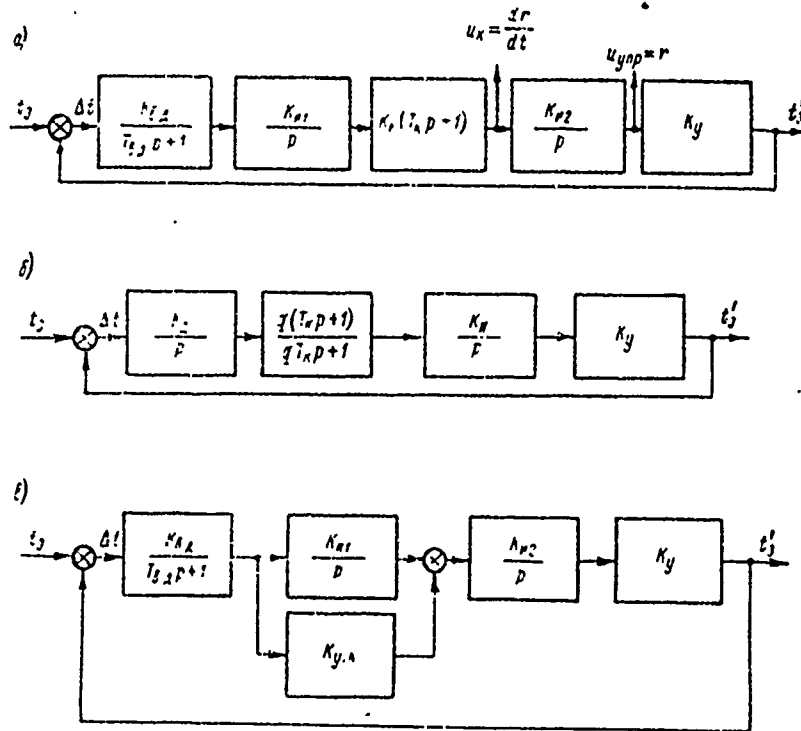
The system is stable only if $T_k > T_{\theta} \Delta$. The nature of the transient processes is determined by the parameters of the system $T_{\theta} \Delta$ and K_3 . When $T_{\theta} \Delta / \sqrt{K_3} < 0.4$ a satisfactory transient state prevails.

The transfer function of the systems described in Fig VI. 15b are /458

$$W(p) = \frac{K_m(1 + T_v p)}{p^2(1 + qT_v p)}; \quad (VI.28)$$

$$\Phi(p) = \frac{K_m q(1 + T_v p)}{qT_v p^3 + p^2 + K_m(1 + T_v p)}; \quad (VI.29)$$

in which $K_m = K_{m1}K_{m2}K_y$.



reproduced from
best available copy.

Fig. VI 15. Block diagrams of an automatic range tracking system with two integrators: a, b -- automatic range tracking systems with boosting elements; c -- automatic range tracking system circuits with corrections for error signals.

This system is stable when $K_m T_k > q K_m T_k$ or when $q < 1$. In such case the stability reserve decreases as q approaches unity.

The characteristics of a system with correction for error (Fig VI 15b) are described by the following transfer functions:

$$W(p) = \frac{K_m}{p^2(1 + T_v p)} \left(\frac{K_m}{p} + K_{y, \kappa} \right); \quad (VI.30)$$

$$\Phi(p) = \frac{K_m(1 + T_v p)}{T_v p^3 + p^2 + K_m(K_y \kappa p + K_m)}; \quad (VI.31)$$

in which $K_m = K_{m1}K_{m2}K_y$.

A stable condition in the system is determined by the inequality $K_{yK} > K_{H1} T_{0D}$; it is insured through the appropriate selection of an amplification factor for one of the branches of the totalizing device.

In systems with corrections for error which use as their first integrator an operating amplifier with capacitive-rheostat feedback, conditions for stability are expressed by the inequality

$$\frac{R_b}{R_a} > K_{H1} T_{0. A}, \quad (\text{VI. 32})$$

in which R_b is the amplifier resistance in the feedback circuit; R_a is the resistance inserted between the discriminator output and the input of the operational amplifier.

In an automatic range tracking system with two integrators errors in range measurement will appear only if the target is in accelerated motion. The acceleration error is expressed in the formula

$$\delta r_{yex} = \frac{a}{K_3}, \quad (\text{VI. 33})$$

in which a is the acceleration of the target.

5. Errors in Automatic Range Tracking Systems Caused by Input Noise and Instability of Time Delay Devices

Automatic tracking system errors due to the effects of noise and various instabilities in time delay devices are of a random nature. The magnitude of these errors is estimated as a mean square value.

The mean square error due to input noise is equal to / 459

$$\sigma_{r_{in}} = \frac{c}{2} \sqrt{\frac{1}{2\pi} \int_{-\infty}^{\infty} S_{b. A}(\omega) |\Phi'(j\omega)|^2 d\omega}, \quad (\text{VI. 34})$$

and the error due to instability of operation of the time delay circuit is

$$\sigma_{r_{in}} = \frac{c}{3} \sqrt{\frac{1}{2\pi} \int_{-\infty}^{\infty} S_{Hc}(\omega) |\Phi''(j\omega)|^2 d\omega}, \quad (\text{VI. 35})$$

in which c is the speed of propagation of electromagnetic energy; $S_{bD}(\omega)$ is the spectral density of the interference voltage at the output of the time discriminator¹ (Note: 1. The expression for $S_{bD}(\omega)$, provided that the time error signal does not extend beyond the limits of the linear portion of the time discriminator curve and the target pulses are not limited in amplitude, will be found in reference [9]); $S_{Hc}(\omega)$ is the spectral density of error signal ϵ_{Hc} due to the unstable operation of the time delay device; $\Phi'(j\omega) = \frac{W'(j\omega)}{1 + W(j\omega)}$ is the frequency characteristic of a closed



Frequency Characteristics of Automatic Tracking Systems in Range

Table VI. 1

	$\Phi' (j\omega)$	$\Phi'' (j\omega)$
Automatic System of Tracking in Range	$\frac{j\omega}{K_A (1 + j\omega T_{ACD})}$	$\frac{j\omega}{K_A (1 + j\omega T_{ACD})}$
With a single integrator (Fig. VI. 12a)	$\frac{j\omega}{K_A (1 + j\omega T_{ACD})}$	$\frac{j\omega}{K_A (1 + j\omega T_{ACD})}$
With one integrator and an aperiodic discriminator (Fig. VI. 12b)	$\frac{1 + j\omega T_{D, \Delta}}{K_{n, \Delta} (\omega^2 T_{D, \Delta}^2 - j2\omega T_{ACD} - 1)}$	$\frac{\omega^2 T_{D, \Delta}^2 - j\omega}{K_A (\omega^2 T_{D, \Delta}^2 - j2\omega T_{ACD} - 1)}$
With one integrator and boosting element (Fig. VI. 15a)	$\frac{K_1 (\omega^2 T_K - j\omega)}{K_{n, \Delta} [\omega^2 + K_2 + j (\omega^2 T_{D, \Delta} - \omega T_K K_2)]}$	$\frac{\omega^2 (1 + j\omega T_{D, \Delta})}{(\omega^2 - K_1) - j\omega (\omega^2 T_{D, \Delta} - K_2 T_K)}$
With two integrators and a boosting element (Fig. VI. 15b)	$\frac{qK_1 (\omega^2 T_K - j\omega)}{K_A [(\omega^2 - qK_2) + j\omega (\omega^2 T_K - qK_1 T_K)]}$	$\frac{\omega^2 (1 + j\omega T_K)}{(\omega^2 - K_1) + j\omega (\omega^2 T_K - K_2 T_K)}$
With two integrators and correction for misalignment (Fig. VI. 15c)	$\frac{K_A [\omega^2 (K_1 K_2 + K_{n1} T_{n, \Delta}) + j\omega (\omega^2 T_{D, \Delta} K_2 - K_{n1})]}{K_{n, \Delta} [\omega^2 - K_2 K_{n1}] + j\omega (\omega^2 T_{D, \Delta} - K_1 K_2)}$	$\frac{\omega^2 (1 + j\omega T_{D, \Delta})}{(\omega^2 - K_1 K_{n1}) + j\omega (\omega^2 T_{D, \Delta} - K_2 K_1)}$

Reproduced from best available copy.

system error signal due to noise; $\Phi^*(j\omega) = \frac{1}{1+W^*(j\omega)}$ is the frequency characteristic of a closed system for the error Δt_{HC} ; $W(j\omega)$ is the frequency characteristic of an open system; $W^*(j\omega)$ is the frequency characteristic of an open system without time discriminator.

Expressions for frequency characteristics $\Phi'(j\omega)$ and $\Phi''(j\omega)$ of automatic range tracking systems are given in table VI. 1.

The mean square range tracking error due to input noise depends on the passband (width of frequency characteristic) of the automatic range tracking system. This error decreases as the system passband decreases. However, it should be borne in mind that as the band is decreased there is a restriction in the frequency spectrum of useful input signal passed by the system, and, therefore, there is an increase in the dynamic tracking error. For that reason the passband of automatic range tracking systems is selected on the basis of compromising considerations.

6. Operating Principles of Automatic Systems of Tracking for Azimuth With Systematic Comparison of Signals

General Information

Automatic systems for tracking in azimuth with successive comparison of signals are continuous operating tracking systems with a single channel for the reception of target signals. Here, formation of the error signal which automatically causes the axis of the antenna system to coincide with the line of sight to the target is achieved by comparing the amplitudes or the phases of the echoes received. Amplitude methods for comparing signals are most commonly used in shipborne radar sets with automatic systems of tracking for azimuth; only one antenna is required. Phase comparison methods require the use of two antennas separately spaced in the plane of the coordinate measured, and four antennas are needed when tracking a target in two planes -- azimuth and elevation.

Depending on the method used in forming the equisignal zone, amplitude systems of azimuth tracking are divided into conical and linear antenna beam scanning systems. The latter, in turn, are subdivided into systems with scanning in one plane and systems with scanning in two mutually perpendicular planes. Automatic systems of tracking for azimuth with conical and linear scanning of the radiation pattern in two planes are used when it is necessary to insure simultaneous tracking of the target by two angular coordinates.

Conical scanning of a radio beam is accomplished either by rotating the exciter, which is located a certain distance away from the focus of the parabolic reflector, or by rotating the reflector about the axis which is not aligned with the direction of maximum radiation of the major lobe of the antenna's radiation pattern. Linear scanning of an antenna radiation pattern in the plane of the tracked coordinate is achieved by successively switching into the radar receiving and transmitting circuits two fixed

exciters disposed symmetrically with respect to the focal axis of the reflector. The successive commutation of exciters is accomplished mechanically or with a ferrite circulator.

In both conical and linear scanning the direction of maximum radiation or reception is shifted relative to the equisignal line by a certain angle γ , the magnitude of which substantially affects precision of tracking and the effective range of the system. The optimal value of angle γ is equal to

Reproduced from
best available copy.

$$\gamma_{opt} \approx 0,4\beta_0,$$

(VI. 35)

in which β_0 is the aperture angle of the major lobe of the radiation pattern through the half power points.

The value of γ_{opt} which is determined by means of formula (VI. 36) is not critical. Decreasing γ makes it possible, at some sacrifice of accuracy in the equisignal method, to extend the operating range and improve the resolution of the system for a particular coordinate; conversely, increasing γ results in greater accuracy with a reduction in range and lowered resolving power. In practical work, therefore, depending on the specific requirements imposed on a system relative to accuracy in direction finding and range of action, angle γ is so selected that the power of the signal received, without error voltage, be no less than 0.8 - 0.65 and rarely 0.5 of the maximum value.

In the case where the antenna is set for receiving only

$$\gamma_{opt} \approx 0,6\beta_0.$$

(VI. 37)

Automatic Systems of Tracking for Azimuth With Conical Scanning

The basic layout of automatic systems for tracking in azimuth with conical scanning of the antenna beam is described in the block diagram shown in Fig VI. 16; such systems vary as to purpose and area of installation.

Figure VI 17 shows the curves of signals at the most characteristic points. The diagrams are offered for those instances where the target deflects away from the equisignal axis (Ox_{p3}) by a certain spatial angle $0 < \gamma$.

The system operates as follows. The scanning motor causes the axis of the radio beam to describe a conical surface in space at a frequency of Ω . This same electric motor turns a two phase generator rotor synchronously with the antenna radiation pattern. The generator develops the azimuthal reference voltage $u_{\alpha} = U_{on} \sin \Omega t$ and the elevation reference voltage $u_{\epsilon} = U_{on} \cos \Omega t$. These voltages are fed without conversion or after conversion into square waves into appropriate phase detectors.

If the antenna axis (equisignal line) does not coincide with the line of sight to the target, i.e. if there is a misalignment error θ , a periodic succession of pulses u_{np} is taken off the receiver output; these are amplitude modulated with an envelope determined by the expression

$$u_{np} = U_{np0} [1 + m \cos(\Omega t + \psi_0)],$$

in which U_{np0} is the amplitude of the signal received when $\theta = 0$; m is the depth of amplitude modulation of radio pulses at the input of the receiver; Ω is the circular frequency of rotation of the antenna beam; ψ_0 is the angular coordinate of the target in a plane perpendicular to the antenna axis, and, accordingly, it is the initial phase of the envelope (measuring from the vertical half plane).

When the misalignment error of $\theta < \gamma$ (tracking cycle) the depth of amplitude modulation is equal to

$$m = \mu \theta$$

in which μ is the slope of the direction finder curve.

When $\theta > \gamma$ (operating cycle during which the equipment locks on the target for automatic tracking) modulation becomes non-sinusoidal and the second harmonic is the most intensive of the higher harmonics.

The periodic sequence of pulses u_{np} proceeds to the error signal meter. To separate out the error signal of frequency Ω i.e. the voltage $u_{co} = U_{co} \cos(\Omega t + \psi_0)$ use is made in the metering devices of peak detectors with a time constant for the discharge circuit of $T_p \ll T$ and resonance filters tuned to the basic harmonic of the amplitude-modulated pulse envelope.

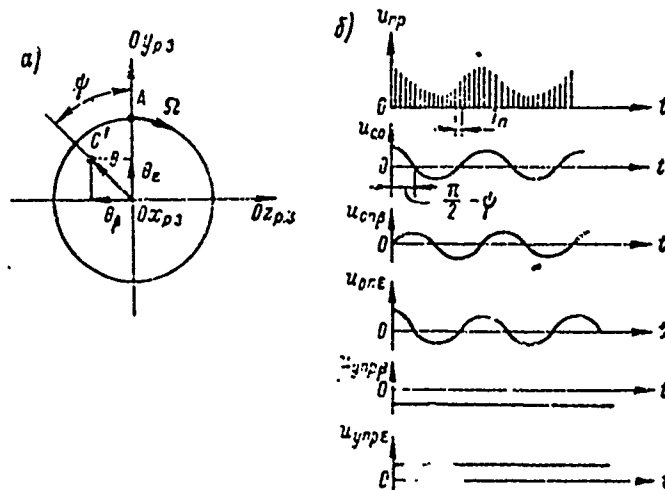


Fig. VI. 17. Component errors of θ in a plane perpendicular to the axis of the antenna (a) and voltage curves of the circuit shown in Fig. V. 16b.

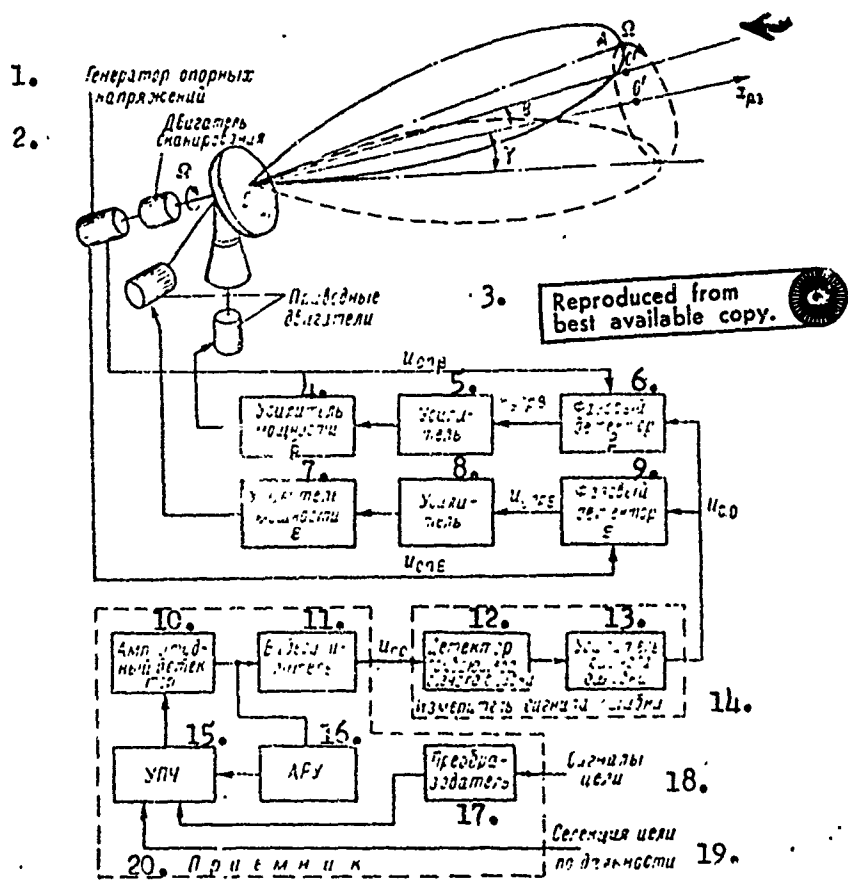


Fig. VI. 16. Block diagram of system for automatic tracking of target in azimuth with conical scanning.

KEY: 1. Reference voltage generator; 2. scanning motor; 3. drive motors; 4. power amplifier; 5. amplifier; 6. phase detector; 7. power amplifier; 8. amplifier; 9. phase detector; 10. amplitude detector; 11. video amplifier; 12. signal error envelope detector; 13. error signal amplifier; 14. error signal meter; 15. IF amplifier; 16. automatic gain control AGC; 17. converter; 18. target signals; 19. target selection in range; 20. receiver.

An automatic system of tracking for azimuth can operate normally only if the error signal amplitude is independent of target dimensions and its distance from the radar set. In actual practice the constancy of U_{co} for various distances away from the target and for various effective reflecting surfaces of targets is insured by the use in the receiver of an automatic gain control system which changes the gain in a manner inversely proportional to the mean value of the pulses. In order that no noticeable demodulation may occur on account of the automatic gain control operation to the error signal, which carries the information about the angular position θ of the target relative to the equisignal direction, the gain control system should have a sufficient degree of inertia with respect to the oscillations of the frequency Ω .

The error signal voltage obtained, whose amplitude is proportional only to the magnitude of angle θ while its phase unambiguously determines the direction to the target, is fed to the two phase detectors. In the phase detectors the error signal voltage is broken down into two direct current voltages, one of which, $u_{\text{ynp}\beta}$, is proportional to the deflection of the target in the azimuthal plane, while the other, $u_{\text{ynp}\epsilon}$, is proportional to the deflection of the target in the elevation plane. /465

The controlling voltage of each channel is amplified and fed to the appropriate drive motor. The latter rotates the antenna in a manner so that $\theta = 0$.

Direct current motors operating jointly with electromechanical amplifiers are most frequently used for driving antennas. Two phase motors with bell-shaped hollow rotors and magnetic amplifiers are used in some systems.

The antenna scanning frequency Ω is the carrier for the input value (movement of target), therefore its lower limit is taken at 5 to 10 times greater than the frequency of the essential harmonics of the input value. The upper frequency limit of conical beam scanning in space is determined by the mechanically feasible speeds of rotation of the antenna elements. Usually, the frequency of present day automatic azimuth tracking systems is between 20 and 100 revolutions per second.

Automatic Systems of Tracking for Azimuth With Linear Scanning

The block diagram of a typical automatic system of tracking for azimuth with linear scanning of the antenna radiation pattern in two mutually perpendicular planes is shown in Fig. VI. 18. Scanning in the azimuthal plane is done by alternately switching in the exciters 1a and 2a to the receiver; in the elevation plane it is done by switching in exciters 1b and 2b. The exciters are switched in to the receiver by means of a ferrite circulator controlled by a commutator. During the first half period of switching, $T_k/2$, the exciters 1a - 2a are switched in, and during the second half period the exciters 1b - 2b are switched in or the other way around. Each exciter remains switched to the receiver for

the period $T_k/2n$ in which n is the number of connections made during a half period.

If the target is on the equisignal zone axis Ox_p , a periodic succession of constant amplitude video pulses is obtained at the receiver output during both half periods of commutation. When the target is displaced from the equisignal line by a certain spatial angle θ amplitude modulation occurs. The pulse envelopes in each half period $T_k/2$ will be square shaped waves. The square wave of the elevation channel is shifted in phase by $\pi/2$ relative to the envelope of the azimuth signal channel. For small values of θ the amplitudes of these envelopes are proportional, respectively, to the θ_β and θ_ϵ components of angle θ , and the phases relative to the reference voltages $u_{0\eta\beta}$ and $u_{0\epsilon}$ developed by the commutator are determined by the direction of deflection of the target.

Inasmuch as the azimuth and elevation channels are identical and operate independently of one another the voltage curves in Fig. VI. 19 are given only for the azimuth channel. The voltage curves $u_{\eta\beta\epsilon}$, $u_{0\epsilon}$, and $u_{0\eta\epsilon}$ differ from the curves of the azimuth channel corresponding to them by the fact that they are shifted in phase by $\pi/2$.

After separating out the $u_{0\beta}$ and $u_{0\epsilon}$ envelopes in the error signal meter they are fed to the phase detectors. As a result of comparison with a suitable reference azimuth at each phase detector output we get a control voltage. The value of this control voltage $u_{\eta\beta}$ is determined by the degree of deflection of the target from the equisignal plane that passes through the Ox_p and Oy_p axes, the sign being determined by the direction of the deflection. The value of the voltage $u_{\eta\epsilon}$ is determined by the degree of deflection of the target from the plane passing through the Ox_p and Oz_p axes while the sign is determined by the direction of deflection away from this plane.

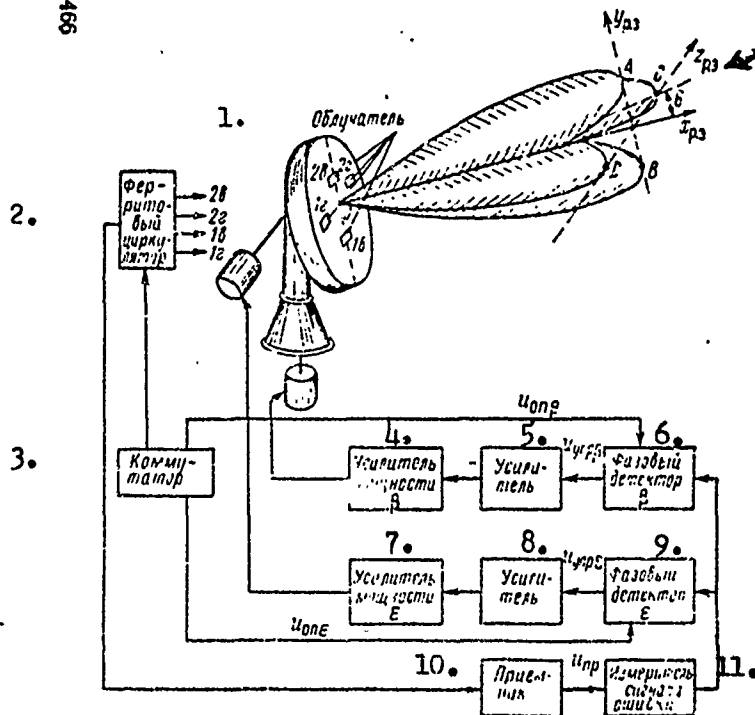
After amplification, the control voltages act on appropriate electric motors which rotate the antenna until the error signal θ becomes zero.

In the automatic system of tracking for azimuth with linear scanning the amplification and error signal conversion channel, as well as the servo mechanisms are not dissimilar to those found in the azimuth tracking systems with conical scanning.

The frequency of scanning cone flipping in one plane varies between 20 and 50 cycles. Moreover, the frequencies may differ for different scanning planes.

Automatic Systems of Tracking for Azimuth With Phase Direction Finders

In automatic systems of tracking for azimuth with phase direction finders



Reproduced from
best available copy.

Fig. VI. 18 Block diagram of automatic system of tracking for azimuth with linear scanning in two mutually perpendicular planes.

KEY: 1. Exciter; 2. ferrite circulator; 3. commutator; 4. power amplifier; 5. amplifier; 6. phase detector; 7. power amplifier; 8. amplifier; 9. phase detector; 10. receiver; 11. error signal meter.

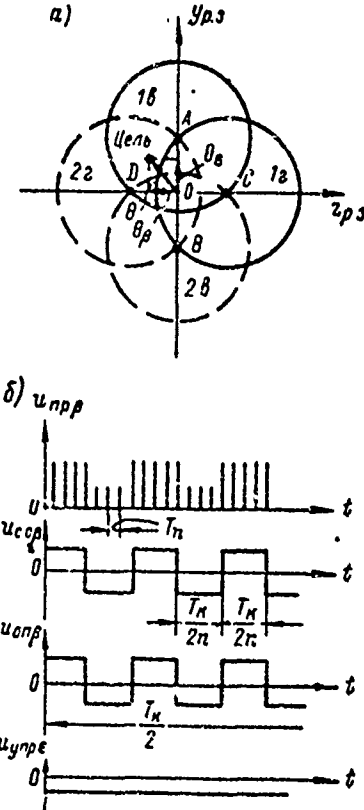


Fig. VI. 19. Components of error signal O in the plane perpendicular to the equisignal zone axis (a), and voltage curves of azimuth channel in the circuit shown in Fig. VI. 18 (b)

[8, 9, 11] and successive comparison of target signals received the azimuth and elevation tracking channels are similar both in operating principle and mechanical design. The block diagram of Fig. VI. 20 is basic to both. The system works as follows. Separated antennas are successively switched in to the error signal phase detector by means of a ferrite circulator controlled by a commutator. A voltage u_{CP} from a synchronous oscillator is fed to this detector to provide information about the angular position of the target relative to the equisignal line. /468

The oscillations of the synchronous oscillator should be synchronized and phased with the oscillations generated for illuminating the target. Therefore, in the automatic systems of tracking for azimuth under consideration the synchronous local oscillator function is performed either by the oscillator in the transmitting system or by an auxiliary, low directivity receiving antenna whose axis coincides with the equisignal line of the main antenna. In both cases additional corrections are made to the phase of the u_{CP} voltage with the aid of a phase inverter. The phase φ_C of the u_{CP} voltage is so selected that if the target is located on the equisignal line the error signal u_{CO} will be equal to zero.

The voltage developed by the error signal phase detector is amplified and then passed to the second phase detector where it is compared with the reference voltage. The reference voltage is the signal of the commutator which controls the operation of the ferrite circulator. The controlling voltage from the second detector is amplified and fed to the antenna rotating motor.

The maximum speed of operation of the automatic system of tracking for azimuth with phase direction finder and successive comparison of signals is determined by the signal averaging time at the input to the second detector; it amounts to several periods of the commutator T_k .

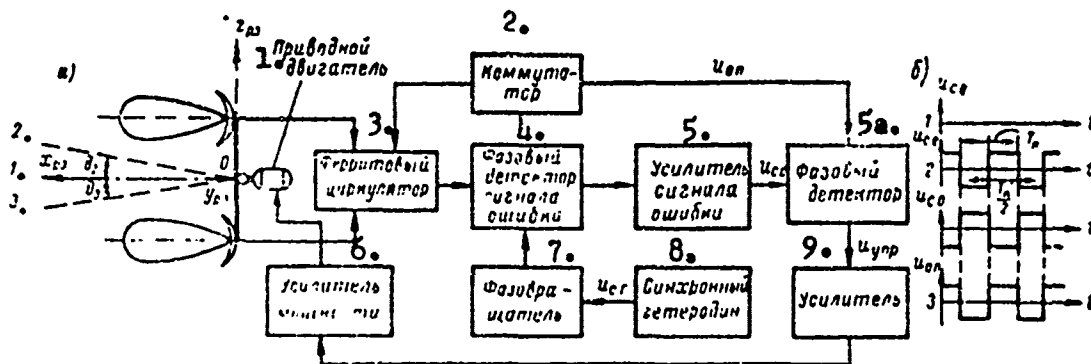


Fig. VI. 20. Simplified block diagram of an automatic system of tracking for azimuth with phase direction finder and successive comparison of signals (a) and voltage curves of error signal u_{CO} for three positions of target relative to the Ox_p axis and the reference voltage u_{CP} (b).

KEY: 1. Drive motor; 2. commutator; 3. ferrite circulator; 4. error signal phase detector; 5. error signal amplifier; 5a. phase detector; 6. power amplifier; 7. phase inverter; 8. synchronous oscillator; 9. amplifier.

7. Operating Principles of Automatic Systems for Tracking in Azimuth With Simultaneous Comparison of Signals

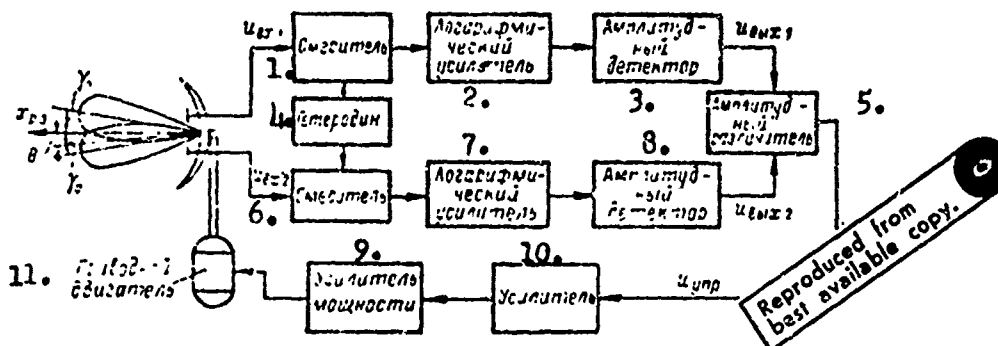
General Information

Automatic azimuth tracking systems with simultaneous comparison of signals are continuous operation tracking systems.

Depending on the principles of direction finding used, monopulse automatic azimuth tracking systems are divided into two types: amplitude tracking systems and phase tracking systems. / 469

Systems of Automatic Tracking for Azimuth With Separate Utilization of Signals

Generally, the amplitude, monopulsed automatic system of tracking for azimuth consists of two closed, independently operating tracking systems: azimuth and elevation systems. The operating principles of these systems are identical.



KEY: 1. Mixer; 2. logarithmic amplifier; 3. amplitude detector; 4. local oscillator; 5. amplitude discriminator; 6. mixer; 7. logarithmic amplifier; 8. amplitude detector; 9. power amplifier; 10. amplifier; 11. drive motor

Fig. VI. 21. Block diagram of a monopulsed automatic system of tracking for azimuth with amplitude direction finder.

The basis of the automatic system of target tracking by only one angular coordinate is seen in the simplified diagram of Fig. VI. 21. The transmitter and auxiliary devices for selecting targets in range are not shown in this diagram.

To describe the equisignal zones coinciding with the plane of the coordinate being measured, the radiation patterns of two antennas are shifted by the angle $2\gamma_0$ determined by formula (VI. 36) when the antennas are operating on reception and transmission, and by formula (VI. 37) when the equipment is for operation on reception only.

Each antenna or exciter shifted with respect to the paraboloid axis is

is switched to a particular signal converter channel. When the target is deflected from the equisignal line Ox_{p3} by a certain angle θ the following voltages will appear on the converter channels: / 470

$$\begin{aligned} u_{u1} &= KF(\gamma_0 \mp \theta) \sin \omega t; \\ u_{u2} &= KF(\gamma_0 \pm \theta) \sin \omega t. \end{aligned}$$

in which K is a coefficient which is a function of the signal strength and antenna voltage gain; $F(\dots)$ is the standardized antenna voltage radiation pattern; γ_0 is the angle between the line of maximum radiation of the directivity pattern and the antenna equisignal line.

These voltages are amplified in the intermediate frequency by logarithmic amplifiers and then fed to the amplitude discriminator (of the subtracting device). In order that a comparison of signal amplitudes only may occur within it these voltages are first passed through the amplitude detectors before being fed into the subtracting device.

After comparing the amplitudes of two simultaneously received signals the control voltage at the output of the direction finding device is equal to

$$u_{yfp} = K_{a.p}(u_{u1} - u_{u2}) = K_{a.p} U_{max,0} \ln \frac{F(\gamma_0 \mp \theta)}{F(\gamma_0 \pm \theta)}, \quad (VI. 38)$$

in which $K_{a.p}$ is the amplitude discriminator gain; U_{DBIX_0} is the initial output voltage of the logarithmic amplifier.

At small angles of target deflection from the equisignal line $\mu \theta \ll 1$ where μ represents the direction finder sensitivity or the absolute value of the relative slope of the radiation pattern at the point of their intersection, the voltage u_{yfp} will be determined as follows:

$$u_{yfp} \approx 2K_{a.p} \mu \theta U_{max,0} \approx 2K_0 \mu \theta, \quad (VI. 39)$$

in which $K_0 = K_{a.p} U_{DBIX_0}$.

The values of direction finder sensitivity for an approximation of patterns by various functions are given in Table VI. 2.

Logarithmic amplifiers are used to eliminate the effects of a strong received signal and the gain of the receiver on the slope of the direction finder curve of the system. In a simple subtraction of detected and amplified signals the control voltage u_{yfp} and, therefore, the slope of the direction finder characteristic curve would depend not only on the error signal angle but also on the factors mentioned above. By using logarithmic amplifiers, however, this drawback is eliminated since the control voltage is proportional not to the difference in amplitudes of the signals received but to the quotient of the division of amplitudes.

Amplitude boosting imposes specific requirements on the parameters

Table VI. 2

Direction Finder Sensitivity Values

Type of approximation of radiation pattern	Values of Coefficient	
	Antenna operating on reception only	Antenna used for reception and transmission
$F(\beta) = \frac{\sin 2,81 \frac{\beta}{\beta_0}}{2,81 \frac{\beta}{\beta_0}}$	$\frac{2,81}{\beta_0} \operatorname{ctg} 2,81 \frac{\gamma_0}{\beta_0} - \frac{\beta_0}{\gamma_0}$	$\frac{5,62}{\beta_0} \operatorname{ctg} 2,81 \frac{\gamma_0}{\beta_0} - 2 \frac{\beta_0}{\gamma_0}$
$F(\beta) = \cos^2 1,14 \frac{\beta}{\beta_0}$	$\frac{2,3}{\beta_0} \operatorname{ctg} \frac{1,14 \gamma_0}{\beta_0}$	$\frac{4,6}{\beta_0} \operatorname{ctg} \frac{1,14 \gamma_0}{\beta_0}$
$F(\beta) = e^{-1,3 \left(\frac{\beta}{\beta_0} \right)^2}$	$2,81 \left(\frac{\gamma_0}{\beta_0^2} \right)$	$5,6 \left(\frac{\gamma_0}{\beta_0^2} \right)$
$F(\beta) = \frac{J_1 \left(\frac{2\pi}{\lambda} R_0 \sin \beta \right)}{\frac{\pi}{\lambda} R_0 \sin \beta}$ <p>A. — функция Бесселя первого рода первого порядка; B. — радиус раскрытия антенны</p>	$\frac{\pi}{4\beta_0^2} \gamma \quad 2,16 \left(\frac{\gamma_0}{\beta_0^2} \right)$	$\frac{\pi^2}{24\beta_0^2} \quad 4,92 \left(\frac{\gamma_0}{\beta_0^2} \right)$

A. — in which J_1 is a first order Bessel Function of the first kind;

B. — is the radius of the antenna aperture.

Reproduced from best available copy.

of each of the channels in the radio system. If there is any inequality in the gain of the separate channels errors will crop up in determining the equisignal direction. Special measures should be taken to maintain similar and stable transfer constants in both amplification channels.

The voltage $U_{\text{гнр}}$, amplified beforehand, whose magnitude is proportional to the absolute value of the error signal θ and whose sign determines the direction of deflection of the target from Ox_p , is fed to the servo mechanism motor in the system to match the equisignal line with the direction to the tracked target. The motor will rotate the antenna toward the target as long as the displacement angle θ is other than zero.

Amplitude Systems in Automatic Tracking for Azimuth With Sum and Difference Processing

In these systems the signal amplitudes of both channels are compared directly at the antenna outputs before they reach the receiver. This kind of comparison of signals greatly reduces the requirements for equality of gain by the receiving channels of the system, and, therefore, it insures higher tracking accuracy.

Comparison or algebraic summation of high frequency signals is accomplished either through the use of "double T" waveguide bridges (Fig. VI. 22a) or waveguide (hybrid) rings (Fig. VI. 22b). Both types of waveguide devices are the same as to characteristics for receiving sum and difference signals. However, the waveguide ring is more sensitive to changes in wavelength and is more compact since it is disposed in a single plane.

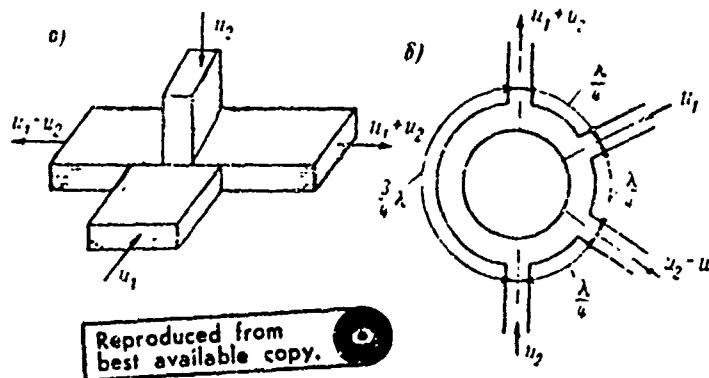


Fig. VI. 22. Waveguide devices for receiving the sum and difference of two signals: a. double "T-shaped" waveguide bridge; b. hybrid ring.

The type circuit shown in Fig. VI. 23 is the basis of multi-channel systems of automatic target tracking in two planes. Shown in Fig. VI. 24 are the directional characteristics of an antenna system used for a summation channel (Fig. VI. 24a) and two difference channels (Fig. VI. 24b, c).

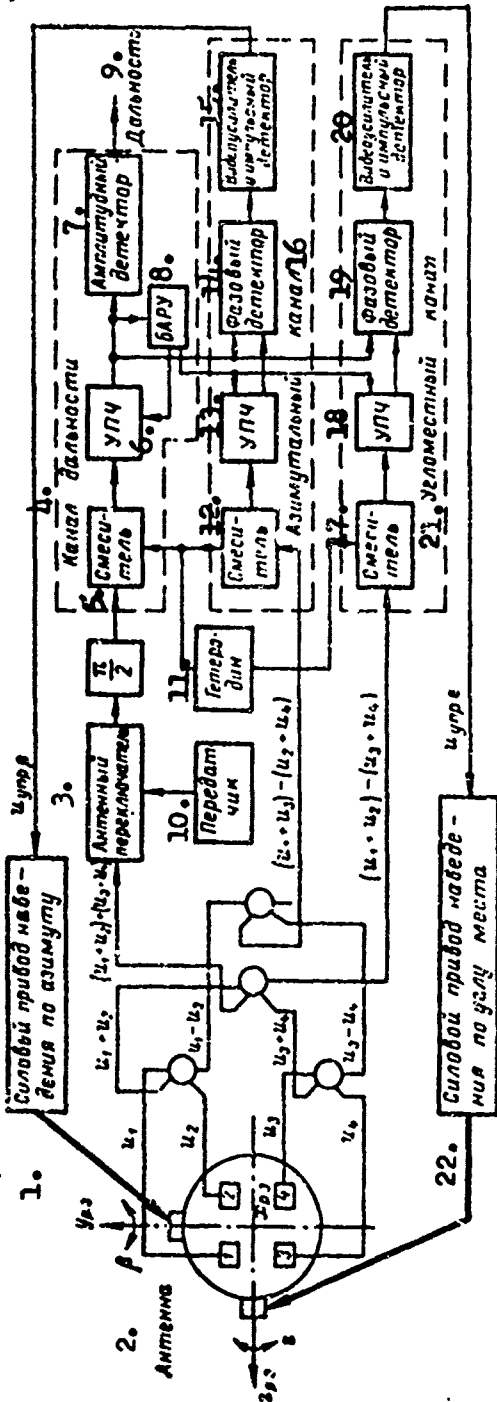


Fig. VI. 23. Block diagram of an amplitude monopulsed automatic system of tracking in azimuth with sum and difference processing.

KEY: 1. Azimuth steering drive; 2. antenna; 3. antenna switch; 4. range channel; 5. mixer; 6. IF amplifier; 7. amplitude detector; 8. fast-acting automatic gain control; 9. range; 10. transmitter; 11. local oscillator; 12. mixer; 13. IF amplifier; 14. phase detector; 15. video amplifier and pulse detector; 16. azimuth channel; 17. mixer; 18. IF amplifier; 19. phase detector; 20. video amplifier and pulse detector; 21. elevation channel; 22. elevation pointing drive.

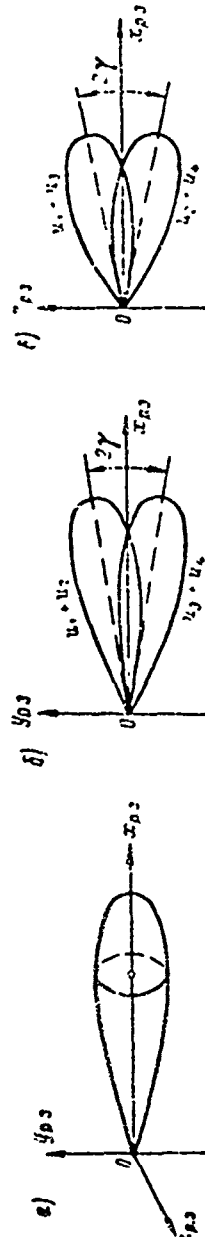


Fig. VI. 24. Antenna radiation patterns; a. range channel; b. elevation error channel; c. azimuth error channel.

99-

The system operates as follows. Three signals are formed from the voltages $u_1, u_2, u_3,$ and u_4 taken off the separately disposed antenna exciters:

summation signal

$$U_{\Sigma} = K [(u_1 + u_2) + (u_3 + u_4)] = \\ = 2K [F(\gamma \mp \theta_{\Sigma}) + F(\gamma \pm \theta_{\Sigma})] \sin(\omega t + \varphi_0);$$

two difference signals

$$u_{\beta} = K [(u_1 + u_3) - (u_2 + u_4)] = \\ = 2K [F(\gamma \mp \theta_{\beta}) - F(\gamma \pm \theta_{\beta})] \sin(\omega t + \beta_0); \\ u_{\Sigma} = K [(u_1 + u_2) - (u_3 + u_4)] = \\ = 2K [F(\gamma \mp \theta_{\Sigma}) - F(\gamma \pm \theta_{\Sigma})] \sin(\omega t + \beta_0).$$

in which K is the factor taking into account antenna gain and signal attenuation in the summation devices; $F(\dots)$ is the standardized radiation pattern; γ is the angle between the maximum radiation direction and the reflector axis--the optimum magnitude of this angle is determined from the conditions set forth in (VI. 36) or (VI. 37); $\theta_{\beta}, \theta_{\Sigma}$ are the azimuthal and angular displacements of the target relative to the paraboloid axis; φ is the fixed phase angle constant.

The signals $u_{\Sigma}, u_{\beta},$ and u_{Σ} go to the input of the three channel superheterodyne receiver. In order that the range voltage u_{Σ} simultaneously be the reference voltage for the azimuthal and elevation signals it is first shifted in phase by the angle $\pi/2$. In the receiver all three signals are converted into intermediate frequency signals, amplified in that frequency, and then fed to the appropriate phase detectors. In the phase detectors the azimuthal signal and the angular elevation signal are multiplied by the reference signal.

Direct current pulses, whose amplitude and polarity impart the magnitude and sign for angles θ_{β} and θ_{Σ} respectively, are taken off the phase detectors of the azimuthal and elevation channels. In order that the amplitude of these pulses may not be dependent on changes in amplitudes of the summation channel signal (range channel) fast response automatic gain control systems operating from the summation channel are used in systems of tracking for azimuth with sum and difference processing of signals. During the process of automatically tracking a target the fast response automatic gain control maintains a fixed signal amplitude at the output of the summation channel and develops a gain control voltage for the azimuth and elevation channels whose change is inversely proportional to the amplitude voltage at the input to the summation channel. Therefore, after the direct current pulses pass through the appropriate video amplifiers and pulse detectors they are converted into controlling voltage

$$U_{\text{ynp } \beta} = \frac{K_{\beta} K_{\text{av}} U_0 [F(\gamma \mp \theta_{\beta}) - F(\gamma \pm \theta_{\beta})]}{K_{\text{per}} [F(\gamma \mp \theta_{\Sigma}) + F(\gamma \pm \theta_{\Sigma})]}; \quad (\text{VI.40})$$

$$U_{\text{ynp } \Sigma} = \frac{K_{\Sigma} K_{\text{av}} U_0 [F(\gamma \mp \theta_{\Sigma}) - F(\gamma \pm \theta_{\Sigma})]}{K_{\text{per}} [F(\gamma \mp \theta_{\Sigma}) + F(\gamma \pm \theta_{\Sigma})]}; \quad (\text{VI.41})$$

in which $K_{\Phi A}$ and $K_{\Phi Y}$ are the transfer coefficients of the phase detector and video amplifier, respectively; U_0 is the amplitude of the output signal of the summation channel if it has a quick response automatic gain control; and K_{per} is the transfer coefficient of the quick response automatic gain control. The power voltages $u_{\text{vnp}\beta}$ and $u_{\text{vnp}\epsilon}$ enter the power drive mechanisms which rotate the antenna until the axis of the paraboloid coincides with the direction toward the target, i.e. when θ_β and θ_ϵ are equal to zero.

Phased Systems of Automatic Tracking for Azimuth

Automatic systems for tracking in azimuth with phased direction finders [9] by the method of changing the spatial position of the equisignal line are divided into the system with mechanical rotation of the antenna and the phase delay (Fig. VI. 25) system.

If there is an angular difference in θ between the direction to the target and the position of the equisignal line Ox_0 , the signals at the output of both antennas are determined by the expressions:

$$u_1 = K_n F(\theta) \left(\omega t + \frac{\pi}{\lambda} d \sin \theta \right);$$

$$u_2 = K_u F(\theta) \left(\omega t - \frac{\pi}{\lambda} d \sin \theta \right),$$

in which K_n is the proportionality factor depending on the signal strength and the antenna gain; $F(\dots)$ is the standardized antenna radiation pattern; λ is the wavelength; d is the distance between antenna foci (base).

The signals u_1 and u_2 are amplified in the appropriate channels of the two channel superheterodyne receiver. To get a direction finding response curve with central symmetry the signal is shifted in phase by the angle $\pi/2$ in one of the receiver channels. Uniformity in the slope of the DF response curve is insured either through automatic gain control devices or by utilizing signal amplitude limiters in the IF amplifier channels.

The following voltages are taken from the intermediate frequency amplifier outputs:

for circuits described in Fig. VI. 25a

$$u_1' = U_{n. \epsilon} \sin \left(\omega_{n. \epsilon} t + \frac{\pi}{2} \right);$$

$$u_2' = U_{n. \beta} \sin \left(\omega_{n. \beta} t - \frac{\pi}{2} \right);$$

For circuits shown in Fig. VI. 25b

$$u_1'' = U_{\text{orp}} \sin \left(\omega_{n. \epsilon} t + \frac{\pi}{2} \right);$$

$$u_2'' = U_{\text{orp}} \sin \left(\omega_{n. \beta} t - \frac{\pi}{2} + \psi \right),$$

in which $U_{\text{пч}}$ is the amplitude of signal pulses at the IF amplifier output whose magnitude is stabilized by the automatic gain control system; ω is the intermediate frequency; $\varphi = 2\pi/\lambda d \sin \theta$ is the phase difference of signals received from the dispersed antennas; $U_{\text{орп}}$ is the amplitude of signal pulses at the output of the limiter; ψ is the variable phase shift introduced by the phase converter.

The signals u'_1 and u'_2 are fed to the phase detector which performs the function of a phase discriminator in these systems. From u'_1 and u'_2 at the phase discriminator output a periodic sequence of direct current pulses is formed. The sequence is determined for the circuit in Fig. VI. 25a by the expression

$$u_{\text{yрп}} = K_{\phi, \text{п}} U_{\text{пч}} \sin \left(\frac{2\pi}{\lambda} d \sin \theta \right), \quad (\text{VI. 42})$$

and for the circuit in Fig. VI. 25b by

$$u_{\text{yрп}} = K_{\phi, \text{п}} U_{\text{орп}} \sin \left(\frac{2\pi}{\lambda} d \sin \theta - \psi \right), \quad (\text{VI. 43})$$

in which $K_{\phi, \text{п}}$ is the transfer coefficient of the phase discriminator.

At small angles of error of θ the voltage at the phase discriminator output is equal to

$$u_{\text{yрп}} = K_{\phi, \text{п}} U_{\text{пч}} \sin \frac{2\pi}{\lambda} d \theta; \quad (\text{VI. 44})$$

$$u_{\text{yрп}} = K_{\phi, \text{п}} U_{\text{орп}} \sin \left(\frac{2\pi}{\lambda} d \theta - \psi \right). \quad (\text{VI. 45})$$

After conversion by the pulse detector and low frequency filter into direct current voltages they trigger appropriate drives which change the spatial position of the equisignal line. In the automatic system of tracking for azimuth shown in Fig. VI. 25a this is achieved by mechanically rotating the antenna mechanism, and in the system shown in Fig. VI. 25b it is achieved through the action on the phase inverter which controls the amount of phase delay in one of the channels of the system.

The marked advantage of the system with phase delay and fixed antenna is its quick response; this condition is possible because large masses do not have to be displaced mechanically.

8. Basic Elements of Systems for Tracking in Azimuth

Phase Detectors (Discriminators)

A phase detector is an electronic device used to convert the difference in phase of two signals having the same frequency into direct current voltage whose magnitude is generally proportional to the amplitudes of the signals, and whose polarity is a function of the phase differences of these voltages.

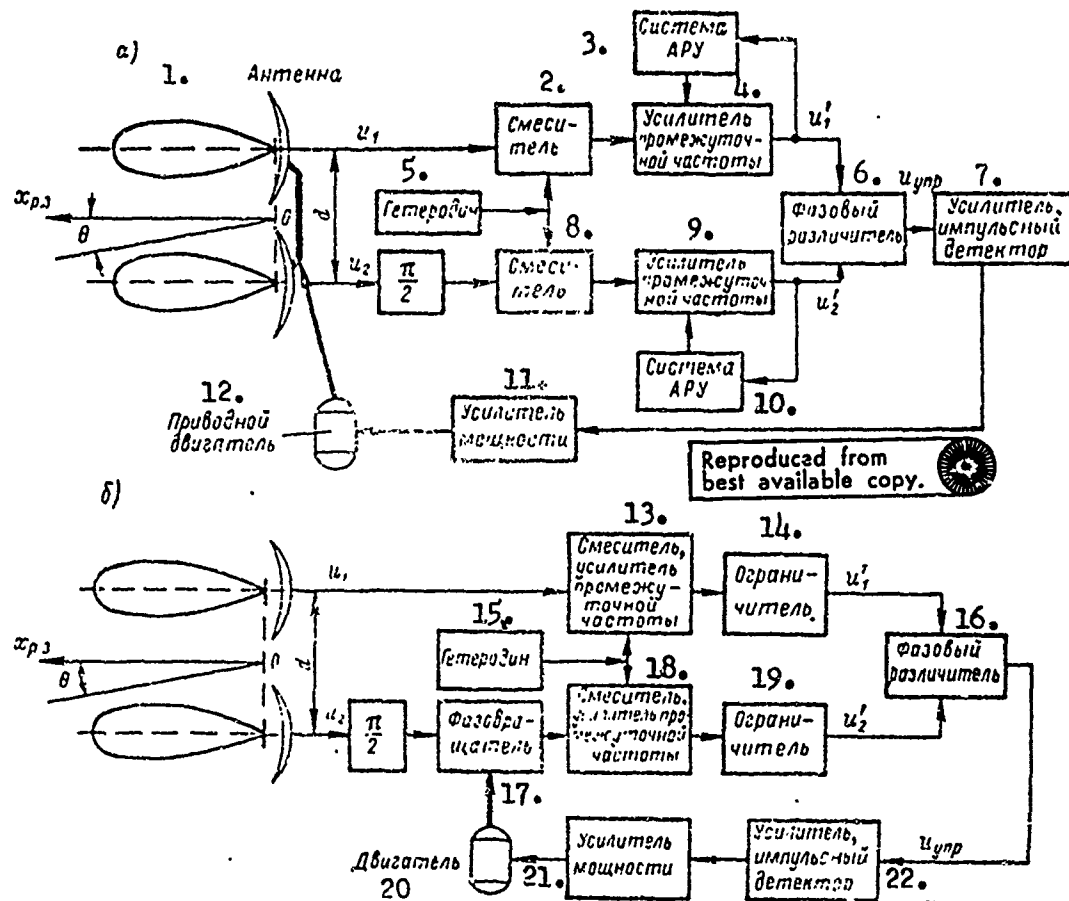


Fig. VI. 25. Block diagram of monopulse automatic systems of tracking in azimuth with phase direction finder: a - with mechanical rotation of antenna system; b. with phase delay.

KEY: 1. Antenna; 2. mixer; 3. automatic gain control system; 4. IF amplifier; 5. local oscillator; 6. phase discriminator; 7. amplifier, pulse detector; 8. mixer; 9. IF amplifier; 10. AGC system; 11. power amplifier; 12. drive motor; 13. mixer, IF amplifier; 14. limiter; 15. local oscillator; 16. phase discriminator; 17. phase inverter; 18. mixer, IF amplifier; 19. limiter; 20. motor; 21. power amplifier; 22. amplifier, pulse detector.

Phase detectors are divided into balanced and circular types. Balanced phase detectors are generally used in radar sets with automatic azimuth tracking systems. The detectors may be diodes or triodes.

Balanced diode detectors are designed in accordance with the circuit shown in Fig. VI. 26. Their operating principle is based on the addition and subtraction of an error signal voltage u_{BX} (of one signal) and a reference voltage u_{ON} (of a second signal). The output voltage of the device is equal to the difference in voltage drops across the resistances R_1 and R_2 .

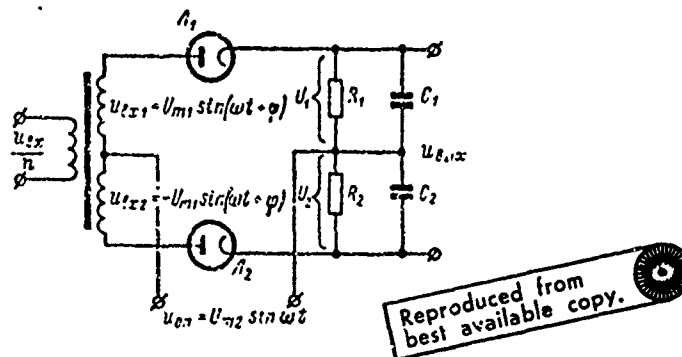


Fig. VI. 26. Schematic diagram of a diode balanced phase detector (in a balanced circuit $R_1 = R_2 = R$; $C_1 = C_2 = C$).

The following disadvantages are peculiar to diode phase detectors:

- they have a low transfer coefficient (less than two);
- the power required from the error signal source depends on the load connected to the output of the circuit;
- circuit balance depends on load balance;
- with large error signals it is difficult to insure the inequality $U_{m1} \ll U_{m2}$.

Triode phase detectors have better performance characteristics. They not only convert the signal but simultaneously amplify it. Depending on the method by which the error signal u_{BX} is fed triode phase detectors are divided into those with symmetrical input and those with asymmetrical input. The former may be single cycle or two cycle. The two cycle phase detector circuits differ from the single circuits in having not one but two pairs of triodes in a two cycle (push-pull) connection.

Amplitude Discriminators

An amplitude discriminator is an electronic or electromagnetic device (for example, a type of magnetic amplifier) whose output voltage is proportional to the difference of the instantaneous values of two input signals.

$$u_{\text{out}} = K_{a.p} (u_{BX1} - u_{BX2}), \quad (\text{VI. 46})$$

in which $K_{a,p}$ is the discriminator transfer coefficient; U_{BX1} and U_{BX2} are the instantaneous values of input signals.

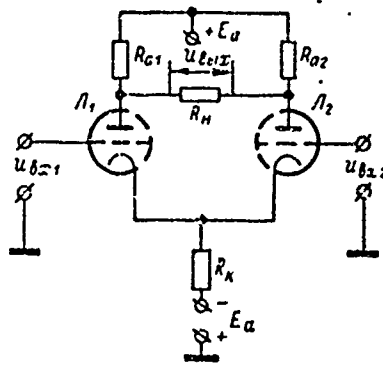


Fig. VI. 27. Circuit of an electronic amplitude discriminator

Because of the low input resistance of electromagnetic amplitude discriminators only electronic types of discriminators are used in azimuth tracking systems. Usually, these discriminators are designed according to a direct current symmetrical differential amplifier (Fig. VI. 27). Circuit symmetry is obtained by equalizing the plate loads ($R_{G1} = R_{G2} = R_G$) and having tubes with identical parameters. Due to the spread in tube parameters the circuits of electronic differential amplitude discriminators are not usually ideally symmetrical; instability of power supplies also affects the output signal. To decrease zero drift on account of instability of power supply, negative feedback, accomplished by applying a large cathode resistance R_k , is used in such circuits.

Actually, zero drift can be disregarded if R_k resistance values are selected in accordance with formula

$$R_k = (10 - j5) \frac{R_i + R_a}{\mu + 1}, \quad (\text{VI. 47})$$

in which R_i is the internal resistance in the tubes; μ is the tube amplification factor.

The transfer constant $K_{a,p}$ of the symmetrical amplitude discriminator depends on the parameters of the tubes used, and the magnitudes of the resistance R_G and load resistor R_H .

$$K_{a,p} = \frac{\mu}{1 + \frac{R_i}{R_G} + \frac{2R_i}{R_H}} \quad (\text{VI. 48})$$

in which $R_H \gg R_G$

$$K_{a,p} = \frac{\mu R_G}{R_i + R_G} \quad (\text{VI. 49})$$

Error Signal Meter

A device which separates out and amplifies an envelope from the periodic train of amplitude modulated video pulses from the output of the automatic azimuth tracking system with successive comparison of signals is known / 480 as an error (misalignment) signal meter.

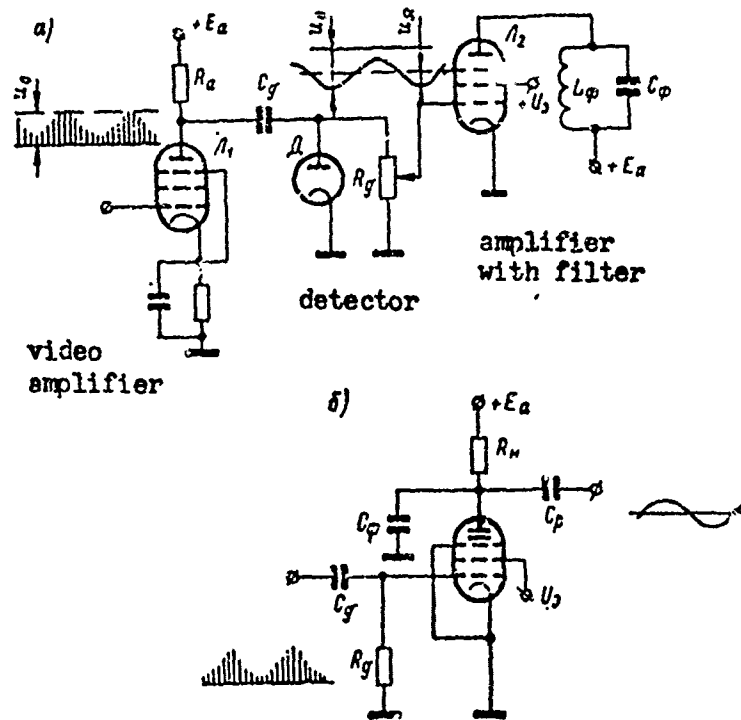


Fig. VI. 28. Error signal meter circuits.

Error signal metering circuits widely used in such systems are shown in Fig. VI. 28. In Figure VI. 28a the signal is demodulated by a separate diode detector, and in the circuit of Fig. VI. 28b demodulation is accomplished by an amplifier tube operating on grid detection.

A condition for non-distorted demodulation of the signal in these circuits is the inequality [6]

$$\frac{T_{\Omega}}{T_{\Theta N}} \gg \frac{2m}{\sqrt{1-m^2}}, \quad (\text{VI. 50})$$

in which $T_{\Theta N}$ is the video pulse tracking period; T_{Ω} is the envelope period; m is the modulation factor.

This condition is usually fulfilled properly in practice because the / 481 ratio $T_{\Omega} / T_{\Theta N}$ has an order of magnitude of 20 - 40, while $m \gg 1$.

For the error signal meter shown in Fig. VI. 28a the transfer constant

of the peak detector is equal to [6]

$$K_A = \frac{U_{\Omega}}{mU_{np}} = \frac{1}{1 + \frac{U_{np}}{S_A R_A}} \quad (VI. 51)$$

in which $S_A = S_1(R_{iA} + R_A)$ is the dynamic slope of the detector response curve; θ_{DM} is the video pulse duty factor; $R_{iD} = 1/S$ is the internal resistance of an open diode; R_B is the plate load resistance of the preceding stage; R_D is the detector load resistance.

The formula is valid if the following conditions are fulfilled:

$$R_A C_A \ll 0.5\tau_{np}; R_{iA} \ll R_B; R_A C_A \gg T_{np}$$

in which τ_{np} is the duration of the main pulse.

Reproduced from
best available copy.

For an error signal meter with grid detection the transfer constant of the detector is equal to

$$K_A = \frac{S_A R_B R_D}{R_A + \theta_{DM}(R_{iA} + R_B)} \quad (VI. 52)$$

in which S_A is the slope of the detector tube response curve; R_B is the plate load resistance; R_{iD} is the resistance of the grid-cathode portion of an open tube.

In addition to the transfer constant K_A peak detectors of error signal meters are characterized by a phase shift φ_D of the output signal relative to the input signal envelope and by a time delay equivalent. Usually, the phase shift is of the order of $46^\circ - 60^\circ$ while the time delay equivalent, which is a function of the detector parameters and the magnitudes R_D and C_D , is considerably smaller than the time constant equivalents encountered in the following elements of the system. Therefore, the delay introduced by the detector is not taken into account. The following voltage is fed from the peak detector to the error signal amplifier input in which U_{np} is the amplitude of the voltage at the receiver output

$$u_c = K_A U_{np} [1 + m \cos(\Omega t + \psi)]$$

In any case, the amplitude of the alternating component of the output voltage of the detector is $U_{\Omega} = K_A m U_{np}$, consequently the meter output voltage is a function not only of the magnitude of deflection of the target from the equisignal line (the coefficient of m) but also of the target's dimensions and its distance from the automatic system of tracking for azimuth. For normal operation of the automatic tracking system, i.e. excluding any possibility of loss of stability it is necessary to insure proportionality only between the error signal and the magnitude of target deflection.

In automatic azimuth tracking systems with successive comparisons of signals this is insured through the use in the receiver of a conventional automatic gain control (an automatic gain control operating on a closed cycle) and through a special operating mode of the error signal amplifier tube

in the metering circuit. The amplifier tube is caused to assume such an operating mode when its characteristic is essentially non-linear; the direct component $U_0 = K_{\Delta} U_{np}$ of the peak detector voltage is fed to the tube grid as a bias voltage. Consequently, the slope change of the amplifier tube response curve is inversely proportional to U_0 i.e.

$$S_{\Delta} = \frac{S_n}{U_0}. \quad (\text{VI. 53})$$

Given the required degree of stabilization of receiver gain by the automatic gain control system the quality of secondary stabilization of the error signal depends on how accurately this condition is fulfilled for the whole range of changes of U_0 . In many instances, and especially when tracking large sized targets at short range, the actual characteristics of tubes may not satisfy this condition. To obtain the required relationship between S_{Δ} and U_0 on a broader section of the tube response curve a small resistance R_k is inserted into the cathode circuit of the amplitude pentode.

Error Signal Meter Band Filters

In azimuth tracking systems band filters serve to separate out the basic harmonic of the envelope of amplitude modulated pulses. Ordinarily, they are a component part of the error signal amplifier contained in the meter.

Resonant LC-circuits (Fig. VI. 29a) and double T-shaped bridges (Fig. 29b) tuned to the scanning frequency of the antenna beam find practical application as filters in automatic systems of tracking for azimuth.

As an element of the servo system, filters are characterized by the transfer function for the envelopes. For a filter representing a resonant oscillating circuit coupled into the plate circuit of the amplifier tube of the error signal meter the transfer function of the envelopes is determined by the formula

$$W(\rho) = \frac{SZ_p}{1 + \tau \rho}, \quad (\text{VI. 54})$$

in which S is the slope of the amplifier tube response curve; Z_p is the dynamic resistance of the filter; τ is the time constant of the circuit $\tau = \frac{2L}{R} = \frac{1}{\Omega_0 Q}$; Ω_0 is its own resonance frequency; Q is the Q-factor of the circuit $Q = \frac{1}{R} \sqrt{\frac{L}{C}}$; B is the filter passband.

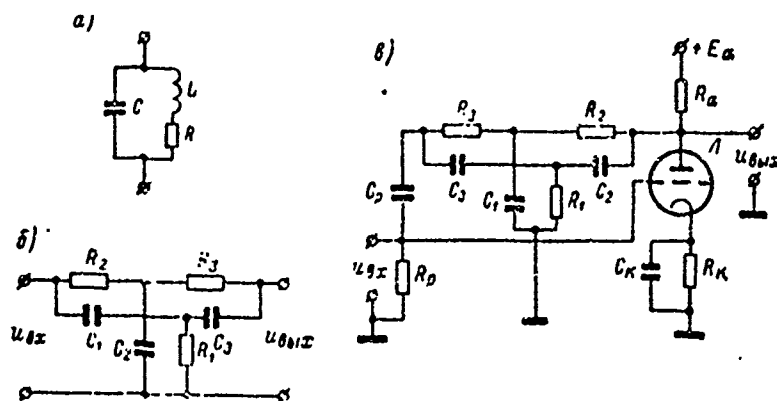


Fig. VI. 29. Narrow band filter circuits used in automatic systems of tracking for azimuth; a - resonant circuit; b. double T-shaped bridge; c. tube narrow band filter.

For a double T-shaped bridge filter

$$W(p) = K \frac{1 + \tau p}{1 + K \tau p}, \quad (\text{VI.55})$$

in which

$$K = \frac{1}{1 + \frac{T_2 + T_{C1} + T_3}{T_1 + T_{C1} - \Omega_0^2 T_1 T_2 T_3}};$$

$$\tau = \frac{2}{\Omega_0^2 (T_1 + T_{C1} - T_1 T_2 T_3)};$$

$$T_1 = R_1 C_1; \quad T_2 = R_2 C_2; \quad T_3 = R_3 C_3;$$

$$T_{C1} = R_1 C_3; \quad T_{C2} = R_1 C_2.$$

Reproduced from
best available copy.

This formula is valid when $K\tau < 1/\Omega_0$, assuming that the "resonant" frequency of the filter Ω_0 is close to the scanning frequency.

The double T-shaped filter is used in azimuth tracking systems in the discriminating amplifier circuit. It is inserted between the control grid and plate of the tube in the amplifier stage on resistances with a large transfer constant K_0 (Fig. VI. 29c). / 484

The transfer function of the amplifier included by the negative feedback through the filter in question is:

$$\Phi(p) = \frac{K_0}{1 + K_0 W(p)} \approx \frac{1}{W(p)} = \frac{1 + K \tau p}{K(1 + \tau p)}. \quad (\text{VI. 56})$$

Symmetrical narrow band double T-shaped filters are used in [9] discriminating amplifier circuits. The parameters of such filters are selected from the relationship

$$\frac{R_2 C_1}{R_1 (R_2 + R_3)} = \frac{C_1 + C_2}{C_2} = 1, \quad (\text{VI. 57})$$

The transfer function of a symmetrical envelope filter is equal to

$$W(p) = \frac{p}{\Omega_0} \cdot \frac{b}{b+1} \quad (\text{VI. 58})$$

and that of an amplifier with such a filter is

$$\Phi(p) = \frac{K_0}{1 + K_0 \frac{p}{\Omega_0} \cdot \frac{b}{b+1}} \quad (\text{VI. 59})$$

here

$$\Omega_0 = \frac{1}{\sqrt{C_1 R_1 C_2 R_2}}; \quad b = \frac{R_1}{R_2} = \frac{C_1}{C_2}$$

Reproduced from
best available copy.

9. Power Drive Boosters

General Information

Electronic, magnetic, and electromechanical amplifiers, as well as combinations of such amplifiers are used in azimuth tracking systems. As boosters, they control the electric motors which direct the antenna toward the target. The kind of system to be used for target tracking by angular coordinates is governed by the type and power of the driving motor.

If the drive motor is a two phase asynchronous unit, provision is usually made for a modulator in the structure of the amplifying device; its function is to convert the dc controlling voltage developed by the phase detector or amplitude discriminator into ac voltage with an amplitude proportional to the magnitude of the input voltage and a phase determined by the polarity of the input voltage. Since it is difficult to get stable amplification with d-c electronic amplifiers, the modulator in systems of this type precedes the voltage amplifier.

If a direct current motor is used as the actuator there is no need to convert the control voltage and the input signal is boosted by the direct current amplifiers. /485

The power amplifier is usually the terminal stage in boosters designed to drive d-c or a-c motors. In the case of lower power motors the power amplifier may be of electronic design with single cycle circuit. A push-pull circuit is used to obtain a relatively greater amount of power; in many instances magnetic amplifiers are used which have an efficiency greater than that of tube power amplifiers. In systems with d-c motors electro-mechanical amplifiers are most often used for power boosters.

Modulators

Modulators are devices which convert a direct current signal into alternating current voltage with an amplitude proportional to the magnitude of the input voltage and a phase determined by the polarity of the input voltage.

Depending on their operating principle modulators are divided into commutator and balanced types. In the former the signal is modulated by the commutator of the vibrator type auxiliary device or by a rectifier. In the case of balanced modulators the signal modulation occurs by disturbing the circuit balance when the direct current voltage is fed to the input.

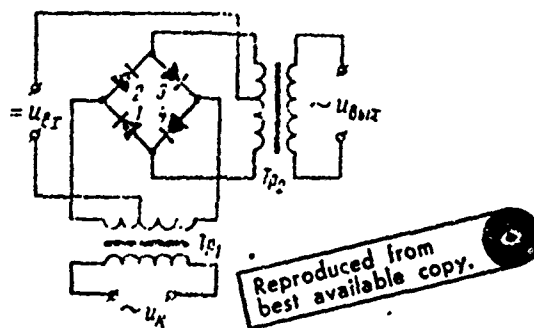


Fig. VI. 30. Ring modulator

- Depending on the elements used modulators are divided into [7]:
- electromechanical types based on the use of vibrator relays;
 - rectifier types based on the use of semiconductor valves or diodes;
 - electronic types with electronic amplifier tubes;
 - magnetic types based on the use of magnetic amplifiers.

The ring modulator (Fig. VI. 30) acts like a commutating type in its operating principle, but as far as the elements used it relates to the rectifier type. Conversion of the direct current input signal into an alternating current signal is based on changing the resistance of the rectifier as a function of the voltage applied. / 486

The circuit operates as follows. The commutating voltage u_k is fed to one of the diagonals of the rectifier bridge by way of the step-up transformer T_{P1} . For normal operation of the modulator the commutating voltage fed to the diagonal of the bridge is taken considerably greater than the input voltage u_{BX} which is fed to the center points of the windings of transformers T_{P1} and T_{P2} . The output voltage u_{BIX} is taken from the secondary winding of the transformer T_{P2} . Because the commutating voltage is considerably greater than the input voltage the operation of the rectifiers in ring type modulators is governed by the voltage u_k . During one half period of this voltage the resistance of rectifiers 2 and 3 is very low, while that of rectifiers 1 and 4 is very high. In the next half period the opposite conditions holds true: rectifiers 2 and 3

operate in a condition of very low resistance, while rectifiers 1 and 4 are operating under conditions of very high resistance.

The circuit in a ring type modulator is symmetrical. Hence, in the absence of an input signal the output voltage $u_{BДIX}$ is equal to zero due to the fact that currents equal in magnitude and opposite in sign flow through the primary winding of transformer Tp_2 .

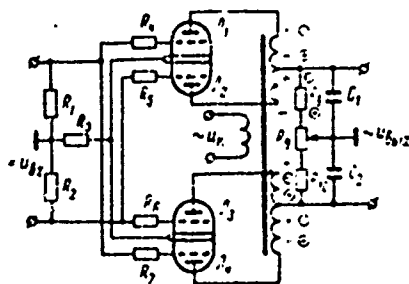


Fig. V. 31. Balanced two half-period type modulator on triodes.

When a direct current signal is fed to the modulator the balance of the resistances in the rectifier bridge is affected. Apart from the two current components caused by the commutator voltage, a third component appears in the primary winding of the output transformer; this one is caused by the source of the input voltage. The current components in the primary winding of transformer Tp_2 which appeared under the influence of the voltage $u_{ДХ}$ are compensated for, just as was true in the case where $u_{ДХ} = 0$. Therefore, the magnitude of the resulting current and voltage on the primary winding of the output transformer are governed by the input voltage. This is an alternating current of square shaped waves with the frequency of the commutating voltage source. When the polarity of the input voltage changes there is a 180° change in the phase of the output voltage.

The balanced, two half-period modulator (Fig. VI. 31) consists of four electronic tubes the plate circuits of which are fed by alternating current u_K . Not only triodes, but tetrodes and pentodes can be used as the modulator tubes. In each particular case the type of tube / 487 used is determined by the amount of modulator amplification required. The direct current voltage $u_{ДХ}$ is converted into alternating current voltage $u_{BДIX}$ with a frequency determined by the source of the commutating voltage in this circuit in accordance with the following.

If no input signal is applied to the control grids of the tubes, currents of equal magnitude flow during the first and second (positive and negative) half cycles of commutating voltage in the secondary windings of the transformer through the plate circuits of the tubes $\mathcal{A}_1, \mathcal{A}_2$ and $\mathcal{A}_3, \mathcal{A}_4$. As a result, the output voltage taken from resistances R_8, R_9 , and R_{10} is equal to zero. When a d-c signal is fed to the input of the modulator the circuit becomes unbalanced, i.e. the current from tube \mathcal{A}_1 becomes

unequal to that of tube \mathcal{N}_3 during the first half-period of the carrier frequency voltage, and the current from tube \mathcal{N}_2 is unequal to that of tube \mathcal{N}_4 in the next half-period. As a result, the output voltage $u_{B_{DIX}}$ determined by the difference in potential between the mean currents of the secondary windings of transformer Tp_1 is not equal to zero. The amplitude of voltage $u_{B_{DIX}}$, which changes with the power supply voltage frequency ω_k , is governed by the magnitude of the direct current voltage which acts on the input to the circuit, whereas the phase is determined by the polarity of the voltage u_{B_X} . When the polarity of the input signal changes the output voltage phase changes 180° .

The linearity of the response curve in the two half-cycle modulator circuit -- the curve represents the relationship of the output voltage amplitude to the magnitude of the input voltage -- is determined by the operating condition of the tubes and the position of the operating point on the triode plate-grid curves.

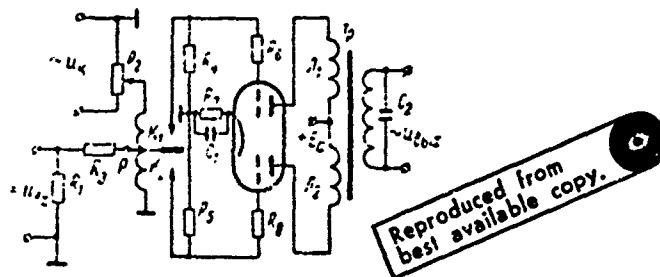


Fig. VI. 32. Electromechanical modulator

The magnitude of the unbalanced output voltage when $u_{B_X} = 0$, which characterizes the zero stability of the modulator, depends on the accuracy of the potentiometer R_9 indicator setting. Tube replacements ordinarily produce a certain unbalance in the modulator due to differences in their parameters; this unbalance decreases with increased values of load resistances R_8 , R_9 , and R_{10} .

Condensers C_1 and C_2 act as filters in the circuit and decrease the amount of distortion in the output voltage wave form.

The electromechanical modulator described in Fig. VI. 32 consists of the electromechanical commutator P which is fed from the commutator power supply and the voltage amplifier on the triodes \mathcal{N}_1 and \mathcal{N}_2 . Contacts K_1 and K_2 of the commutator are closed periodically as a result of which a direct current taken from the resistance R_1 is fed alternately to the control grids of the tubes. /488

The commutator period of oscillation is equal to the voltage period u_k . During the first half period of the alternating voltage contact K_1 is closed, and during the second half period contact K_2 is closed. When commutator contact K_1 is closed the grid potential in tube \mathcal{N}_1 is determined by the bias voltage (R_7 , C_1) and by a drop in the input voltage

across resistances R_4 and that of tube \mathcal{A}_2 is determined only by the bias voltage. And conversely, when contact K_2 is closed the grid potential of tube \mathcal{A}_1 is determined by the bias voltage, whereas the potential on the grid of tube \mathcal{A}_2 is determined by the bias voltage and direct current voltage drop across resistance R_5 which is equal to the resistance of R_4 . As a result, during each half cycle of carrier frequency voltage the tube plate currents are unequal. During the first half cycle the current of one tube is greater, and during the next half cycle the current from the other tube is greater.

The plate currents of the tubes are pulsed and contain direct and alternating current components. Due to circuit symmetry or balance the positive components of the currents are the same in magnitude but opposite in direction. Therefore, when flowing through the primary winding of the input transformer they mutually compensate one another. The alternating components of the plate currents produce a magnetic field in the transformer which has a square shaped wave with the periodicity of the commutating voltage and initial phase determined by the polarity of the input voltage.

A reversal in the polarity of the input voltage changes the phase of the alternating magnetic field, as well as the phase of the output voltage by 180° .

Electronic Amplifiers

The electronic amplifiers contained in the servo drives of automatic azimuth tracking systems are designed to amplify the error signals; the principal function of the amplifier in the servo mechanism is to amplify error signal intensity. Ordinarily, electronic amplifiers in servo drives are used when the output power is under 100-150 watts.

Electronic amplifiers of servo drive mechanisms used in azimuth tracking gear are classed as low frequency amplifiers of 50 hertz and above. Direct current amplifiers are used when it is necessary in the servo drive to boost the mis-alignment (error) signals which change very slowly at a frequency of from 0 to 10-12 hertz.

The operating characteristics of direct and alternating current amplifiers include the following: coefficient of amplification; power and voltage on the load; efficiency; and distortions introduced by the amplifier. Circuits of electronic amplifiers used in the servo drives of automatic azimuth tracking systems are shown in Figs. VI. 33-VI. 35.

The push-pull direct current amplifier (Fig. VI. 33) responds not only to changes in the magnitude of the input signal but also indicates its sign. Resistance R_3 in the cathode circuits performs the functions of a stabilizer of the zero position of the amplifier in addition to creating an automatic bias.

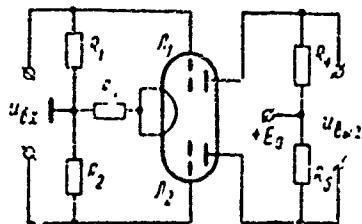


Fig. VI. 33. Push-pull direct current amplifier

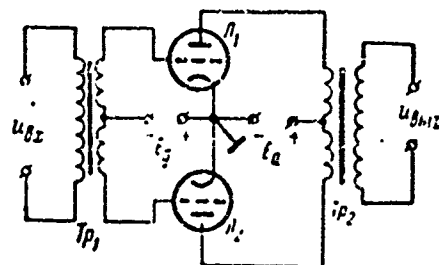


Fig. VI. 34. Push-pull alternating current amplifier with d-c power supply

The operating principle of the push-pull alternating current amplifier circuits shown in Figs. VI. 34 and 35 is similar to that employed in a push-pull direct current amplifier. As was the case in the d-c amplifier, the alternating current amplifier tubes operate simultaneously. Here, in the alternating current fed amplifier they operate only during the positive half cycle of the feed voltage. If the error signal u_{BX} is equal to zero the plate currents of the tube are equal to one another provided the branches of the circuit are symmetrical with one another. Since these currents flow through the primary winding of the output transformer T_p in opposite directions the magnetic fields they produce are mutually cancelled out and $u_{BX2} = 0$. If $u_{BX} \neq 0$ voltages that are 180° out of phase act on the grids of the tubes. Accordingly, the plate current increases in one of the tubes and decreases in the other; the voltage at the output of the circuit has the same frequency as the input signal. 1490

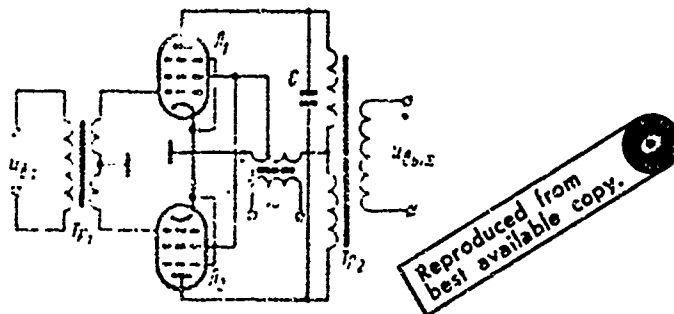


Fig. VI. 35. Push-pull a-c amplifier with a-c power supply.

A very important advantage of push-pull circuits is the fact that with complete symmetry of the branch circuits the output voltage has no even harmonics.

In a-c amplifiers the transformer T_{p2} serves to match the load resistance R_L with the resistance between the plates of the tube R_g . Here, the necessary match is accomplished by selecting the right transformation ratio.

$$n = \sqrt{\frac{R_{L1}}{R_n}}$$

The condenser C in the amplifier circuit connected in parallel to the primary winding of the output transformer serves to derive the greatest amount of power from the tubes. The capacitance value of the condenser is selected such as to resonance tune the circuit to the frequency of the alternating current of the power supply.

Magnetic Amplifiers

Magnetic amplifiers [10] are electromagnetic devices which amplify the power and voltage of electrical signals. Despite the multiplicity of magnetic amplifier circuits used they are all designed around the same physical principle -- utilizing the ratio of the magnetic permeance of ferromagnetic materials with alternating current μ_{\sim} to the magnitude of a magnetizing field.

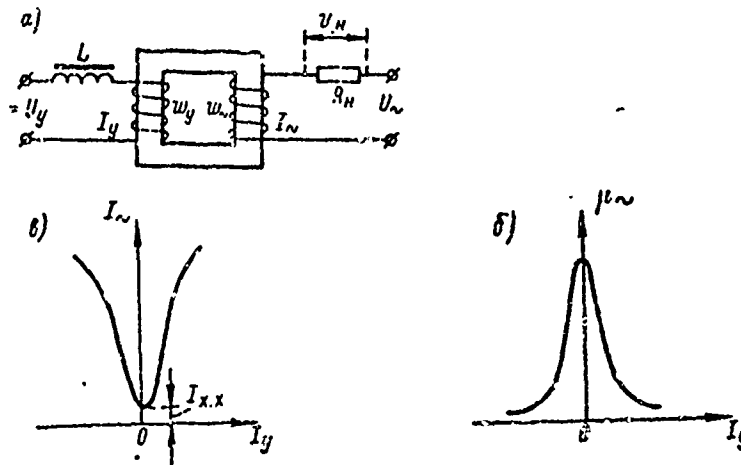


Fig. VI. 36. A simple choke-coupled amplifier: a. circuit; b. the function $\mu_{\sim} = f(I_y)$; c. the function $I_{\sim} = f(I_y)$.

In its simpler aspects the magnetic amplifier consists of a choke with two windings, one of which is fed by an alternating power source and the other is connected to the direct current power supply (Fig. VI 36a). The core is simultaneously magnetized by a direct current I_y flowing in the control winding w_y and the alternating current I_{\sim} , flowing in the winding w_y . Due to the constancy of the power source voltage U_{\sim} and the non-linear nature of the core magnetization curve the value of magnetic permeance is determined only by the current of the control winding I_y . The approximate form of the relationship $\mu_{\sim} = f(I_y)$ for a choke coupled amplifier is shown in Fig. VI. 36b.

At small values of active resistance compared to the inductive reactance of the choke winding the magnitude of the current I_{\sim} flowing through it is determined by the expression

$$I_{\sim} = \frac{U_{\sim}}{\omega L}, \quad (\text{VI. 61})$$

in which U_{\sim} is the power voltage; ωL is the inductive reactance of the winding W_{\sim} ; and L is the inductance of the winding,

$$L = \frac{0.4\pi w^2 S_0}{l_0 10^9} \mu_{\sim};$$

S_0 is the cross section of the magnetic circuit; and l_0 is the mean length of the magnetic circuit.

Increasing or decreasing the magnetizing current results in increasing or decreasing the current I_{\sim} in the winding w_{\sim} ; changes in the current I_{\sim} are considerably greater than the changes in the current I_y . The function $I_{\sim} = f(I_y)$ is the magnetic amplifier control characteristic. Its nature depends on the material used in the core and on the parameters of the amplifier.

In a simple, magnetic, choke-coupled amplifier, because of the fact that a reduction in the magnetic permeance μ_{\sim} is not a function of the direction of current flow in the winding w_y the response curve of $I_{\sim} = f(I_y)$ is symmetrical to the ordinate axes (Fig. VI. 36c).

The current amplification factor of the magnetic amplifier is equal to

$$K_I = \frac{I_{\sim}}{I_y}, \quad (\text{VI. 62})$$

and the amplification factor for voltage is

$$K_P = \frac{I_{\sim}^2 R_{\sim}}{I_y^2 R_y}, \quad (\text{VI. 63})$$

in which R_y is the resistance in the control circuit.

To increase the gain in magnetic amplifiers use is made of ferromagnetic materials with a very marked relationship between the μ_{\sim} and the value of the magnetizing current I_y as well as the positive feedback; this means that a certain portion of the power of the output circuit is used to control the magnetic amplifier along with the input signal that enters the winding w_y . Of the many existing varieties of feedback (external, / 492 internal, and crossed) the most commonly used in servo drives are the external and internal positive feedback systems. External feedback is ordinarily used with high voltages and small currents, whereas the internal system is used with small voltages and large currents.

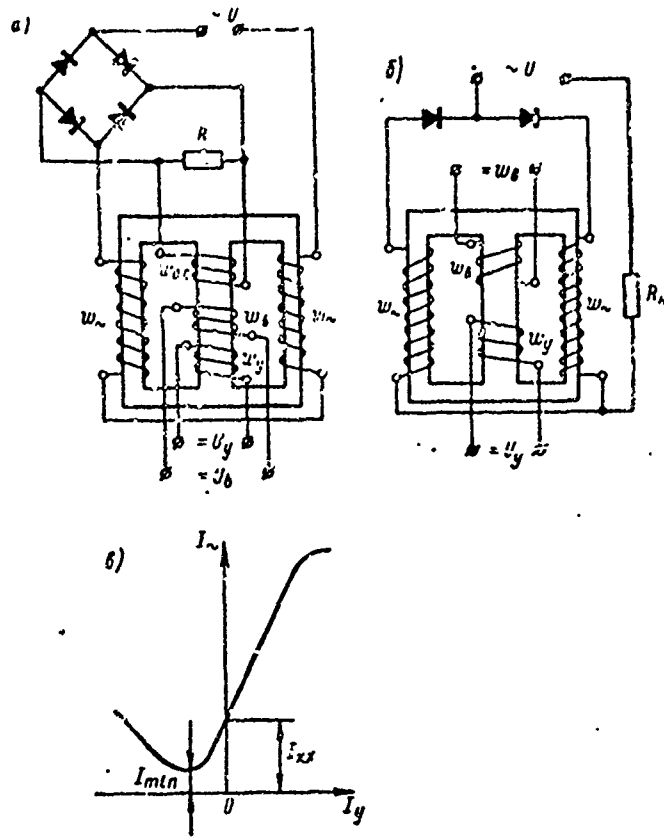


Fig. VI. 37. Schematic diagrams of the simpler type magnetic amplifiers with positive feedback: a. with external coupling; and b. with internal coupling; the function $I_w = f(I_y)$.

Diagrams of simpler magnetic amplifiers with positive feedback are given in Fig. VI. 37. External positive feedback is obtained by introducing a supplementary positive feedback winding w_{oc} which is connected into the circuit so that a direct current proportional to the load current may flow through it.

At a particular polarity of the input signal U_y the magnetic fluxes of the windings w_y and w_{oc} are additive; this condition corresponds to positive feedback. With a change in the polarity of the input signal magnetic fluxes of the windings of w_y and w_{oc} act in opposite directions thus weakening the resulting magnetized field; this corresponds to negative feedback. In view of the fact that positive feedback becomes negative with changes in the polarity of the input signal, magnetic choke-coupled amplifiers with negative feedback are used only to amplify signals having a fixed polarity.

Internal feedback is accomplished by coupling in single half cycle rectifiers in series with each of the alternating current winding w_w .

As a consequence, pulsing currents flow in the windings creating a magnetic field feedback. This will be positive for one polarity of the input signal and negative for the other.

The power amplification factor K_p for a magnetic amplifier with feedback can be determined in accordance with the following

$$K_p = \frac{i_{\sim}^2 R_H}{I_y^2 R_y} = \frac{R_H}{R_y} K_T^2 = \frac{R_H w_y^2}{R_y w_{\sim}^2 (1 \mp K_{oc})^2}, \quad (\text{VI. 64})$$

in which $K_{oc} = w_{oc}/w_{\sim}$ is the feedback coefficient.

The feedback coefficient is regulated in amplifiers by changing the number of coil turns or by bypassing the winding w_{oc} through shunting of the feedback rectifiers or by changing the alternating component of the magnetizing force.

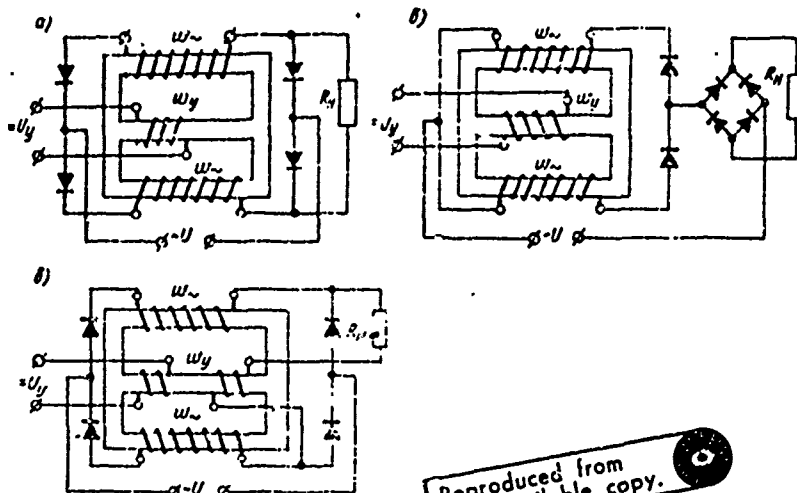
In the simpler single cycle choke-coupled magnetic amplifiers with positive feedback the no-load current I_{xx} increases with an increase in the feedback coefficient K_{oc} . In many cases provision is made for special windings (bias windings w_b) to shift the response curve of $I_{\sim} = f(I_y)$ along the abscissa axis in order to decrease the current I_{xx} and select the necessary operating portion on the control curve in amplifier circuits. The bias windings may either be alternating or direct current fed. The most commonly used method is that in which the bias is obtained by feeding the windings with a direct current.

Multiple stage magnetic amplifiers for servo drives are usually designed as push-pull circuits with stages having separate input and output (Fig. VI. 38a); or with common input and output (Fig. VI. 38b); or with separate and common input, as well as separate and common outputs (Fig. VI. 38c).

An advantage of the structured amplifie. circuit made up of stages with separate input and output is the relative simplicity of matching the stages and more completely utilizing the stages for power yield and gain. The drawback of such systems is the marked influence the following stages have on the preceding ones and the relative instability of the circuit with changes in the U_{\sim} voltage and the temperature.

The chief advantage of amplifier circuits made up of stages with / 495 common input and common output, i.e. with series connected w_y windings, is the lessened effect the following stages have over the preceding stages than is true of circuits with separate input and output, and the comparatively greater stability of the amplifier's characteristics when it is operating under conditions other than normal. The drawback of these structural diagrams is their lesser amplification factor and greater complexity of design.

Combination block diagrams of magnetic amplifiers (amplifiers made up of both primary and secondary type stages) are free of the shortcomings peculiar to amplifiers having stages with separate input and output, and those having stages with common input and output. For that reason they are most commonly used in servo drive mechanisms.



Reproduced from
best available copy.

Fig. VI. 39. Diagrams of choke coils used in the intermediate stages of magnetic amplifiers with series (a), bridge (b), and parallel (c) coupling of rectifiers.

The types of intermediate stages to be used in multiple cascade magnetic amplifiers are determined by the kind of amplifier circuit selected. The choke coil systems most commonly used for the intermediate stages are described in Fig. VI. 39a, b, c.

Most widely used in the output stages of servosystems with alternating current low and medium power drive motors are feedback magnetic amplifiers with differential and bridge circuits. In the case of servosystems with high power motors, bridge amplifiers without positive feedback are most commonly used. Typical circuits of output amplifiers are shown in Fig. VI. 40.

When using a direct current motor that is directly controlled by a magnetic amplifier in an automatic system of tracking for azimuth the circuit shown in Fig. VI. 41a can be used for the output stage of the magnetic amplifier. When the direct current motor is controlled by an electromechanical amplifier the circuit shown in Fig. VI. 41b can be used in the output stage.

Within the limits of the linear portions of the curve $I \sim (L_y)$ push-pull single stage magnetic amplifiers can be regarded, with certain allowances, as aperiodic elements with a transfer function

$$\omega(p) = \frac{K_y}{1 + T_p p} \quad (\text{VI. 65})$$

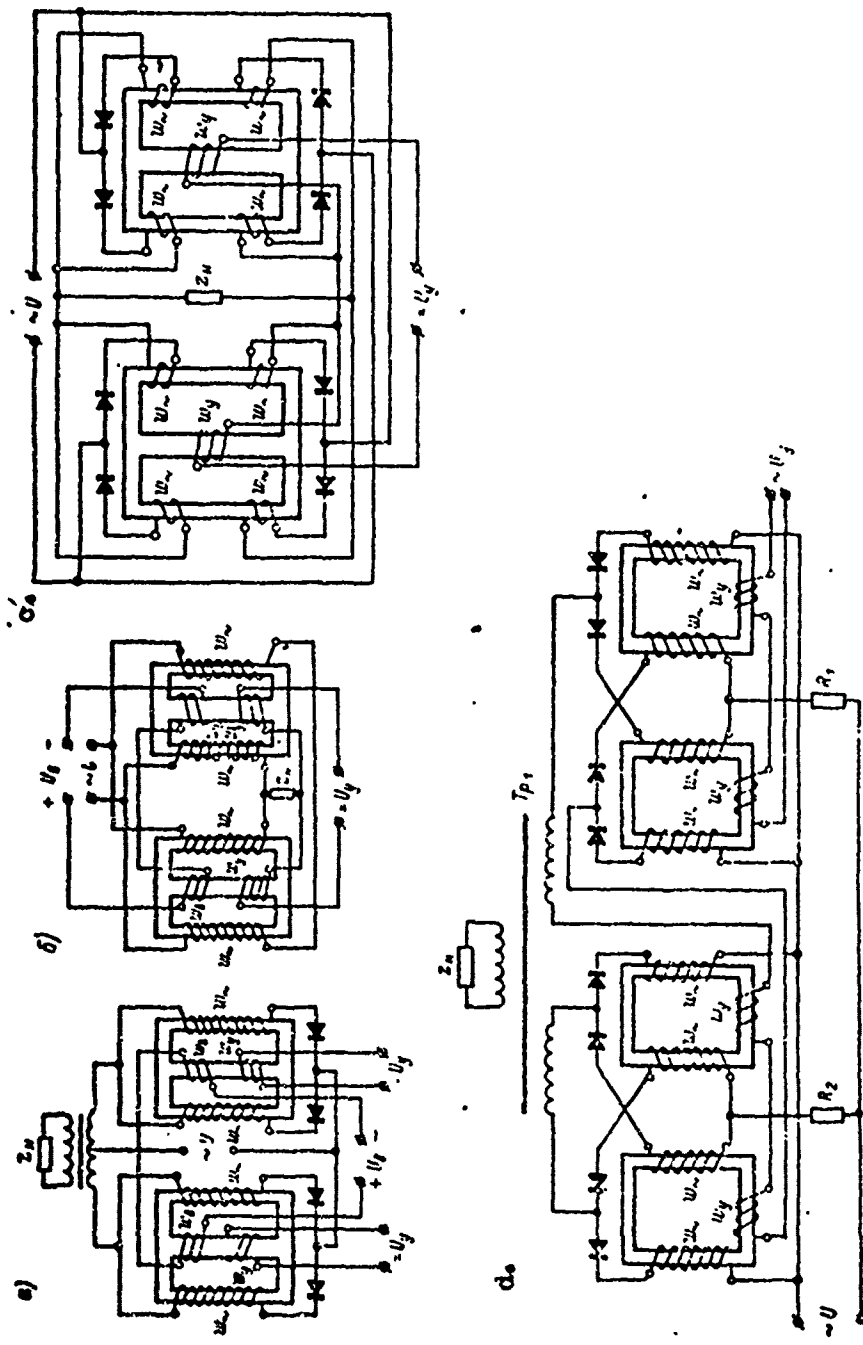
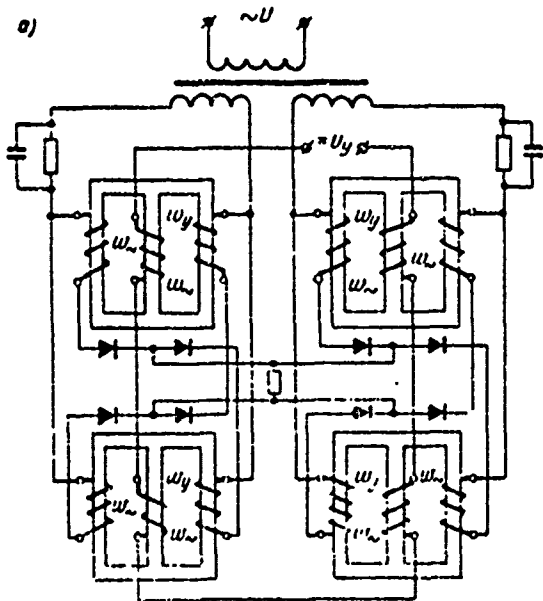


Fig. VI. 40. Types of output stages of magnetic amplifiers for servo drives with alternating current motor: a. differential circuit diagram with positive internal feedback; b. bridge amplifier circuit without feedback; c. bridge amplifier circuit with positive feedback; c. quick response full wave amplifier output.



Amplidyne excitation windings

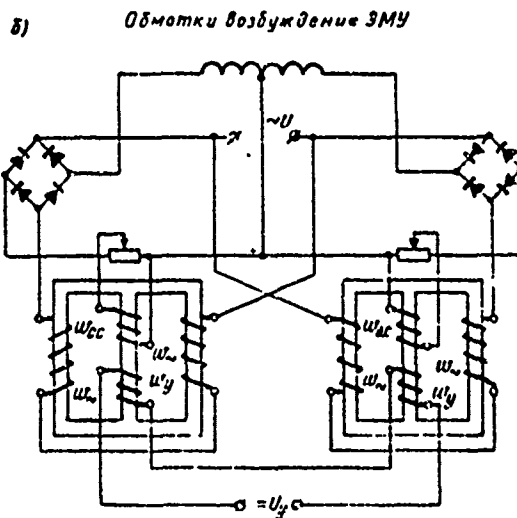


Fig. VI. 41. Circuit diagrams of magnetic amplifier stages for servo drives with direct current motors: a. push-pull circuit for direct control of motor; b. differential circuit for control of excitation windings of amplidyne.

in which K_y is the static voltage gain of the stage; T is the time constant of the stage (seconds) determined from the expression

$$T = \frac{0.4\pi S_0 \omega_y (\omega_y + K_y \omega_{ac}) \mu_{\Delta\Phi}}{R_{y0} I_0}, \quad (\text{VI. 66})$$

in which R is the resistance of the amplifier control circuit; $\mu_{\Delta\Phi} = \partial B_0 / \partial H_0$ is the differential magnetic permeability.

For multiple stage magnetic amplifiers in which the following stages exert only a mild effect on the preceding stages -- this is accomplished either through series coupling or bypassing the control windings of the stages with capacitances -- the transfer function in its general form is determined by means of the expression

$$\omega(p) = \frac{K_y}{(1 + T_1 p)(1 + T_2 p) \dots (1 + T_n p)}, \quad (\text{VI. 67})$$

in which $T_1, T_2, T_3 \dots T_n$ are the time constants of the individual stages.

Reproduced from
best available copy.

Amplidyne

The amplidyne is a direct current generator with longitudinal and lateral excitation caused to rotate by a built-in direct or alternating current motor.

The following are some of the desirable features of the amplidyne: it can be driven by motors of up to 10 kw in power; has a great power amplification coefficient ($\sim 10^2 - 10^4$); capable of comparatively high operating speed; has low operating power requirements (about 1 watt); and has a simple system for totalizing several signals.

Among the drawbacks of this type of amplidyne are: its requirement for a special system to improve commutation; instability of its parameters due to a lateral short circuited circuit and a tendency to oscillate when over-compensated.

/ 499

Electrodynes are used in the servo systems of automatic azimuth tracking systems as power amplifiers to control d-c drive motors.

The chief static features of an amplidyne include its no-load characteristic, which is expressed by the ratio of the electromotive force E to the magnitude of the control current, and its internal characteristic, which is expressed by the ratio of the output voltage $U_{\Delta\Phi X}$ to the load current I_H with $I_y = \text{constant}$. The effect of controlling the magnitude of the output power is evaluated by the power gain K_p which is equal to the ratio of the amplidyne output power to the power fed to the control windings

$$K_p = \frac{E^2}{I_y^2 R_u R_y}, \quad (\text{VI. 68})$$

in which R_y is the resistance of the control windings; R_h is the load resistance.

10. Controlling Actions of Automatic Systems of Tracking for Azimuth

Automatic Tracking Errors

Controlling Actions

In general, the controlling actions of automatic systems for tracking in azimuth are the angular displacements of the targets in two mutually perpendicular planes: the bearing angle plane and the elevation plane of the target. If the target travels at uniform speed in a straight line at constant altitude (Fig. VI. 42) the changes with respect to time of the real angular coordinates of the tracked target and their first derivatives are determined by the following expressions:

$$\beta(t) = \arctg \frac{V_u t}{p}; \quad (VI.69)$$

$$\frac{d\beta}{dt} = \frac{V_u}{p \left(1 + \frac{V_u^2}{p^2} t^2 \right)}; \quad (VI.70)$$

$$\epsilon(t) = \arctg \frac{H}{p \sqrt{1 + \frac{V_u^2}{p^2} t^2}}; \quad (VI.71)$$

$$\frac{d\epsilon}{dt} = - \frac{H V_u^2 t}{\sqrt{p^2 + V_u^2 t^2} (p^2 + V_u^2 t^2 + H^2)}; \quad (VI.72)$$

in which V_u is the target velocity; H is the flight altitude of the target; p is the course parameter. / 500

Course parameter is defined as a segment of a straight line perpendicular to the target's course projected on the horizontal plane and passing through the point where the automatic azimuth tracking system is positioned.

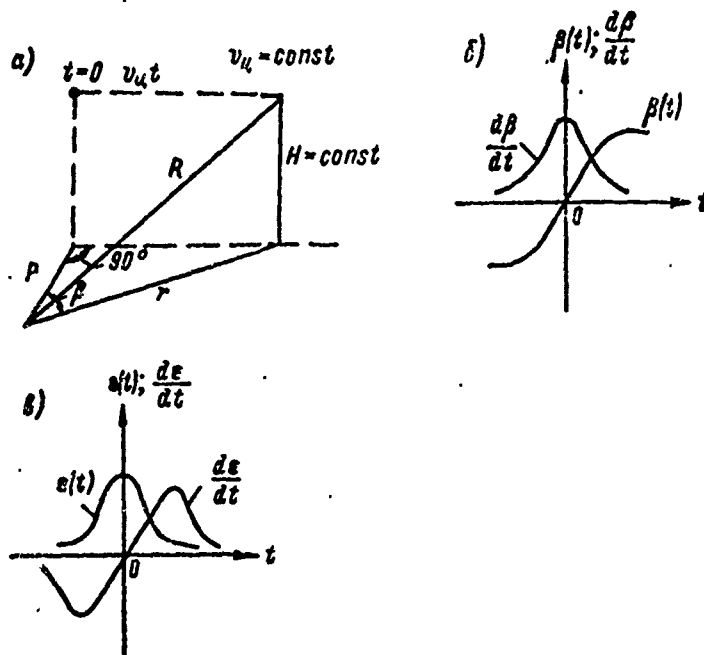


Fig. VI. 42. Uniform rectilinear movement of target at constant altitude (a); graphs of changes in angular coordinates and first derivatives from them (b, c).

Errors in Automatic Systems of Tracking For Azimuth

Automatic azimuth tracking system errors are divided into those caused by the controlling actions and fluctuating or random errors resulting from the effects of interfering signals (static), noises, parasitic changes of target pulse parameters, etc.

Errors due to changes in the coordinates of a target describe the accuracy of an automatic tracking system for a specific channel with normal operating changes of input effect. Because of the identical characteristics of the channels for target bearing angle tracking and tracking in elevation the overall angular error of the system is $\sqrt{2}$ times greater than the error of one channel. / 501

The magnitude of total error for a specific system for any of its channels depends on the parameters of the system and the principles underlying changes in a particular action, i.e. $\beta(t)$ or $\alpha(t)$. The total amount of system error for any channel is determined by the expression

$$\Delta X(t) = C_0 X_{sx}(t) + C_1 \frac{dX_{sx}}{dt} + \frac{1}{2!} C_2 \frac{d^2 X_{sx}}{dt^2} + \dots + \frac{1}{3!} C_3 \frac{d^3 X_{sx}}{dt^3} + \dots \quad (\text{VI. 73})$$

in which $\Delta X(t)$ is the automatic tracking error for a particular coordinate; $X_{BX}(t)$ is the input signal of the system; $C_0, C_1, C_2,$ and C_3 are the error coefficients computed through the use of the formula

$$C_i = \left(\frac{d^i}{dp^i} \left[\frac{1}{1+W(p)} \right] \right)_{p=0}, \quad (\text{VI. 74})$$

in which $W(p)$ is the transfer function for a particular channel of an open system.

The first member of the series in VI. 73 determines the static error; the second determines the dynamic velocity error; and the third member determines the dynamic acceleration error, etc.

Automatic systems of tracking for azimuth with first and second orders of astatism are used in field operations. The error coefficients of such systems have the following values:

for systems with first order astatism

$$C_0 = 0; C_1 = \frac{1}{K}; C_2 \approx -\frac{t_{p \max}}{K};$$

For systems with second order astatism

$$C_0 = C_1 = 0; C_2 \approx \frac{2}{K},$$

Reproduced from
best available copy.

in which K is the transfer constant of an open automatic tracking system; $t_{p \max}$ is the maximum time constant of the system.

Therefore, with acceptable values of stability reserve, accuracy in tracking targets by angular coordinates with automatic azimuth tracking systems is governed by the magnitude of the transfer constant and, therefore, by the effective passband ΔF_{eff} . The latest tracking systems have K values running to the several hundreds.

In this case the passband of the servo system is equal to

/ 502

$$\Delta F_{\text{eff}} \approx \frac{1-1.5}{2\pi \sqrt{C_2}}. \quad (\text{VI. 75})$$

The speed of operation of a system and the tracking error components due to the effects of interfering signals are dependent upon the effective passband. The wider the ΔF_{eff} the higher the speed of operation of the system and, therefore, the smaller the dynamic automatic tracking errors of a maneuvering target. At the same time, the various kinds of interferences exert a stronger effect.

For optimal frequency characteristics the stabilization time in a system (responsiveness of a system) is related to ΔF_3 by the expression

$$t_p \approx \frac{1,0-2,5}{\Delta F_3}. \quad (\text{VI. 76})$$

The magnitude of random errors, i.e. errors showing up in automatic azimuth tracking systems due to the effects of various disturbing factors, is assessed by their mean square values in terms of the spectral density of perturbation and by the transfer function of the system determined with respect to the point of application of a particular disturbance

$$\sigma_i = \sqrt{\frac{1}{2\pi} \int_{-\infty}^{\infty} S_i(\omega) |\Phi_i(j\omega)|^2 d\omega}, \quad (\text{VI. 77})$$

in which σ_i is the mean square error of the system due to the i-th disturbance; $\Phi_i(j\omega)$ is the transfer function of the system with respect to the disturbance, and $S_i(\omega)$ is the spectral density of the i-th disturbance.

Automatic systems of tracking for azimuth have a sufficiently narrow passband ΔF_3 which falls within the limits extending from 0 to .5-2 hertz. Therefore, in the first approximation the error value due to some disturbance of a statistical nature can be determined as

$$\sigma_i \approx \sqrt{S_i(0) \Delta F_3}, \quad (\text{VI. 78})$$

in which $S_i(0)$ is the spectral density of the i-th disturbance on the zero frequency of the system.

The total error of any automatic azimuth tracking system is the mean square value of all the errors.

- - - - -

BIBLIOGRAPHY

1. Artamov, V. M., Elektroavtomatika sudovykh i samoletnykh radiolokatsionnykh stantsiy (Electrical Automatic Systems in Shipborne and Aircraft Radar), Moscow, Gosenergoizdat, 1962.
2. Bayda, L. I., and Semenkovich, A. A., Elektronnyye usiliteli postoyennogo toka (Direct Current Electronic Amplifiers), Moscow, Gosenergoizdat, 1953.
3. Desekerskiy, V. A., et al, Proyektirovaniye sledyashchikh sistem maloy moshchnosti (Designing Low Power Servo Systems), Leningrad, Sudpromgiz, 1958.
4. Vasil'yev, V. P., et al, Raschet elementov impul'snykh radiotekhnicheskikh ustroystv (Designing Radar Pulsing Equipment), Moscow, Gosenergoizdat, 1963.
5. Gitis, E. I., Avtomatika radiustanovok (Automation in Radio), Moscow, Energiya, 1964.
6. Gutkin, L. S. Preobrazovaniye sverkhvysokikh chastot i detektirovaniye, (Conversion of Superhigh Frequencies and Detection), Moscow, Gosenergoizdat, 1953.
7. Dobrogurskiy, S. O., et al, Schetno reshayushchiye ustroystva (Computers), Moscow, Oborongiz, 1959.
8. Dulevich, V. Ye., et al, Teoreticheskiye osnovy radiolokatsii (Theoretical Principles of Radar), Moscow, Sovetskoye Radio, 1964.
9. Krivitskiy, B. Kh., Avtomaticheskiye sistemy radiotekhnicheskikh ustanovok (Automatic Systems in Radio and Radar Equipment), Moscow, Leningrad, Gosenergoizdat, 1962.
10. Rozemlat, M. A., Magnitnyye usiliteli (Magnetic amplifiers), Moscow, "Sovetskoye Radio", 1960.
11. Snybel', A. G., Osnovy radiolokatsii (Principles of Radio), Moscow, "Sovetskoye Radio", 1961.